Il processo di una scoperta scientifica è, in effetti,

un continuo conflitto di meraviglie.

Albert Einstein

Alla mia famiglia

Contents

Abbreviations:

AC: adenylyl cyclase
CaM: calmodulin
cAMP: cyclic adenosine monophosphate
CCPs: clathrin-coated pits
CCVs: clathrin-coated vesicles
CI: clathrin-independent endocytosis
CI-M6PR: cation-independent mannose-6-phosphate receptor
CMG2: capillary morphogenesis protein 2
CLICs: clathrin-independent carriers
CT-B: cholera toxin B subunit
DCs: dendritic cells
DTA: catalytic domain of diphtheria toxin
EdTx: edema toxin
EEA1: early endosomal antigen 1
EEs: early endosomes
EF: edema factor
EGFR: epidermal growth factor receptor
ESCRT: endosomal-sorting complex required for transport
FP59: N-terminal portion of LF fused to *Pseudomonas* exotoxin A
FRET: fluorescence resonance energy transfer
ILVs: intralumenal vesicles
LAMP1: lysosomal-associated membrane protein-1
LBPA: lysobisphosphatidic acid
LeTx: lethal toxin LEs: late endosomes
LF: lethal factor
LF_N: first 255 residues of lethal factor
LRP6: low-density lipoprotein receptor-related protein 6
MAPKKs: mitogen-activated protein kinase kinases
MIDAS: metal ion dependent adhesion site
MVEs/MVBs: multivesicular endosomes/ multivesicular bodies
PA: protective antigen
PI3P: phoshatidylinositol 3-phoshate
PI-4,5-P_2: phosphatidylinositol(4,5)bisphospate
siRNA: short interfering RNA
SV40: Simian virus 40
TEM8: tumor endothelial marker-8
Tf-R: transferrin receptor epidermal growth factor receptor
TGN: *trans*-Golgi network
VPS: vacuolar protein sorting
VWA: von Willdebrand factor type A

Chapter I

1 Sommario

L'antrace è una zoonosi causata da *Bacillus anthracis,* un batterio Gram-positivo in grado di formare spore. Il batterio è in grado di secernere tre proteine, chiamate antigene protettivo (PA), fattore letale (LF) e fattore edematoso (EF), che si assemblano in maniera binaria per formare due complessi tossici chiamati tossina letale (LeTx: PA+LF) e tossina edematosa (EdTx: PA+EF) . LF è una zinco-metalloproteasi che taglia la maggior parte delle isoforme delle *mitogen-activated protein kinase kinases* (MEKs), interferendo con questa importante via di segnale intracellulare; EF, invece, è una adenilato ciclasi calmodulina dipendente che catalizza un forte aumento di cAMP, importante secondo messaggero, portando ad una alterazione dell'equilibrio osmotico della cellula.

PA, dopo essersi legato a specifici recettori cellulari, viene tagliato da proteasi cellulari, ciò ne promuove l'attivazione e porta all'assemblamento di omo-oligomeri in grado di legare LF ed EF. Il complesso viene quindi internalizzato attraverso il processo di endocitosi e raggiunge i compartimenti tardivi, il cui pH acido favorisce un riarrangiamento conformazionale che porta alla traslocazione delle subunità catalitiche nel citoplasma cellulare.

In questa tesi, l'attività delle tossine, in particolare di EF, è monitorata con diverse tecniche di microscopia e particolare attenzione è rivolta al processo di entrata e *trafficking* nella cellula facendo uso di chimere di LF ed EF fuse al C-terminale con proteine fluorescenti.

1.1 Summary

Anthrax is a severe zoonosis, which may also affect humans, caused by pathogenic strains of the Gram-positive, spore forming *Bacillus anthracis*. The bacterium secretes a three-components toxic complex consisting of the protective antigen (PA), the lethal factor (LF) and the edema factor (EF). These elements combine to form lethal toxin (LeTx: PA+LF) and edema toxin (EdTx: PA+EF). LF is a zinc metalloprotease that cleaves mitogen-activated protein kinase kinases (MEKs), thereby interfering with the MAPK cascade; EF is a calmodulin-activated adenylate cyclase, which catalyses the formation of cAMP, thus altering cell signalling and tissue ion fluxes.

PA binds its specific cellular receptors, then it is proteolytically activated by cellular proteases and self-associates into homo-oligomers capable of binding LF and EF. These complexes enter surface rafts, are endocytosed and reach late endosomal compartments, whose acid luminal pH causes a conformational change, which results in LF and EF release into the cell cytosol.

Here, the activity of anthrax toxins, in particular of EF, is monitored with fluorescent imaging techniques and particular attention is focused on the cell entry and trafficking of anthrax toxins using LF and EF chimerae C-terminally fused to the EGFP or mCherry fluorescent proteins.

Chapter II: Introduction

2.1 Anthrax

''The hand of the Lord is upon the cattle which is in the field, upon the horses, upon the asses, upon the camels, upon the oxen, and upon the sheep: there shall be a very grievous murrain''

Such were the words of Moses, about 1491 B.C., to Pharaoh who refused to let his people leave Egypt, in Exodus book of the Holy Bible; the warning was fulfilled and the resultant fifth plague was likely anthrax, a disease caused by *Bacillus anthracis*. From then up to now, anthrax still represents a problem for herbivores, as well as for human beings, particularly in developing countries.

Humans and animals may become infected by anthrax spores through skin abrasions, ingestion, or inhalation. Cutaneous anthrax is mild and can be treated with antibiotics. Gastrointestinal or inhalational anthrax, if left untreated, usually leads to fatal systemic disease. Inhalational anthrax is the most severe form. When anthrax spores are inhaled, they are deposited in alveolar spaces and ingested as inert particles by local macrophages. The spores are then transported by the infected macrophages to mediastinal lymph nodes, where they germinate into vegetative bacilli. The bacilli escape from the macrophages and begin extracellular multiplication within the lymphatic system. The bacilli then spread into the bloodstream and continue rapid replication. All the while, the bacilli secrete high levels of toxins that intoxicate the host.

The initial symptoms, such as malaise, fatigue, and cough, are nondescripted and resemble those of influenza and other common upper respiratory infections, and this makes early specific diagnosis difficult. After 2 to 5 days, there is a sudden onset of acute symptoms, which may include fever, chills, subcutaneous edema widening of the mediastinum and pleural effusions. Death usually occurs within 24 hrs due to respiratory failure associated with bacteremia.

Indeed, the 2001 anthrax letters crisis has stricken public attention leading to a massive investment in research on the various aspects of anthrax biology and pathology. An unprecedented wealth of discoveries resulted in a restricted period of time, such as the genome of several strains of *B. anthracis*, many aspects of functional genomics and gene regulation, the definition and formulation of anti-anthrax vaccines for human use. This great progress has changed the face of anthrax research.

2.2 Spores and vegetative cells

B. anthracis is a Gram-positive, rod-shaped, spore-forming bacterium. It is found either as vegetative cells or as spores. The latter are ideal infectious agents for the disease, they can remain dormant in the environment for extended periods, when nutrient is limited, until the opportunity to leave this state to begin a process, called germination, which is required for the expression of toxins and capsule, the two major bacterial virulence factors [Driks 2009]. Spores are resistant to a variety of stesses and contribute to dissemination such as *Bacillus thuringiensis* and *Clostridium perfringens* spores.

Sporulation is a complex and long process (about 8 hours) that leads to the formation of a series of concentric shells (Fig. 1): the core, the most internal compartment where the spore chromosome is protect; the cortex, a peptidoglycan layer that provides considerable protection against stresses including heat and UV radiations and keeps the core relatively dry; the coat, a shell which prevents the entry of degradative molecules and predation of other microbes but plays also important roles in facilitating spores survival inside the hosts; the exosporium, the outermost structure separated from the coat by an interspace, whose content is still unknown. The exosporium proteins have recently received much attention because they are good candidates to develop vaccines. This layer plays a fundamental role in interactions with the host and the major surface protein, BclA, influences spore adherence to macrophages.

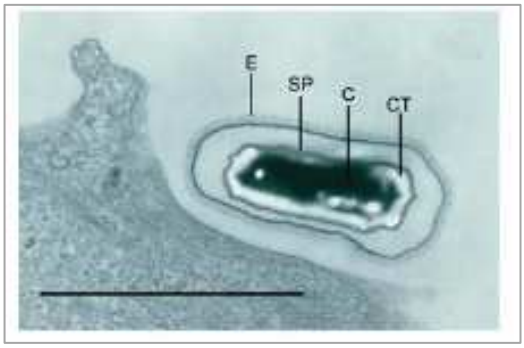

Fig. 1 : **Bacillus anthracis spore.**
From Russell et al., a transmission EM image showing a *B. anthracis* spore in close proximity to the plasma membrane of an HT1080 cell. The structural components of the spore are indicated. E, exosporium; SP, spore coat; C, spore core; CT, cortex. [Russell2007]

When a set of receptors in the spore inner membrane bind amino acids, ribonucleosides and/or peptidoglycan fragments, collectively known as germinants, there is a cascade of events by which spores can leave the dormant state and begin the germination process. It includes the influx of water into the spores, swelling the spore core, dismantling of the cortex and coat and is followed by the resumption of metabolic activity and cell growth. In *B. anthracis* the trigger for germination seems to be more complex than the presence of nutrients, since successful pathogenesis appears to require a germination restricted to specific locations in the host.

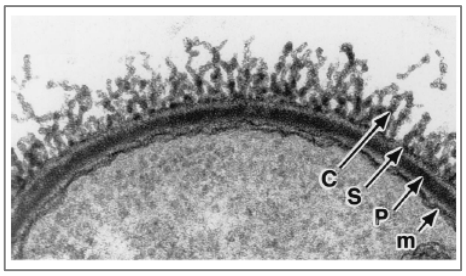

Fig. 2: **Thin section of an encapsulated *B. anthracis*.**
From Mesnage et al., *B. anthracis* surface components. C, capsule; S, S-layers; P, peptidoglycan; m, membrane. [Mesnage1998]

The vegetative form displays a typical Gram positive cell wall which comprises peptidoglycan, a 20-50 nm thick layer apposed to the membrane. This is followed by S-layers, bi-dimensional proteinaceous subunit assemblies which completely cover the bacterial cell surface and are involved in cell adhesion and bacterial protection. The bacterial outermost layer is a polysaccharidic capsule [Fouet2009], which consists of a polymer of D-glutamic acid and functions as anti-phagocytic system (Fig. 2). Although the capsule is an important virulence factor for the establishment of anthrax, the symptoms associated with the disease are the result of toxin production following septicaemia (see section *Anthrax toxins and the host immune defenses*).

2.3 Anthrax toxin

The idea that *B. anthracis* could secrete a molecule involved in pathogenesis was already mentioned by Pasteur in 1887. Only in the late 1950s, Smith and colleagues isolated and characterized the tripartite complex which appeared in the plasma and exudates of infected animals [Smith 1956, Smith 1962].

The genes encoding these proteins are carried by a virulence plasmid called pXO1 and their expression is regulated by host-specific factors, such as temperature (≥37°C), carbon dioxide concentration (≥5%), presence of serum components; conditions similar to those met by the bacterium inside the mammalian host. The expression system is under the regulation of the transcriptional activator AtxA, whose activity appears to be affected by the host-specific factors mentioned above [Koehler 2009].

The three toxin polypeptides belong to the family of bacterial A-B toxins characterized by an A moiety, which contains the catalytic activity and acts within the cytosol of target cells and by a B moiety that binds the toxin to its receptor and translocates the A moiety into the cytosol [Ascenzi 2002]. Anthrax toxins are composed of a single B unit called protective antigen (PA), and two

alternative A subunits: the lethal factor (LF) or the edema factor (EF). Among the known binary toxins, anthrax toxin is unique in using a single B moiety , protective antigen, for the delivery of two alternative A subunits. The three toxin components combine to form two toxins, called lethal toxin (LeTx: LF+PA) and edema toxin (EdTx: EF+PA) because the former caused death of experimental animals after intravenous injection, whereas intradermal treatment of the latter produces edema in the skin. It is worthy to note that none of the three proteins is individually toxic.

2.3.1 Protective antigen

Protective antigen, so named for its use in vaccines, is a long, flat protein of 83 KDa (PA_{83}). The proteolytic activation on the host cell surface removes a 20 kDa fragment (PA_{20}) and the remaining part, called PA_{63}, forms a membrane inserting homo-oligomer that translocates the toxic enzymes into the cytosol. The monomer is a 735-amino-acids protein organized mainly into antiparallel β-sheets and four domains (Fig. 3) [Petosa 1997, Lacy 2004].

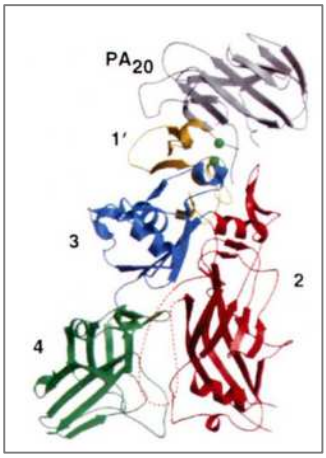

Fig. 3: **Orthogonal view of PA.** From Petosa et al., orthogonal view of PA with domain 1 that comprises PA_{20} (grey) plus domain 1' (yellow) and two calcium ions (green).

The amino-terminal domain, or domain 1 (residues 1-258), contains two calcium ions which help to stabilize the structure and the cleavage site (RKKR) for proteases that release the N-terminal PA_{20} (residues 1-167) which has been reported to affect gene transcription in human peripherial blood leukocytes and to induce apoptosis [Hammamieh 2008]. The remaining part, called 1' (residues 168-258), forms the N terminal of the active PA_{63} which provides a site for binding LF and (or) EF. The domain 2 (residues 259-487) is implicated in membrane insertion and contains a disordered loop (the β2-β3 loop) that ultimately forms the membrane-penetrating element of the pore, a structure that actively catalyzes the polypeptide translocation which requires LF and EF unfolding [Wesche 1998, Zhang 2004, Krantz 2005].

It is followed by a domain 3 (residues 488-595) which has a role in PA_{63} oligomerization [Mogridge 2001]. The carboxy-terminal domain 4 is the receptor-binding domain (residues 596-735) and has a limited contacts with domains 1, 2 and 3 which are intimately associated. Recently, the co-crystal

structure of PA-receptor complex has revealed that the β3-β4 loop of domain 2 also significantly contributes to the receptors interactions (for further details see section *Anthrax toxin receptor*).

Homologues of PA have been found in several spore-forming Gram-positive bacteria namely *Clostridium perfringens*, *Bacillus cereus* and *Bacillus thuringensis*, and share the ability to translocate toxic enzymes into the host cytosol.

The homo-oligomer has a central lumen, polar and negatively charged, which also includes a conserved phenylalanine (Phe427) in a solvent exposed loop. It is water soluble at neutral or basic pH and inserts into membranes at acidic pH. At low pH PA oligomer inserts into membrane by forming 14-stranded β-barrel that function as a selective channel (with estimated size of ~12-15 Å) in both artificial lipid bilayers and cells [Blaustein 1989, Milne 1993]. The cell membrane bound PA oligomer is likely to be oriented with domain 1' exposed to extracellular environment available to bind LF and (or) EF and with domain 2 and the bottom of domain 4 next to the membrane.

Point mutations in two luminal loops of PA are of particular interest because block its biological activity. PA carrying mutations at Lys397, Asp425, and/or Phe427, might co-assemble with wild-type PA and act as dominant-negative inhibitors of the toxin action *in vivo* [Sellman 2001, Sellman 2001#1]. Recently the strongly dominant effects of the D425A and F427A mutants have been directly demonstrated. Each mutant protein was mixed with a 20-fold excess of wild-type PA, the mixture was activated with trypsin, and the prepore fraction, containing co-oligomerized mutant and wild-type PA_{63} protomers, was isolated. Heteroheptamers with a single mutated subunit were then purified from the heterogeneous mixture of prepores and characterized. The presence of the single D425A protomer within an otherwise wild-type prepore was found to inhibit pore formation by $>10^4$, to block prepore-to-pore conversion, and to abrogate PA activity in a standard cytotoxicity assay. The single F427A protomer inhibited cytotoxicity ~100-fold, resulting from strong inhibition of translocation, together with smaller effects on pore formation and ligand affinity [Janowiak 2009].

It is noteworthy that PA homo-oligomers can translocate heterologous proteins and this ability suggests that PA may function as general protein delivery system for therapeutic agents.

2.3.2 Lethal factor

Lethal factor (776 residues) is an extraordinarily selective metalloprotease that site specifically cleaves MAPKK family of proteins near to their N-termini and removes the docking sequence for the downstream cognate MAP kinase.

LF comprises an N-terminal domain which contains all the sequences essential for binding to PA and a C-terminal catalytic domain (Fig. 4). The crystal structure of lethal factor reveals that it consists of four different domains [Pannifer 2001]. Domain 1 (residues 1–262) is perched on top of the other three domains which are intimately connected; it has a high structural similarity with EF domain 1 (Fig. 4, right panel A) indicating its role in binding to PA. A major part of this LF domain folds very similarly to its metalloprotease domain 4 (Fig. 4, right panel B), but the zinc-binding motif HExxH is replaced by YEIGK, suggesting that domain 1 originates from a metalloprotease domain which has been mutated during evolution in such a way as to lose its enzymatic activity and acquire PA binding properties [Tonello & Montecucco 2009].

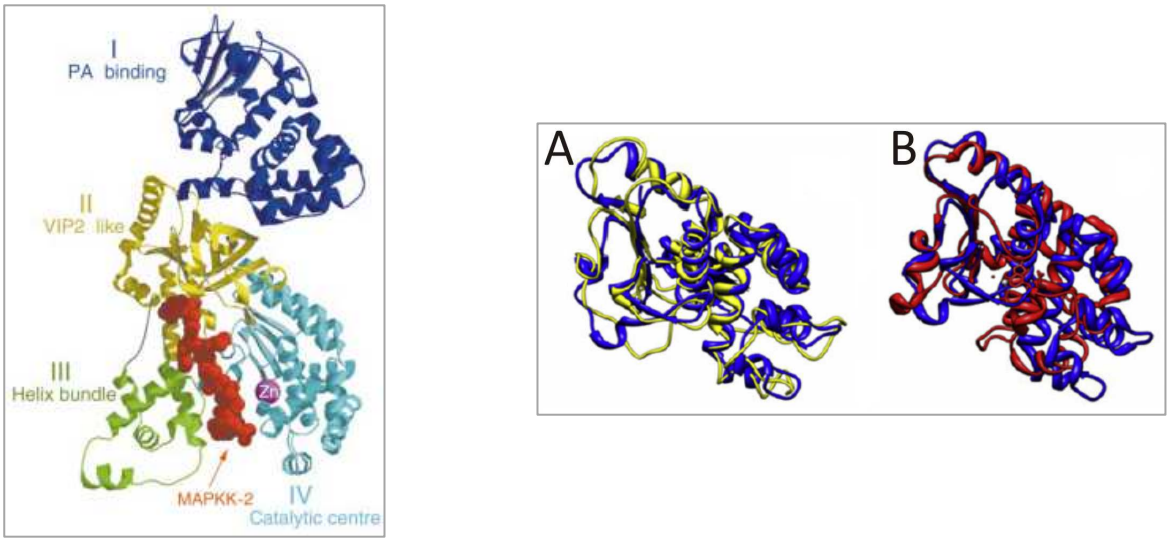

Fig. 4: **Lethal factor**. In the left panel, stereo ribbon representation of LF**.** From Pannifer et al.; the MAPKK-2 substrate is shown as a red ball-and-stick model, and the Zn^{2+} ion is labelled. In the right panel, LF N-terminal domain folding similarities. From Tonello and Montecucco, crystallographic structure similarities among the N-terminal domains of LF (blue) and EF (yellow) are depicted in A; and domain 4 of LF (red) in B.

The peptide corresponding to the first 255 residues of LF (LF_N) can be linked to different polypeptides, such as portions of *Pseudomonas* exotoxin A (FP59) [Arora 1992, Arora & Leppla 1993], the Shiga toxin A subunit or the enzymatic A chain of diphtheria toxin (DTA) [Arora & Leppla 1994, Milne 1995] and a short sequences of positively charged residues fused to the DTA [Blanke 1996]; which can bind to PA and translocate through the PA channel into the cytosol.

The last helix of domain 1 makes an abrupt change into the first helix of domain 2 which is formed by two non contiguous segments (residues 263-297 and 385-550). The folding of domain 2 is similar to that of the catalytic part of the *Bacillus cereus* toxin, VIP2, but it does not conserve neither residues involved in NAD binding and catalysis nor an NAD-binding pocket. Some residues of this domain (Leu-253, Lys-254, Arg-491, Leu-514 and Asn-516) are important for the binding of the substrate MAPKK in the cytosol [Liang 2004], indicating that the interaction of LF with its substrate is not limited to the segment containing the cleavage site. A short LF segment, called domain 3 (residues 303–382), is characterized by the presence of four repeats (LKKLQIDI) of segment 293–300 of domain 2. These five repeats probably arose from duplication of the first sequence and are arranged as a bundle of short a-helices. This domain is required for the enzymatic activity of LF as it contributes to form, with domain 4, a long cleft which is essential for the recognition and correct placement of the substrate at the active site. Domain 4 (residues 552-776) has an active site HEXXH sequence that is common to metalloproteases and constitutes part of the zinc-binding and catalytic machinery.

Whilst sequence comparison shows little homology, more than the presence of the HExxH fingerprint of a zinc-metalloprotease, with other proteins, there is an extensive 3-D similarity with the clostridial neurotoxin metalloprotease domains. Not surprisingly, the major difference between LF and clostridial metalloproteases is in their substrate binding regions [Tonello&Montecucco2009].

2.3.3 Edema factor

Edema factor is a calmodulin (CaM)-activated adenylyl cyclase (AC) that increases the cyclic AMP (cAMP) concentration in infected host cells, thereby disrupting intracellular signalling pathways. There are at least six classes of adenylyl cyclase based on their primary sequences; to date, the structure of three of these classes are available. Class II adenylyl cyclases are bacterial AC toxins which are secreted by pathogenic bacteria and require host cellular factors for their catalytic activation. This class includes anthrax EF, CyaA from *Bordetella pertussis*, the causative agent of whooping cough, and ExoY from *Pseudomonas aeruginosa*, bacteria responsible for various nosocomial infections [Ladant & Ullmann 1999]; as well as a number of gene products from

Yersinia pseudotubercolosis, *Vibrio cholera*, and *Burkholderia thailndesis* that may have AC activity [Tang & Guo 2009].

Class III adenylate cyclase are found from bacteria to humans; among them, the most studied member is the mammalian AC. Both EF and CyaA have at least 1,000 fold higher AC activity than those of class III AC.

While it is difficult to determine the molecular basis for the turn-over differences among these two classes of AC, the fundamental variation in domain movement for catalytic activation and the composition at the catalytic site likely provides the major contribution. It is known that the motion required for the activation of EF and CyaA is significantly smaller than that of mAC [Drum 2002].

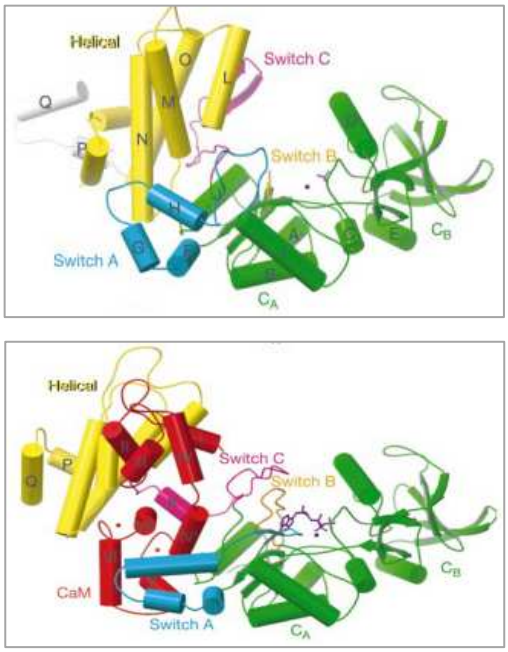

Fig. 5: **Secondary structures of EF.** In the upper panel: C-terminal domains of EF. In the lower panel, the EF-CaM-3'-deoxy-ATP complex. CaM (red) and 3'-deoxy-ATP analogue (purple). From Drum et al. 2002.

Furthermore, there are fundamental differences at the catalytic site [Shen 2002], which would dictate their ability to lower the transition state energy. EF can be divided into N- and C-terminal functional domains. The N-terminal domain bears strong homology to that of lethal factor and is centrally involved in association with PA and entrance into host cells. The C-terminal domain (291-800 residues) comprises three globular domains: the AC domain, which can be divided structurally into the C_A and C_B domains, and the helical domain. The structure of EF AC domain alone significantly differs from that CaM-bound EF AC domain (Fig. 5) and it reveals that the disordered catalytic loop triggered by the interaction of the EF helical domain with the catalytic core domain is the key mechanism to keep EF in the inactive state in the absence of CaM [Drum 2002].

2.4 Anthrax toxin entry into cells

The current model of toxin entry into host cells proposes that the full-length form of PA binds cell surface receptors and is subjected to a necessary cleavage by cellular proteases.

The remaining activated PA_{63} protein then self-assembles into a heptameric ring structure, called prepore, and this oligomerization is accompanied by receptor clustering into the plasma membrane. The receptor–toxin complex is then taken up into cells by endocytosis. Translocation of LF and EF into the cytosol requires a low pH-dependent conformational change in the PA prepore that results in pore formation in an intracellular membrane and the toxin A-moieties are translocated into the host cell cytosol.

2.4.1 Anthrax toxin receptors

The first step of intoxication involves binding of PA to specific cellular receptors [Van Der Goot & Young 2009]. Two types of cell surface receptor have been identified: TEM8 (tumor endothelial marker-8) and CMG2 (capillary morphogenesis protein 2) also known as ANTXR1 and ANTXR2, respectively. The identification of TEM8 was done with a genetic complementation approach on CHO cells [Bradley 2001] and interestingly it is conserved among different species, in particular in the extracellular domain; CMG2 is the protein most similar to TEM8 and it was discovered to support intoxication of a stably transduced population of PA receptor-deficient CHO-R1.1 cells [Scobie 2003]. At least three different isoforms of each receptor have been described and they are the result of alternative mRNA transcripts splicing and differ only in their cytoplasmic tails [Liu & Leppla 2003, Scobie & Young 2005]. Both ANTXR1 and ANTXR2 are type 1 transmembrane proteins with a single membrane-spanning domain and their most distinctive feature is an extracellular region that is highly related to von Willdebrand factor type A (VWA) domain (located between residues 44 and 216) which is present in the extracellular portions of a variety of cell surface proteins, including integrins. Recently, crystallografic structures have been determined for the CMG2 VWA domain alone and complexed with PA or the prepore [Lacy 2004, Santelli 2004]. The VWA domain of these receptors contains a metal ion-dependent adhesion site (MIDAS) motif (DxSxS. . .T. . .D) which binds a divalent cation (i.e Mg^{2+}, Mn^{2+}) and it was demostrated that it is involved in PA binding because the mutation of a MIDAS residue (Asp50) causes a loss of binding of TEM8 to PA [Bradley2003]. These receptors share 40% overall amino acid identity and 60% identity within their VWA domain. The PA affinity for VWA domain of CMG2 was reported to be approximately 1000-fold higher than for that of TEM8 [Wigelsworth 2004]; in a recent paper, the affinities of PA for TEM8- and CMG2-expressing cells were reported to be similar [Liu 2007] but

now this is challenged because it was found that the apparent affinity of PA for CMG2 is 11-fold higher than it is for TEM8 [Liu 2009]. Nevertheless, the lower affinity of ANTXR1 for PA has physiological consequences because it was demonstrated that the pH threshold for conversion of the prepore to the pore and for translocation differs by about a pH unit, depending on whether ANTXR2 or ANTXR1 is the receptor [Rainey 2005]. These findings suggest that translocation may occur at different points in the endocytic pathway, depending on the specific receptor to which the PA is bound.

Recently, it has been also demonstrated that CMG2 has higher activity than TEM8 as anthrax toxin receptor in MEF cells with various ANTXR1 and ANTXR2 genotypes and it is the major receptor in mediating lethality *in vivo* in TEM8- and CMG2-null mice [Liu 2009]. This is surprising in view of the previous *in vitro* cell-culture studies showing that the robust efficacy of TEM8 as an anthrax toxin receptor [Bradley 2001, Liu 2003].

It is noteworthy that these receptors are internalized slowly by the host cell, but PA-receptor complex can be rapidly internalized once it dimerizes making proper oligomerization a critical step in the internalization pathway. Now, there is evidence that the ANRTX1 receptor may exist in a dimeric state on cell surface [Go 2006].

These receptors are ubiquitously expressed [Bradley 2001, Scobie 2003, Bonuccelli 2005, Liu 2009] and their normal functions are associated with binding to extracellular matrix components. It is noteworthy that EdTx can stimulate the expression of both receptor types in macrophages by a mechanism that requires its associated adenylate cyclase activity [Maldonado-Arocho 2006] and TEM8 expression is modestly upregulated in response to interleukin-1β treatment [Rmali 2004] raising the possibility that it can serve to amplify the effects of anthrax toxin on host cell types. It is currently unclear if *B. anthracis* has evolved to use these two types of receptor only because they serve as efficient portals of entry into the cell or whether there are additional aspects of these molecules (e.g. their associated cell-signaling pathways) that are also important for various aspects of anthrax pathogenesis.

Recently, Banks and colleagues have shown that CMG2 and toxins are implicated as factors that help the *B. anthracis* bacterium escape the acidic environment of phagolysosome following spore germination [Banks 2005].

2.4.2 Formation of PA63 prepore

Receptor-bound PA_{63} then self-associates to form a ring-shaped homo-oligomer complex, the prepore, which has been shown to be heptameric [Milne 1994].

Recently, Kintzer and colleagues have demonstrated the existence of a small population (25-30% *in vitro*, 20-30% in CHO expressing CMG2) of octameric oligomers which assemble in the presence of ligand (such as LF, LF_N, EF, EF_N or dimeric soluble receptor domain).

Because each bound ligand molecule effectively occludes two subunits of these holigomers, only three ligand molecules can bind to the heptamer [Mogridge 2002, Young & Collier 2007] and four molecules to the octamer simultaneously [Kintzer 2009].

A 4.5 Å structure and a later 3.6 Å structure of the water-soluble PA_{63} heptamer [Petosa 1997, Lacy 2004] shows a hollow ring with the subunits packed like pie wedges. There are no major conformational changes from the structure of monomeric PA_{83}. Domains 1' and 2 are lumen-facing, and domains 3 and 4 are on the outside. A conserved phenylalanine (Phe427) in a mobile, solvent-exposed loop in the lumen plays a major role in protein translocation through the pore [Krantz 2005].

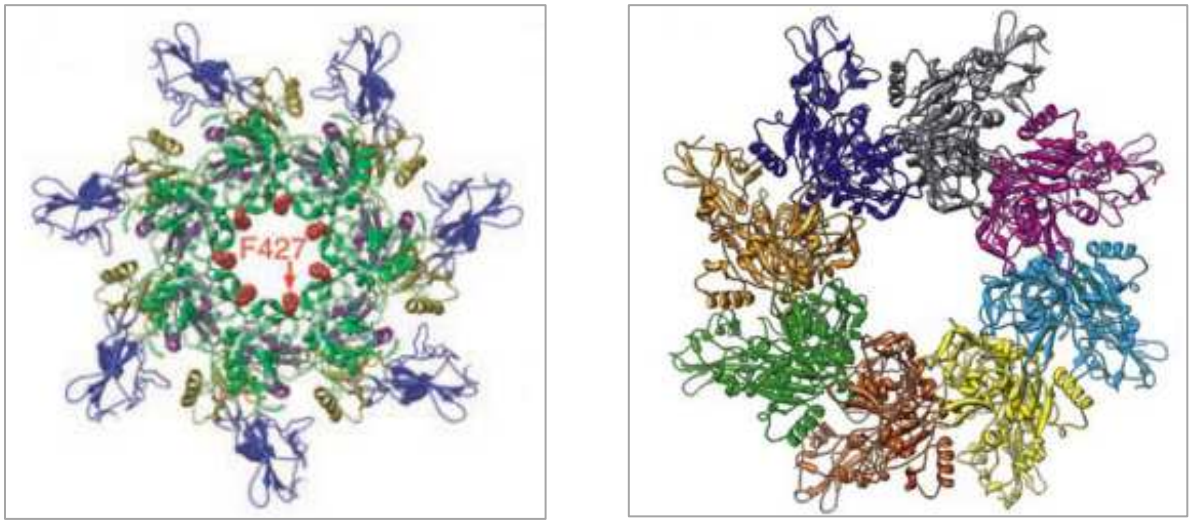

Fig. 6**: PA prepore.**
In the left panel, a ribbons rendering of the PA_{63} prepore, viewed axially, where domain 4 is proximal. Domains are colored: 1' (magenta), 2 (green), 3 (gold), and 4 (blue). F427 (red, space filling) is modeled into the structure [from Krantz 2005]. In the right panel, axial view of the $PA^{\Delta MIL}$ (PA mutant with no possible hydrophobic interactions between domain 4 and the neighboring membrane insertion loop). Monomer subunit chains are colored uniquely [from Kintzer 2009].

Two other functionally important features of the prepore are a large, flat hydrophobic surface exposed on domain 1' at the top of the structure, which serves as binding site for LF and EF, and

the 2β2–2β3 loop of domain 2, which is involved in pore formation. Recently, Kintzer *et al.* has solved the 3.2 Å octamer structure of $PA^{\Delta MIL}$, a mutant which disrupted the hydrophobic interface between two PA subunits at the interface of domain 4 and the neighboring membrane insertion loop (MIL) in the adjacent PA subunit. The octamer is not a regular octagon, but it is rather composed of four PA dimer pairs arranged in a square planar symmetry.

The heptameric and octameric channels have similar translocase activity but octameric oligomers are more stable under physiological pH and temperature. Thus, it is possible that these two oligomerization states have different functions during anthrax pathogenesis.

2.4.3 Internalization of the toxin-receptor complex by endocytosis

Besides proteolytic activation, another factor affecting anthrax toxin action is acidic pH within an intracellular, membrane-bound compartment. The dependence on acidic pH is reminiscent of that found in certain other bacterial toxins, such as diphtheria, botulinum, and tetanus toxins, which are endocytosed and undergo translocation across endosomal membranes in response to acidic intravesicular conditions (Sandvig and Olsnes, 1980).

Thus, since recently our knowledge on endocytosis mechanisms has enormously grown an overview of this basic cellular process is needed.

2.4.3.1 Endocytosis: an overview

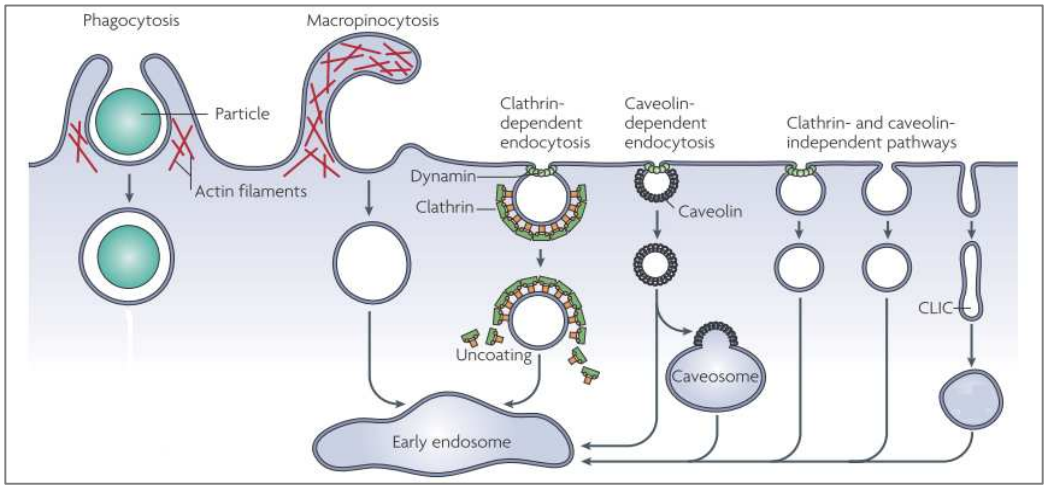

Fig. 7: **Multiple portals of entry into the mammalian cells.** The endocytic pathway differ with regard to the size of endocytic vesicles, the nature of cargo and the mechanism of vesicle formaton. Modified from Mayor & Pagano 2007.

Endocytosis is a basic cellular process that is used by cells to internalize plasma membrane lipids, integral proteins and extracellular fluid. It does not simply negatively regulate interactions with

external world but it also controls other processes as mitosis, antigen presentation, cell migration, many intracellular signalling cascades.

In addition, pathogens often exploit endocytic routes to enter host cells. Endocytosis occurs by multiple mechanisms that can be divided in two categories: clathrin-dependent and clathrin-independent (Fig. 7).

Clathrin-dependent endocytosis

Clathrin-dependent endocytosis is the most well-characterized mechanism for the entry of molecules (such as receptors, nutrients, growth factor, antigens and pathogens) into cells.

The central defining feature of this process is the recruitment of soluble clathrin molecules from the cytoplasm to the plasma membrane. Clathrin unit, called triskelion (a three-legged structures consisting of three heavy and three light chains), assembles into a polygonal lattice at the plasma membrane to form clathrin-coated pits (CCPs), a complex structure, that concentrate surface proteins for internalization (Fig. 8 , stage 1). Endocytic adaptors first specify the location of clathrin assembly on the plasma membrane interacting with phospholipids such as phosphatidylinositol(4,5)bisphospate (PI-4,5-P_2), which is the prevalent phosphoinositide specie present on the plasma membrane, and then they bind to clathrin directly to initiate internalization process. In addition, adaptors also recognize cargo proteins interacting with amino acid sequences, such as the YXXϕ (where X represent a non-specific amino acid and ϕ a bulky hydrophobic residue) and [DE]xxxLL motifs, either structural features or added ubiquitin molecules in the cytosolic tail of the membrane protein to mediate their endocytosis.

Coated pits bud and pinch off from the membrane (Fig. 8, stage 2 and 3) in a dynamin-dependent manner and give rise to clathrin-coated vesicles (CCVs). In addition to those used in endocytosis, CCVs can also bud from various intracellular compartments with the use of different adaptor proteins [Doherty & McMahon 2009]. Deeply invaginated coated pits are characterized by the presence of a neck structure that connects the forming vesicle to the plasma membrane and specifies the site of fission. The neck has to be constricted sufficiently to bring the opposing membrane together in order to cause fusion within the neck and the formation of a free CCVs from the plasma membrane [Mousavi 2004]. The fission machinery includes different proteins including dynamin, a large GTPase, that has a central role because it self-assembles into helical collar around the neck of the invaginated CCPs and regulates the actin filament assembly at sites

of endocytosis which can provide force to induce the scission of forming vesicles. CCVs are uncoated after endocytosis (Fig. 8, stage 4) and then undergo further trafficking within the cell before the appropriate delivery through fusion with a destination intracellular compartment.

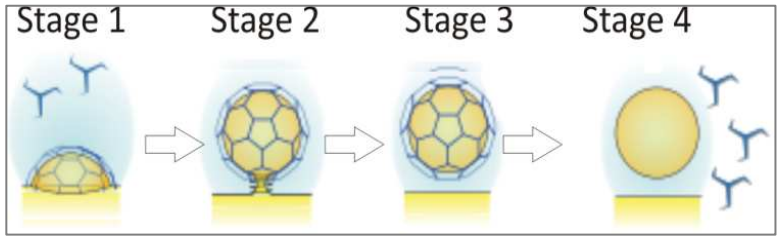

Fig. 8**: Schematic diagram of clathrin recruitment and coated-vesicle formation.** Clathrin-dependent endocytosis begin with nucleation of clathrin-coated structure (stage 1), then continue with invagination of CCPs (stage 2), scission and uncoating (stage 3 and 4, respectively) of CCVs [modified from Doherty & McMahon 2009].

Clathrin-independent endocytosis

Many years ago, it was demonstrated that the plant toxin ricin, which binds all over the cell surface (since it binds to both glycoproteins and glycolipids with terminal galactose) provided some of the early evidence for clathrin-independent (CI) endocytosis [Moya 1985, Sandvig 1987].

In fact, for many years clathrin-dependent endocytosis was believed be the only mechanism accounting for the uptake from the cell surface [Sandvig & van Deurs 2005]. The recent development of new techniques has provided new insights into CI internalization pathways. Clathrin-independent routes are sensitive to cholesterol depletion and to inhibitors of actin polymerization but they differ in their mechanism and kinetics of formation and molecular machinery involved. Little is known about how cargo is selected for the different clathrin-independent pathways. In contrast to clathrin-dependent endocytosis, in which specific adaptor molecules that recruit cargo molecules to coated pits have been identified, no such well defined adaptors for CI have been found. One potential mechanism that has been considered is sorting based on the association of cargo with membrane microdomains.

I will begin this simplified overview with a brief discussion of phagocytosis (known as ‘cell eating’) and macropinocytosis (called also ‘cell drinking’) that belong to a separate class of CI endocytic processes involving internalization of large patches of the membrane.

Phagocytosis

Phagocytosis is an essential process by which specialized mammalian cells (including macrophages, monocytes and neutrophils) internalize pathogens, apoptotic cells and other foreign particles that are >0.5 μm in diameter.

It often occurs by a zippering mechanism, in which actin-driven protrusions of the plasma membrane engulf a cargo by repeated receptor-ligand interactions. It is an active and highly regulated process that involves specific cell-surface receptors and signalling cascades. For example, Fc receptors on macrophages recognize and are activated by antibodies bound to surface antigens on bacteria. A signalling cascade (involving activation of Cdc42 and Rac) triggers actin assembly and the formation of cup-like membrane extension that zipper up around the antibody-coated pathogen and engulf it (Fig. 9).

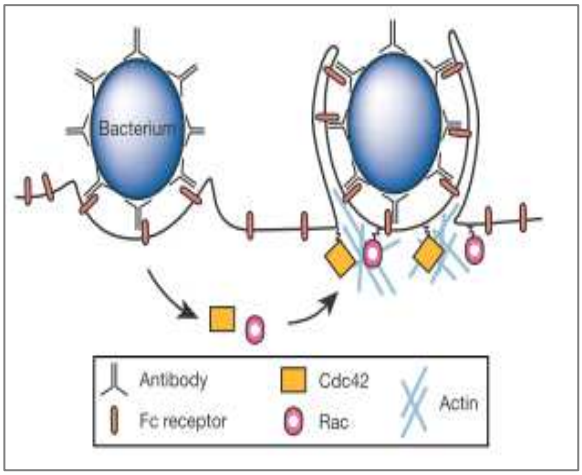

Fig. 9 **: Phagocytosis.**
Fc receptors on the surface of macrophages activate a signalling cascade that triggers actin rearrangements, protrusion of the membrane around the bacterium, and its engulfment into a phagosome. [Conner&Schmid2003]

These signals also activate the cell's inflammatory response, so once the bacteria are inside vesicles, they are destroyed by bactericidal weapons (for example acid hydrolase, acids, free oxygen radicals) and the residual peptides are then presented on the surface of macrophages to elicit immune response.

Phagocytosis triggers the activation of many signalling pathways that lead to the reorganization of actin cytoskeleton and the formation of a sealed intracellular compartment: the phagosome. Now there is evidences that the phagosome "matures" by multiple transient interactions with endosomal compartments, including lysosomes, to form a hybrid organelle termed phagolysosome where phagocytosed particles are degraded.

Macropinocytosis

It is used to internalize large amount of fluid and grow factors. Unlike phagocytosis, the membrane protrusions do not 'zipper-up' along a particle, but they collapse onto and fuse with plasma membrane to generate large vesicles, called micropinosomes. Actin ruffles caused by actin rearrangement are a fundamental part of this process of internalization that has many functions such as down-regulation of activated signalling molecules, regulation of cell migration and immune surveillance. Finally, some bacteria inject toxins into cells that trigger the process and ensure their its own uptake into micropinosomes, which are suitable to their replication.

Caveolin dependent endocytosis

Caveolae are defined as plasma membrane invaginations with a diameter of 60-80 nm. These pits have a common uncoated flask shape. They are formed by the polymerization of caveolins (Cav1 and Cav2 in non-muscle cells and Cav3 in muscle cells) that associate with cholesterol-rich lipid rafts domains. Caveolins show an unusual topology with N and C termini in the cytoplasm and a long hairpin intramembrane domain. An highly conserved region of these proteins might have a specific role in cholesterol interactions (Fig. 10) through conserved basic (+) and bulky hydrophobic residues (as shown in Fig. 10 as red circles). The C-terminal domain, which is close to the intramembrane domain, is modified by palmitoyl groups that insert into the lipid bilayer. Cholesterol depletion or sequestration disrupts the structure of caveolae and inhibits the internalization of several cargo molecules. Caveolae at the cell surface forms a stable functional unit, that is also maintained upon endocytosis. Budded caveolae, known as endocytic caveolar carrier, can fuse with the caveosome in a Rab5-independent manner or with the early endosomes in a Rab5-dependent manner or can fuse back to the plasma membrane without the involvement of any endosomal intermediate. The caveosome is a distinct endosomal compartment with specific properties: it is negative for endosomal markers typical of clathrin-dependent endocytosis, such as early endosome antigen-1 (EEA1) and internalized transferrin; furthermore, it has a neutral lumenal pH, which is in contrast to early endosomes, late endosomes and lysosomes, which have an acidic pH.

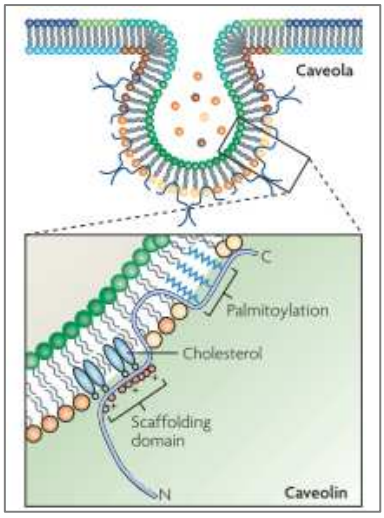

Fig. 10**: Caveolin insertion into the caveolar membrane.**
From Parton & Simons, 2007.

Caveolae remain for long periods at the plasma membrane, but their internalization can be stimulated by various agents such as small viruses, i.e. Simian virus 40 (SV40) and polyoma virus, and large pathogens (*Pseudomonas aeruginosa, Porphyromonas gingivalis*, etc). The bacteria, that are larger than a single caveola, do not use caveolae as such, but they seem to be internalized in caveola-rich areas of the cell. It is known that these invaginations might exist as single pits or can form a cluster of caveolae with non-caveolar membrane between the pits. Clathrin-coated pits can even be observed in continuity with caveolae within these clusters. So, pathogens can exploit

these invaginations as portal to facilitate their entry into host cell and avoid their degradation in lysosomes.

Caveolae endocytosis shares many common features with clathrin-mediated pathway, including the same dynamic requirement of molecular machinery in the fission process with a crucial role for dynamin that sever vesicles from plasma membrane.

The study of caveolar endocytosis is complicated by the possibility that the same endocytic cargo may be internalized by different mechanisms in different cell types or may switch pathway in a single cell type under different conditions.

Clathrin- and caveolin-independent endocytosis

This pathway is insensitive to inhibitors of clathrin-mediated endocytosis and it may represent a more primordial endocytic pathway [Kirkham&Parton2005]. It was initially identified in Hela cells, in which the expression of a mutant dynamin-1 blocked receptor-mediated endocytosis but apparently increased fluid-phase uptake via a CI pathway.

Clathrin- and caveolin-independent endocytosis seems to be the main route for the uptake of CT-B as well as for the *Helicobacter pylori* vacuolating toxin (VacA) and the plant protein ricin.

The primary carriers, that bud from the cell surface, are called clathrin-independent carriers (CLICs), they have long and relatively wide tubular surface invaginations, in contrast to the small spherical vesicles that are characteristic of the clathrin and caveolar pathways. These carriers also represent the main mechanism of fluid-phase internalization in many cell types, and are mainly devoid of cargo from the clathrin-mediated pathway [Mayor&Pagano2007].

This route of internalization may be dynamin-independent, as described above, or dynamin-dependent as rit has been ecently discovered for IL-2 receptor β chain and γc cytokine receptor.

Internalized cargo trafficking into mammalian cells

Typically endocytosed molecules are delivered to a sorting station, early endosomes (EEs), where two distinct circuits are well separated, both topologically and functionally, to ensure that proteins that need to be recycled to the cell surface remain separate from those that are destined to degradation. After leaving EEs, recycling molecules are found in distinct tubular structures that correspond to recycling endosomes and trafficking of cargoes, destined to degradation pathway,

involves multivesicular (MVEs) and late endosomes (LEs), before lysosomes, their destination compartment.

It is important to note that it is difficult to draw the line between early organelles, multivesicular and late endosomes and the boundary between late compartments and lysosomes is even more elusive; for this reason, to date it is not possible to find in literature a unique nomenclature of these organelles; in many cases, MVEs are considered a form of late endosomes and the latter of lysosomes. Now a brief description of the endocytic organelles will be given.

Early endosomes and recycling endosomes

In the classical view, newly formed vesicles, following fission from the plasma membrane, fuse with early organelles. The early endosomes are well-defined but dynamic compartments (lumenal pH 6.0-6.5) with high homotypic fusion capacity that function as the first sorting station in the endocytic pathway [Gruenberg 2001]. They display a highly complex organization (Fig. 11) that consists in cisternal regions with occasional intralumenal vesicles (ILVs), which arise from invagination and fission of EEs membrane and therefore contain cytosol, and an array of tubular subdomains, including endosome to *trans*-Golgi network (TGN) transport carriers and the tubular sorting endosome or tubular endosomal network, where membrane cargoes destined for a range of other compartments are sorted [Cullen 2008]. For example, a recent study proposes that transferrin receptor (Tnf-R), epidermal growth factor receptor (EGFR) and cation-independent mannose-6-phosphate receptor (CI-M6PR) can all pass through the same early endosome but they exit through distinct compartments [Mari 2008]. Tnf-R is recycled back to the plasma membrane, either directly, or more slowly via a tubular compartment, that presumably represents an intermediate of the recycling pathway; EGFR is retained within the limiting membrane of the EE until fusion with or maturation into multivesicular endosomes; CI-M6PR is sorted for retrieval back to the TGN. 'Geometric sorting', facilitated by the different membrane area/volume ratio of vacuolar and tubular domains, may account to some extent for separation between recycling and degradation pathways [Woodman & Futter 2008].

Recently, growing evidence indicates that EEs are a morphologically and functionally heterogeneous population whose complexity is enhanced by the presence of biochemically distinct membrane subdomains within individual organelles (Fig. 11). Small GTPases and phosphoinositides are considered as endosomal markers for their restricted distribution.

In particular, the small GTPase Rab5, along with 3-phosphorylated phosphoinositides, coordinates the assembly of effector complexes important for the function and maturation of early endosomal compartments. Efficient recruitment of some effectors is based on its simultaneous binding to Rab5 and phoshatidylinositol 3-phoshate (PI3P); for example, early endosomal antigen 1 (EEA1) interacts specifically with PI3P through a conserved FYVE motif and its distribution is restrict to EEs.

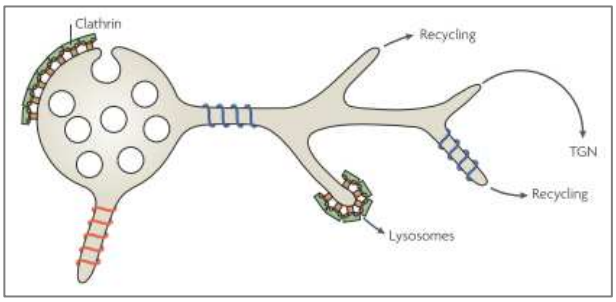

Fig. 11 **: Early endosome complex organization.**
The endocytic network comprises a series of interconnected membranous organelles, many of which contain elaborate arrays of tubular subdomains through which cargo sorting occurs [modified from Cullen2008].

However, endosomal proteins and lipids that help to define organelle identity are not only found in a single compartment. For example, Rab5 is also associated with plasma membrane and CCVs and PI(3)P is present on EEs, multivesicular endosomes and Golgi complex.

As mentioned before, in the early compartments some bound ligands dissociate from their receptors in the acidic lumen allowing recycling of molecules destined to be reused at the cell surface in distinct structures that correspond to recycling endosomes. These organelles are less acidic than EEs and Rab4 and Rab11, two small GTPases involved in recycling, show a distinct, but partially overlapping, distribution *in vivo* with early endosomal Rab5, which probably corresponds to different effector platforms. These membrane domains are dynamic but do not significantly intermix over time and their distribution does not change at different stages of recycling [Sönnichsen 2000].

Multivesicular endosomes

Multivesicular endosomes, often referred as multivesicular bodies (MVBs), are large organelles, typically spherical with a diameter of ~400-500 nm which contain a characteristic accumulation of vesicles in their lumen. Indeed, all endosomes along the degradation pathway contain multivesicular elements, including early and late endosomes, MVEs represent the transport intermediates between EEs and LEs along the degradation pathway. Whether these organelles change in composition as they undergo a maturation process, or whether they mediate the

transport between two stable compartments, is subject of much debate but, either way, once formed and after the complete removal of recycling proteins, MVEs move from the cell periphery to cell centre, in a microtubule-dependent fashion, towards late endosomes, with which eventually fuse.

Cargoes destined for degradation are sorted into ILVs of endosomes through the concerted action of the conserved Class E *VPS* machinery, first identified from studies of vacuolar protein sorting (*vps*) mutants in the yeast *Saccharomyces cerevisiae.* Most of Class E *VPS* proteins are found within the endosomal-sorting complex required for transport (ESCRT) that has a role in endosomal membrane deformation and ILVs formation, although accumulating data suggest that, at least in mammalian cells, other machineries also participate in this process [Woodman & Futter2008]. ESCRT machinery consists of four complexes, ESCRT-0, -I, -II, -III, plus other accessory components. ESCRT-0 complex consists of the subunits Hrs and STAM; they both contain an ubiquitin-interacting motif and a clathrin-binding domains but Hrs can also bind PI3P through its FYVE zinc-finger domain [Gruenberg 2004]. Thus, PI3P binding recruits Hrs, and thereby ESCRT-0, to endosomal membrane; even if another subunit of ESCRT-II can bind 3-phosphorylated phosphoinositides, it is tempting to speculate that ESCRT-0 is the first recruited to endosome membranes by PI3P binding [Raiborg 2009] and is fundamental for ESCRT complexes (ESCRTs) functions because they are recruited and work sequentially (in the order that corresponds to their number).

It is worth noting that the 'inverse' budding (compared with clathrin-coated vesicles budding from the plasma membrane) requires that vesicles can bud into the lumen of an endosome and needs a distinct machinery specialized for severing vesicles of membrane filled with cytosol that is recruited from inside the membrane stalks; accumulating evidence indicates that ESCRT-III represents this membrane fission apparatus.

Late endosomes

Late endosomal elements (lumenal pH 5.2-5.5) are highly pleiomorphic, with a complex organization, containing cisternal, tubular and vesicular regions with numerous membrane invaginations. They function as an important sorting station in the endocytic pathway, for example, the CI-M6PR cycles, at least in part, from late endosomes back to the TGN, whereas class

II major histocompatibility complex molecules are efficiently transported from LEs to plasma membrane in maturing dendritic cells.

The mechanism by which these organelles (and MVEs) are formed from early endosomes has been subject of much debate with two models emerging: a maturation model and a vesicular transport model in which endocytic carrier vesicles, formed from EEs, are required for cargo transport to late compartments. Up to now, recent studies [Rink 2005] have demonstrated that both models are partially correct; live imaging experiments show that large vesicles (400-800 nm diameter) arise from early endosomes and undergo a conversion in which they lose the small GTPase Rab5 and recruit Rab7, classical marker of the late organelles.

Typically late endosomes, in their limiting membrane, contain high amounts of so called lysosomal glycoproteins, in particular lysosomal-associated membrane protein-1 (LAMP1) and LAMP2, even though they can occasionally be detected within internal membranes, which are very abundant in both LEs and lysosomes. In addition, internal membranes accumulate large amounts of lysobisphosphatidic acid (LBPA) that cannot be detected on the cytoplasmic surface of the limiting bilayer or in other organelles; for this reason, it is considered a specific late endosomal marker.

LBPA accounts for ~15% of total late endosomal phospholipids [Kobayashi 1998], it is an inverted cone-shaped lipid, a structure that prefers curved membranes; thus, it promotes both the multivesicular morphology characteristic of these organelles, inducing membrane invagination, and 'back-fusion' of lumenal membranes with the perimeter of LEs, which is typical of endosomes that have a non-degradative function. It is important to note that not all late compartments are functionally equivalent, for example EGF and EGFR traffic through a subpopulation of endosomes that are morphologically identical to other late organelles but lacking of LBPA and containing annexin I [White 2006]. There is evidence that in mammalian cells LBPA is enriched in a subset of late endosomal membranes [Kobayashi 2002] that are distinct from those where ubiquitinated proteins, destined to degradation, are sorted [Russell 2006]. These data might resolve the confusion derived from studies indicating that late endosomal lumenal membranes are involved in both the degradation and recycling of proteins and lipids, if the membranes are located in different ILVs subpopulations.

Lysosomes

Lysosomes, the terminal degradative compartment of endocytic pathway, are membrane-bound organelles with an acidic (pH 4.6-5.0) lumenal environment, due to the presence of proton-pumping vacuolar ATPases, and they often present electron-dense deposits and membrane whorls, structures that have the appearance of being multi-lamellar or arranged in spirals, when observed in cross-section [Luzio 2007].

It is well established that endocytosed macromolecules are delivered to lysosomes after their sequential passage through late compartments, however, the mechanism of transfer of endocytic cargo remained controversial as many theories have been proposed.

The maturation model (Fig. 12) proposes that LEs mature into lysosomes by the gradual addition of lysosomal and removal of late endosome components but it cannot explain how lysosomes undergo content mixing with late endosomes; the vesicular model (Fig. 12) suggests that vesicles carry cargoes from the late compartments into lysosomes. Recently, as supposed by the kiss-and-run model (Fig. 12), live-cell microscopy experiments [Bright2005]

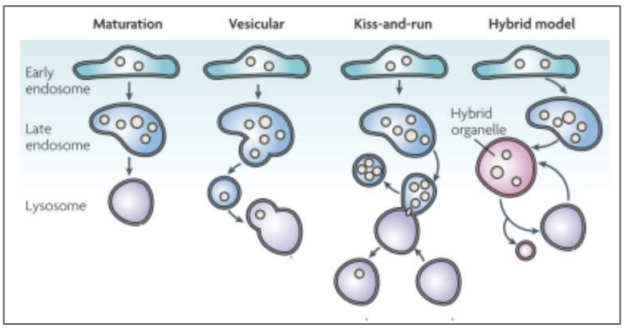

Fig. 12: **Delivery of endocytosed cargoes to lysosomes.**
Different models proposed to transfer endocytosed material from late endosomes to lysosomes (modified from [Luzio 2007]).

have shown that a continuous cycle of transient contacts (“kisses”) followed by dissociations (“run”) between endosomes and lysosomes which contribute to mix the contents but vesicle-mediate trafficking was not observed. Moreover, these compartments either transiently fuse or undergo permanent fusion, creating hybrid organelles in which the cargo molecules are degraded, as proposed by the hybrid model (Fig. 12). In this case, lysosomes are then reformed by the selective retrieval of membrane, export of digested products and recondensation of lysosome contempt for further rounds of fusion. It has been recognized that “kiss-and run” and “hybrid organelle” models are not mutually exclusive. Although the essential features of lysosomes fusion with late compartments have been established, the regulation of this processes is far from being clear.

To degrade endocytosed molecules, lysosomes contain acid hydrolases; now, considerable information is available concerning how these newly synthesized enzymes are delivered from TGN to degradative compartments into mammalian cells. Many acid hydrolases are tagged with mannose-6-phosphate in the *cis*-Golgi, subsequently bind to M6PRs in the TGN. They are first delivered to endosomes, where they dissociate from the receptors as a result of acidic lumenal pH; so, the receptors can recycle back to the TGN and the hydrolases reach lysosomes. For this reason, a criterion to distinguish lysosomes from endosomes is the lack of mannose-6-phosphate receptors. Unlike soluble hydrolases, newly synthesized lysosomal proteins do not require their binding to M6PRs but use a common delivery pathway from late endosomes. Moreover, in proximal kidney tubule cells the enzyme cathepsin B is secreted as pro-cathepsin B that binds the cell surface receptor megalin, the newly formed complex is then internalized by clathrin-mediated endocytosis and delivered to lysosomes [Pryor 2009].

It is important to note that cellular entry of many pathogens, which need to reach the cytoplasm or an intracellular compartment of a target cell to survive and replicate, requires the use of endocytic and phagocytic pathways, which terminate in fusion with lysosomes. Therefore, survival of the microorganism involves preventing or delay phagolysosomes biogenesis (as in *Escherichia coli* K1 or *Mycobacterium tubercolosis*, respectively), escaping into the cytosol by degrading the phagosomal membrane (as in *Listeria monocytogenes* that secrete a pore-forming toxin) or surviving in the harsh environment of lysosome itself, as in the case of *Leishmania* species.

2.4.3.2 Anthrax toxins endocytosis

The current model of *B. anthracis* toxin cell entry (Fig. 13) is a much debated question that point out the differences between the anthrax toxin and other endocytosed toxins [Puhar & Montecucco 2007]. According to the recent literature, *B. anthracis* protective antigen, released as soluble 83 KDa monomer, associates with its receptors on cell surface. Recently, the low-density lipoprotein receptor-related protein 6 (LRP6) was reported, using a genome-wide antisense RNA screening approach, to act as an essential co-receptor in M2182 prostate carcinoma cells, treated with PA and FP59 but several other lines of evidence in support the idea that LRP6 is an accessory protein to toxin internalization [Wei 2006]. For example, macrophages were also protected from PA and LF when a specific short interfering (siRNA) corresponding to antisense strand of *lrp6* was

expressed. Furthermore, it was also observed that overexpression and silencing of the toxin receptors leading to the post-translational down-regulation of LRP6 into cells [Abrami 2008].

By contrast, it was found that $LRP6^{+/-}$ and $LRP5^{-/-}$ mice were just as susceptible to killing after LeTx injection as wild-type mice; in addition, mouse embryo fibroblasts that were isolated by $LRP6^{-/-}$ or $LRP5^{-/-}$ were just susceptible to intoxication by PA and FP59, and to MEK1 cleavage by LF and PA, as those isolated from wild-type mice [Young 2007]. In addition, siRNA-mediated knockdown of LRP6 and/or LRP5 levels has not impact on the kinetics of anthrax toxin entry into human Hela cells [Rayan & Young 2008]. These authors suggest that LRP6 might function in either a human-specific or cell type specific manner. Whether LRP6 affects endocytosis of the toxin however remains controversial and it is necessary to further investigate this question because anthrax toxin cell entry is an essential step for host cells intoxication.

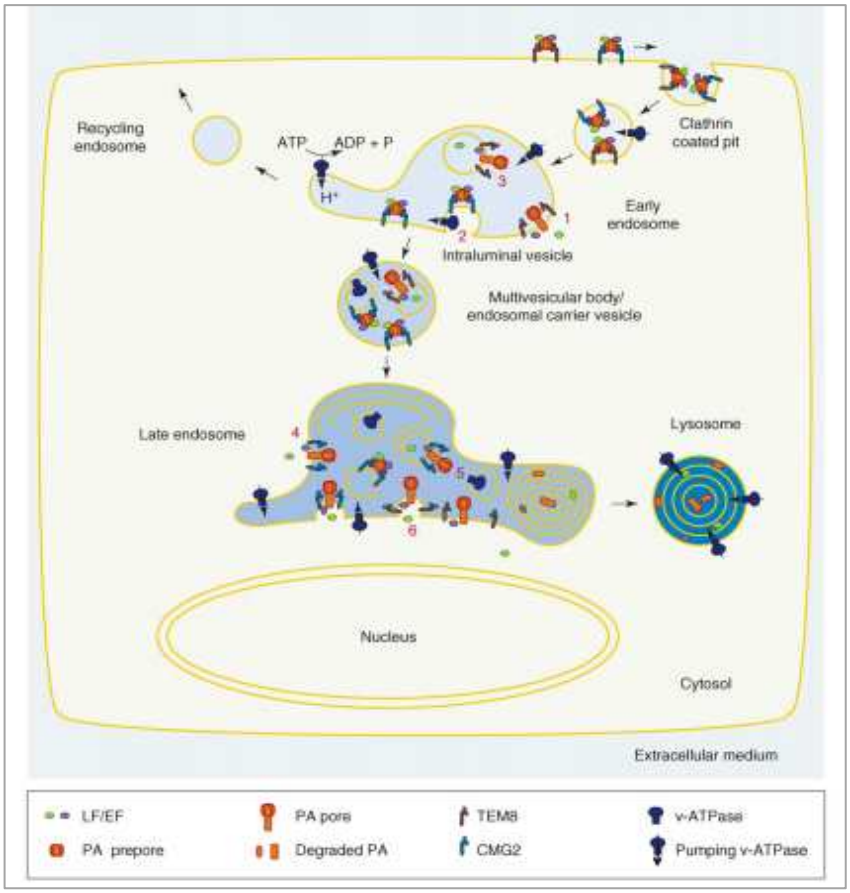

Fig. 13: **Cell entry and trafficking of anthrax toxins in the endocytic pathway.**
PA associates with either TEM8 or CMG2 on the cell surface, and subsequently binds EF and LF. The toxin–receptor complexes are endocytosed. The moderate acidity of the early endosomal lumen is sufficient to induce detachment of PA from TEM8 and formation of pores in the limiting membrane of EEs (1). There is evidence that toxin-receptor complexes end up in ILVs which form by invagination of the EE limiting membrane. This could lead to translocation of EF and LF into ILVs (2, 3). The ILVs toxins or toxin–CMG2 complexes enter the increasingly acidic intermediate compartment ECVs/MVBs and finally conveyed to the more acidic LEs. The low pH of LEs induces PA to form pores in the limiting (4) and internal (5) membranes of LEs, allowing the passage of EF and LF into the cytosol or eventually into ILVs, respectively. The low LE pH allows the back-fusion of ILVs with the limiting membrane of the organelle (6). Modified from [Puhar & Montecucco 2007].

After the binding to the cell surface, the N-terminal portion of PA is removed and the remaining PA_{63} protein forms homooligomer which binds the enzymatic subunits. Formation of this complex induces its entry into lipid rafts [Abrami 2003] and ubiquitination of the cytosolic domain of the receptor [Abrami 2006], which in turn triggers internalization of the complex by endocytosis.

Receptor-mediated endocytosis of many bacterial protein toxins ensures their passage through an acidified endosomal compartment. In addition to anthrax toxin, diphtheria toxin and the botulinum neurotoxins all require exposure to a low-pH environment for the delivery of their respective catalytic domains to the cytosol.

Following endosomal acidification, the complex is thought to dissociate from the receptors and inserts into the lipid bilayer forming a transmembrane ion channel (for further details, see section of *Translocation*). The low-pH conditions of the endosome can be conceived to facilitate unfolding of the catalytic subunits as a prelude to their entry into the PA_{63} pore, a concept commensurate with the estimated size of the PA_{63} channel and with the fact that at lower pH values predominate a molten globular state, a compact, partially folded state observed under mildly denaturing conditions in which much of the original secondary structure is retained, which facilitates their translocation through the PA channel [Young and Collier 2007].

Up to this point, anthrax toxin cell entry fits the general scheme of cytosolic delivery of bacterial toxin exploiting the endocytic route but it has unique features. The toxin-receptor complex is located within EEs *in trans* with respect to the cytosol (Fig. 13) but, due to the fact that PA has different affinities for its receptors [Rainey 2005], the catalytic subunits can translocate into the cytosol at different stages of the endocytic pathway. The available data suggest that LF [Abrami 2003] and EF [Dal Molin 2006] reach the cytosol mainly from late endosomal compartments but these studies need further investigations.

Endocytosed toxins are generally thought to translocate across the endosomal membrane directly to the cytosol but, a recent report [Abrami 2004] proposes that LF is first translocated into intralumenal vesicles and then delivered to the cytosol, by back-fusion of ILVs with the limiting membrane of LEs (Fig. 13), as recently proposed for vesicular stomatitis virus [Le Blanc 2005].

These considerations call for further analysis with particular attention to the receptor type expressed on target cells, endocytic trafficking and cytosolic localization after translocation.

2.4.4 Translocation

Up to now, the efficiency of translocation of EF and LF from the endosome is not known. An electrophysiological system for studying translocation across planar phospholipid bilayers involving only toxin proteins has yielded invaluable data on the process [Krantz 2005; Zhang 2004]. An elegant study demonstrated that deleting more than about 20 residues from the N-terminus of LF_N ablated the ability of this protein to block conductance and strongly inhibited its translocation across the plasma membrane of CHO-K1 cells in response to low pH [Zhang 2004]. These results strongly suggest that translocation is initiated by entry of the N-terminus into the pore and that translocation proceeds in an N- to C-terminal direction. There is evidence that entry of the N-terminus of LF_N into the pore depends primarily on its having a net positive charge. The notion that positive charge is key to initiating translocation through the PA_{63} pore is supported by the finding that fusing a His_6 tag to the N-terminus of N-terminally truncated forms of LF_N [Zhang 2004] or of LF [Neumeyer 2006] increased the ability to undergo translocation across the $(PA_{63})_7$ transmembrane channel.

In addition, a structure formed by the seven (or eight) Phe427 side chains within the PA_{63} pore, the Phe clamp, creates a constriction in the pore lumen that may be viewed as an active site, crucial for protein translocation, an environment that reduce the energy penalty of exposing hydrophobic side to the solvent in the unfolding molten globular protein chains. Evidence from electron paramagnetic resonance spectroscopy (EPR) measurements suggested that these residues moved into close proximity (<10 Å) during prepore-to-pore conversion; thus, the Phe clamp may function primarily to form a seal around the translocating polypeptide, blocking the passage of ions and preserving the proton gradient across the membrane as a potential energy source for driving translocation; and to assist EF and LF through their passage across the pore [Krantz 2005, Krantz 2006, Melnyk 2006, Collier 2009].

A further area to be investigated is the possible involvement of chaperones in the transmembrane translocation of EF and LF. The DT catalytic subunit seems to be assisted by two cytosolic chaperones in EEs membrane crossing and cytosolic refolding [Ratts 2003]. DT was previously assumed to refold by itself from an extended conformation acquired at low pH. EF and LF are considerably larger than DT (21 kDa) and are multidomain proteins, hence the requirement of cytosolic chaperones for EF and LF seems even more stringent than for DT. Recently, it was has been demonstrated that the addition of cytosolic extracts to partially purified early endosomal

vesicles, preloaded with PA_{63} and LF_N-DTA, greatly stimulates LF_N-DTA translocation across the endosomal membrane *in vitro* and release into the external medium. The COPI coatomer complex or COPI-associated proteins are suggested as a key component of a cytosolic translocation complex for LF similar to those required for the translocation of the diphtheria toxin catalytic domain [Tamayo 2008]. As mentioned, ILVs arise from invagination and fission of EEs membranes and therefore contain cytosol. As a consequence, participation of cytosolic chaperones is consistent with anthrax toxin translocation into ILVs. Also, the possible involvement of chaperones is not inconsistent with the documented permeation of the enzymatic subunits through PA pores in artificial lipid bilayers because chaperones could be needed to increase the efficiency of the process.

2.5 Anthrax toxin effects

2.5.1 MAPK kinase-specific metalloprotease activity of lethal factor and its cellular and systemic effects

LF is an endopeptidase with highly restricted specificity. The only known protein substrates are mitogen-activated protein kinase kinases (MAPKKs), except MAPKK-5, which are cleaved within their N-terminus [Duesbery 1998; Vitale 1998, 2000]. It is important to note that MAPKK-4 and -7 are cleaved at two similar and close peptide bonds, whilst isoforms 1, 2 and 6 are cleaved at single sites. It is known that the N-terminus of MAPKKs is essential for the formation of a productive complex with its phosphorylation substrate MAPKs (Erk1/2, Jnk and p38), and therefore the cytosolic LF activity disrupts major signalling pathways implicated in a variety of responses, including immune response.

The alignment of the N-termini of the cleaved MAPKK isoforms defines a consensus motif for the cleavage site consisting of one to four positively charged residues located within the positions P7, P6, P5, P4 and hydrophobic residues at P2 and P1' [Vitale 2000; Tonello 2002]. Based on the MAPKK cleavage consensus, several artificial peptide substrates were developed to study enzyme kinetics, such as peptide substrates based on the consensus motif with C-terminal chromogenic (p-nitrophenylanilide) or fluorogenic (amidocoumarin) groups, which change spectroscopic characteristics following LF cleavage [Tonello 2002, 2003]; a fluorescence resonance energy

transfer (FRET) based substrate with a N-terminal fluorophore and a C-terminal quenching group [Cummings 2002]. Recently, other peptide substrates efficiently cleaved by LF were selected from a phage display peptide library [Zakharova 2009]. Altogether, these LF peptide substrate studies lead to the conclusion that the most important determinants for a rapid hydrolysis by LF are an upstream basic cluster followed by an hydrophobic amino acid (in P5–P3 positions) and an hydrophobic residue at the P1' position.

LF is an important potential target for small molecule drugs, which may be used in combination with antibiotics, given the limited success of this kind of therapy. Different experimental approaches have been used to develop toxin inhibitors for example receptor decoys that bind the toxin and prevent it binding to the cognate cell-surface receptors [Bradley 2001, Scobie 2003], neutralizing antibody against PA [Maynard 2002] and LF [Zhao 2003], dominant negative inhibitors of PA pore formation [Sellman 2001] or small molecules and polypeptide substrate analogues [Tonello 2002, Turk 2004]. The development of novel therapeutic approaches to counteract toxin activity is promising, however, it is likely that each of these inhibitors will need to be refined to generate antitoxins with therapeutically useful potency.

2.5.2 The adenylyl cyclase activity of anthrax edema factor

EF belongs to a family of bacterial toxins that can specifically elevate the intracellular cAMP level, which is an important second messenger that regulates diverse cellular responses. The biological effects of cAMP are mediated by the binding of cAMP to three families of signal transducers: cAMP-dependent protein kinases, cyclic nucleotide-gated channels and EPAC, the guanine nucleotide exchange factor for Ras GTPase homologs Rap1 and Rap2.

There are two major mechanisms by which bacterial toxins can raise the intracellular cAMP level. The first mechanism is by the action of the bacterial AC toxins, which possess AC activity, such as EF and CyaA of *Bordetella pertussis*. Their AC activities are activated only upon their entrance into host cells and association with the specific cellular proteins that serve as the activator: EF and CyaA share CaM as a common activator. The second mechanism by which intracellular cAMP is increased by bacteria is the ADP-ribosylation of heterotrimeric G proteins by bacterial toxins, resulting in increased catalytic activity of host membrane-bound AC. For example, Cholera toxin from *Vibrio cholera* can ADP-ribosylate G_sa, rendering it constitutively active to stimulate host ACs.

Targeting a different G protein subunit, pertussis toxin from *Bordetella pertussis* ADP-ribosylates G_ia, uncoupling G protein-coupled receptor from inhibiting host ACs.

These differences between AC proteins have permitted to develop small molecular inhibitors which can specifically inhibit the activation of these toxins without affecting host ACs. These inhibitors can be targeted to compete with the binding of ACs to substrate or CaM [Shen 2004]. Such inhibitors (Adefovir, Tenofovir) are widely use as an anti-anthrax treatment to be administered in combination with traditional antibiotics.

2.5.3 Anthrax toxins and the host immune defences

All bacterial pathogens have to deal with the complex barrier opposed by the host immune system. Regardless of the route of entry, *B. anthracis* needs to keep the immune system at bay to achieve effective colonization but it also relies on phagocytes, used as a Trojan horse, to reach the lymph node. There the spores germinate to become vegetative bacteria which, upon release from the phagocytes, multiply and eventually enter the bloodstream [Tournier 2009].

LeTx inhibits the release of pro-inflammatory cytokines and of NO from macrophages and dendritic cell lines [Pellizzari 1999] and their chemotaxis through its enzymatic activity. It blocks also the differentiation of monocytes into macrophages, thereby preventing them from destroying pathogens. Furthermore, LeTx induces a rapid lysis of murine macrophages from some imbred mice. It is worthy to note that different mouse strains display markedly different susceptibility to LeTx dependent cytotoxicity, suggesting that this process is independent of MAPKK cleavage [Friedlander 1986, 1993].

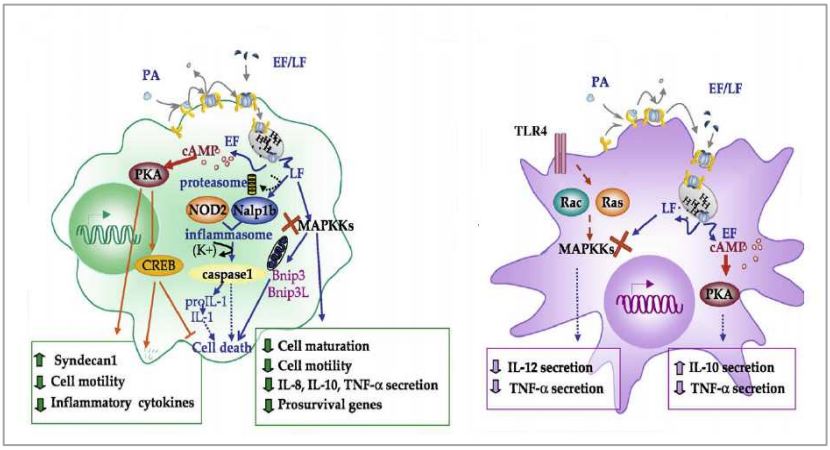

Fig. 14: **Anthrax toxin effects on macrophages and dendritc cells.** In the left panel, LeTx inhibits macrophage activation, expression of pro-inflammatory cytokines and cell motility by disrupting the pathways regulated by MEKs. LeTx also promotes macrophage apoptosis. In the right panel, LeTx and EdTx inhibit expression of TNF-a and modulate expression of cytokines (IL-10, IL-12) implicated in helper T cell differentiation in DCs stimulated with TLR agonists. Modified from Tournier 2009.

The identification of *Nalp1b* (also known as *Nlrp1b*) as the LeTx sensitivity locus (Fig. 14) has highlighted this inflammasome component as potential target of LF [Boyden & Dietrich 2006]. Inflammasome formation involves the recruitment and the activation of caspase-1, which in turn activates the pro-inflammatory cytokines IL1-β and IL-18. Inflammasome-mediated caspase-1 activation is not only involved in the innate immune response leading to cytokine processing and release, but also cell death in response to many stimuli. Besides its effect on MAPKK, LF acts at the crossroads of the mitochondria, the proteasome and the inflammasome pathways (for excellent reviews see Moayeri & Leppla 2009, Tournier 2009). It is not clear yet whether LeTx acts by direct physical interactions with components of these pathways or through indirect consequences of MAPKK cleavage.

EdTx rescues macrophage cells (Fig. 14, right panel) from apoptosis via the downstream activation of protein kinase A (PKA) and CREB [Park 2005]; and it enhances their spontaneous migration but inhibits their chemotaxis [Rossi Paccani 2007].

It was demonstrated a strong inhibitory effect of LeTx on pro-inflammatory cytokine secretion in mouse spleen-derived dendritic cells (DCs) and EdTx has a cumulative effect. Interestingly, immature DCs can be killed by LeTx, while mature cells in lymph nodes are unaffected. Thus, anthrax toxins may finely tune the balance between signals delivered by DCs, inducing terminal differentiation of T cells. Although impairment of DC activation and maturation would be by itself sufficient to prevent the development of the specific and long-lasting response against the pathogen mediated by T and B lymphocytes, *B. anthracis* affects the activation and effector functions of these cells through the combined activities of LeTx and EdTx. Anthrax toxin are potent suppressors of human and mouse T cell activation and proliferation; their inhibitory activity on T cells activation derives from the interference with T cell antigen receptor signaling through their respective enzymatic activities [Rossi Paccani 2009]. Both anthrax toxins have been reported to suppress T cell chemotaxis, this event may prevent initiation of the adaptive immune response but also with migration of effector armed T cells out of the lymph node to peripheral tissues.

2.5.4 Anthrax toxins in vivo studies

Studies with *B. anthracis*-derived LeTx in animal models confirm discoveries made in the 1960s by Smith and colleagues.

It was demonstrated that LeTx induces an atypical vascular collapse in mice and rats without classic hallmarks of endotoxic shock, marked by absence of thrombosis or cytokine involvement but it is still not known how LeTx induces vascular collapse. In contrast, EdTx used at doses that are lethal for mice is associated with hemorrhaging lesions in many organs [Moayeri and Leppla 2009]. It is noteworthy that LeTx-induced vascular shock kills mice with LeTx resistant macrophages as well as macrophage-deficient mice [Moayeri 2004].

An important issue to address is the dose relevance of toxins secreted by the bacterium in infected animals. Recently, a detailed analysis of *in vivo* toxin production levels in anthrax infected rabbits found a 5:1 ratio of LF:EF in most samples [Dal Molin 2008]. This finding confirms what was reported for *in vitro* toxin production (PA:LF:EF, 20:5:1) [Sirard 1994]. Based on the 5:1 ratio, it is likely lethal doses of ET for mice are actually not achieved in infection. However, the pathology associated with lower nonlethal doses of ET which does include nonlethal haemorrhaging in multiple organs and extreme changes in adrenal glands are more likely to be the relevant ET effects in infection [Firoved 2005]. Clearly, further investigation of the timing and levels of toxins produced in early stages of infection will be important.

Chapter III: cAMP imaging of cells treated with pertussis toxin, cholera toxin, and anthrax edema toxin

Biochemical and Biophysical Research Communications 376 (2008) 429–433

Contents lists available at ScienceDirect

Biochemical and Biophysical Research Communications

journal homepage: www.elsevier.com/locate/ybbrc

cAMP imaging of cells treated with pertussis toxin, cholera toxin, and anthrax edema toxin

Federica Dal Molin [a,1], Irene Zornetta [a,1], Andrea Puhar [a,2], Fiorella Tonello [a], Manuela Zaccolo [b], Cesare Montecucco [a,*]

[a] Dipartimento di Scienze Biomediche and Istituto C.N.R. Neuroscienze, Università di Padova, Viale G. Colombo n. 3, 35121 Padova, Italy
[b] Neuroscience and Molecular Pharmacology, Faculty of Biomedical Sciencess, University of Glasgow, University Avenue, G12 8QQ Glasgow, UK

ARTICLE INFO

Article history:
Received 1 September 2008
Available online 13 September 2008

Keywords:
cAMP imaging
Cholera toxin
Pertussis toxin
Edema toxin
Adenylate cyclase

ABSTRACT

The enzymatic activity of the three most studied bacterial toxins that increase the cytosolic cAMP level: pertussis toxin (PT), cholera toxin (CT), and anthrax edema toxin (ET), was imaged by fluorescence videomicroscopy. Three different cell lines were transfected with a fluorescence resonance energy transfer biosensor based on the PKA regulatory and catalytic subunits fused to CFP and YFP, respectively. Real-time imaging of cells expressing this cAMP biosensor provided time and space resolved pictures of the toxins action. The time course of the PT-induced cAMP increase suggests that its active subunit enters the cytosol more rapidly than that deduced by biochemical experiments. ET generated cAMP concentration gradients decreasing from the nucleus to the cell periphery. On the contrary, CT, which acts on the plasma membrane adenylate cyclase, did not. The potential of imaging methods in studying the mode of entry and the intracellular action of bacterial toxins is discussed.

Many pathogenic bacteria produce toxins that elevate the intracellular cAMP concentration and this activity has a major impact on different cell types [1,2]. The finding that targeting cAMP-dependent processes allows toxins to modulate the immune response of the host can, at least partially, account for the wide distribution of this evolutionary strategy [3–5]. Further, cAMP-elevating toxins are indispensable tools in cell biology and cellular microbiology [6,7].

The most intensively studied cAMP-elevating toxins are: pertussis toxin (PT) from *Bordetella pertussis*, cholera toxin (CT) from *Vibrio cholerae*, and edema toxin (ET) from *Bacillus anthracis*. Although the common outcome of their activity is a rise of the intracellular cAMP concentration, their mechanisms of action are distinct. In fact, ET is an adenylate cyclase (AC) [8], whereas PT and CT ADP-ribosylate distinct intracellular G proteins [9]. PT ADP-ribosylates the inhibitory $G_{i\alpha}$ protein of the plasma membrane AC and relieves its inhibition with ensuing increase of cytosolic cAMP [10]. However, PT also affects other G proteins which control different cell functions [3], including the dynamics of the actin cytoskeleton with changes in cell shape typically observed in PT-treated Chinese hamster ovary (CHO) cells [11,12]. Similarly, CT ADP-ribosylates the stimulatory $G_{s\alpha}$ protein of the plasma membrane AC leading to its up-regulation [13]. The consequent rise of cAMP causes loss of water and ions through cAMP-gated ions channels in intoxicated intestinal epithelial cells.

PT, CT, and ET also differ in their modes of cell entry. CT is endocytosed and is retrogradely transported from the endosomal compartment to the Trans Golgi Network, to the Golgi and then to the endoplasmic reticulum, wherefrom it reaches the cytosol and diffuses to its targets [13]. ET is endocytosed after binding to either of its two cell surface receptors, tumor endothelial marker 8 (TEM8) or capillary morphogenesis protein 2 (CMG2) [14]. Available evidences indicate that the catalytic subunit of ET translocates into the cytosol from late endosomes and then remains attached to the endosomal membrane, where it produces cAMP [15–17]. Comparably less is known on how PT reaches the cytosol [18,19]. These distinct mechanisms of action and modes of cell entry are expected to result in different dynamics and intracellular distribution of cAMP elevation. Indeed, space and kinetics of the toxin-induced intracellular cAMP variations are the two crucial parameters of the intoxication process. On the one hand, mounting evidence indicates that signal compartmentalization is an essential mechanism to determine the specificity of signaling events [20,21].

Abbreviations: AC, adenylate cyclase; CMG2, capillary morphogenesis protein 2; CT, cholera toxin; Caco-2, human colonic adenocarcinoma cells; ET, anthrax edema toxin; FRET, fluorescence resonance energy transfer; HBE, human bronchial epithelial cells; PT, pertussis toxin; TEM8, tumor endothelial marker 8.

* Corresponding author. Fax: +39 498276049.
E-mail address: cesare.montecucco@unipd.it (C. Montecucco).

[1] These authors contributed equally to the present work.

[2] Present address: Unité de Pathogénie Microbienne Moléculaire, Institut Pasteur, 28 rue du Dr Roux, 75724 Paris Cedex 15, France.

0006-291X/$ - see front matter © 2008 Elsevier Inc. All rights reserved.
doi:10.1016/j.bbrc.2008.09.012

Therefore, both for infection-oriented research and for the use of toxins as tools in cell biology, it is important to know the site of cAMP increase. On the other hand, the time taken by a toxin to reach the cytosol, corresponding here to the onset of cAMP rise, can provide information about the mode of cell entry [22]. Moreover, the kinetics of the enzymatic action of these three toxins can lead to different levels of cAMP with distinct alterations of cellular functions.

Here, we have used a recently established powerful method [23] to provide novel information on the action of cAMP-elevating toxins in different cell lines in culture. Fluorescence resonance energy transfer (FRET)-based single-cell imaging allows one to monitor the spatially- and temporally-resolved increase of intracellular cAMP levels [24]. The PT, CT, and ET action was measured in three different cell lines, to evaluate the role of the cellular environment in cAMP elevation and to obtain results of rather general validity. Human bronchial epithelial (HBE) cells were chosen because airways epithelial cells are targeted by cAMP-elevating toxins during respiratory tract infections with *B. pertussis*. Similarly, Jurkat T cells are a relevant model for anthrax toxins as well as for PT and CT [3]. Intestinal epithelial cells are directly affected by CT during infection with *V. cholerae* and by anthrax toxins in intestinal anthrax, and therefore we have used here human colonic adenocarcinoma cells (Caco-2).

Materials and methods

Reagents, plasmids, and proteins. Cell culture media, fetal calf serum (FCS), L-glutamine, and antibiotics were purchased from Gibco. Fibronectin, poly-D-lysine, non-essential amino acids, forskolin, IBMX, Hepes and CT were from Sigma; bovine serum albumin (BSA) and FuGENE HD from Roche, collagen type I from BD Biosciences, and PT from List Biological Laboratories, Inc. (CA, USA). The plasmids pCDNA3-RIIRI-CFP and pCDNA3-C-YFP coding, respectively, for the regulatory subunit of PKA fused to CFP and for the catalytic subunit of PKA fused to YFP were previously described [25]. Protective antigen (PA) and edema factor (EF) were obtained as previously described [16,26].

Cell culture. HBE cells and CaCo-2 cells were maintained in minimum essential medium (MEM) with Earle's Salts supplemented with 15% heat-inactivated FCS, 100 U/ml penicillin, and 100 μg/ml streptomycin. Further, 1% of non-essential amino acids was added to the medium for CaCo-2 cells. Jurkat JEG-1 cells were cultured in Roswell Park Memorial Institute (RPMI) 1640 medium containing 10% heat-inactivated FCS, 100 U/ml penicillin, 100 μg/ml streptomycin, 2 mM L-glutamine, and 10 mM Hepes. CHO cells were kept in F12-K medium supplemented with 10% heat-inactivated FCS, 100 U/ml penicillin, 100 μg/ml streptomycin, and 1% non-essential amino acids. Flasks and glass coverslips used to grow HBE cells were treated for 2 h at 37 °C with a coating solution containing 20 μg/ml fibronectin, 100 μg/ml BSA, and 30 μg/ml collagen type I in MEM with Earle's Salts, which was removed by aspiration. Cells were maintained at 37 °C and 5% CO_2 in a humid environment.

Cell transfection and FRET imaging of intracellular cAMP dynamics. Live imaging of intracellular cAMP dynamics was performed as previously described. Briefly, 1×10^5 HBE, and CaCo-2 cells were plated on glass coverslips and immediately transfected with 1 μg each of pCDNA3-RIIRI-CFP and pCDNA3-C-YFP in Opti-MEM, using 6 μl FuGENE HD. Jurkat cells (9×10^6) were prepared the evening before transfection and 20 μg each of pCDNA3-RIIRI-CFP and pCDNA3-C-YFP were introduced into cells kept in 400 μl of culture medium and electrically shocked at 250 V and 950 F in electroporation cuvettes with 0.4 cm gap (Bio-Rad) using a GenePulser Xcell electroporator (Bio-Rad). Cells were then plated at 5×10^5 cells/ml on poly-D-lysine-coated glass coverslips, and 24–48 h after transfection, were transferred to a microscope-adapted micro-incubator equipped with a temperature controller (HTC s.r.l., Italy) at 37 °C and constant 5% CO_2 pressure in 135 mM NaCl, 5 mM KCl, 0.4 mM KH_2PO_4, 1 mM $MgSO_4$, 20 mM Hepes, 1.8 mM $CaCl_2$, and 5.4 mM glucose, pH 7.4. The toxins (5 nM CT or 20 nM PT or 10 nM EF + 20 nM PA) were added, and, after 5–10 min of equilibration, images were acquired every 20 s. An oil immersion 60 × PlanApo 1.40 NA objective was used in a IX81 inverted microscope (Olympus), equipped with an MT20 illumination system with 150 W Xe arc burner (Olympus), a Dual-View beam splitter (Optical Insights, Germany) with a 505DCXR dichroic mirror and D480/30 and D535/40 band filters (Chroma Technologies Corp., USA), and an F-View II digital camera (Olympus). The acquisition software was cell^R (Olympus) and the integration time 100 ms or less. Images were processed with WCIF ImageJ v1.37 (http://rsb.info.nih.gov/ij). The intracellular cAMP level was determined as the ratio between the background-subtracted cyan emission (480 nm) and the background-subtracted yellow emission (540 nm) upon excitation at 430 nm (CFP/YFP ratio). Ratio images were created in pseudo-colors ranging from blue to red, which indicates increasing cAMP levels.

Results

Dynamics of intracellular cAMP rise induced by pertussis toxin

A fluorescent biosensor based on the cAMP-binding protein kinase A (PKA) which exploits the phenomenon of FRET was employed for space- and time-resolved live imaging of intoxicated cells. This probe was generated by fusing the regulatory RII-β subunit and the catalytic C-α subunit of PKA to the cyan (CFP) and the yellow (YFP) variants of the green fluorescent protein, respectively [23–25]. In quiescent cells, the R-CFP and C-YFP subunits are associated in a holotetrameric complex and FRET occurs among them, but cAMP induces theirs separation with loss of FRET. HBE, Caco2, and Jurkat T cells were transfected and expressed good levels of C-YFP and R-CFP. These fluorescent cells were treated with toxin doses defined in preliminary experiments not to saturate the fluorescent signal and this was verified at the end of each experiment by addition of 25 μM forskolin.

Fig. 1 shows the effect of PT on the intracellular cAMP level monitored by FRET in HBE cells, as a change of pseudo-colors in a scale going from blue (low cAMP) to red (high cAMP). The increase of cytosolic cAMP is evident after 1 h from toxin addition, though it appears to be rather low as compared with that obtained by addition of forskolin (Fig. 1E). The level of cAMP in different microdomains of the cells can be determined by selecting subareas of the cells where the ratiometric signal is monitored. This provides a quantitative, though relative, evaluation of cAMP which is particularly valuable when followed in time. Fig. 1F shows that about 30 min after PT addition the cytosolic cAMP level begins to rise. cAMP rises similarly in different sub-areas of the HBE cells (Fig. 2A); these profiles are representative of many cells ($n = 10$) which have been transfected and imaged. Fig. 2B shows that PT induces in Jurkat T cells a sharper rise of cAMP which begins after a lag phase of 20–30 min ($n = 7$ cells); in these cells the signal was recorded on the entire cell area owing to the small size of this lymphocytic cell. At variance, PT did not alter the basal level of cAMP in Caco2 cells, which are very reactive to forskoline (Fig. 2C).The purified B oligomer, lacking the enzymatic S1 subunit of PT, has not effect on the level of cAMP of HBE and Jurkat cells (not shown). Taken together, the imaging profiles obtained with Jurkat and HBE cells indicate that the time course of entry of the enzymati-

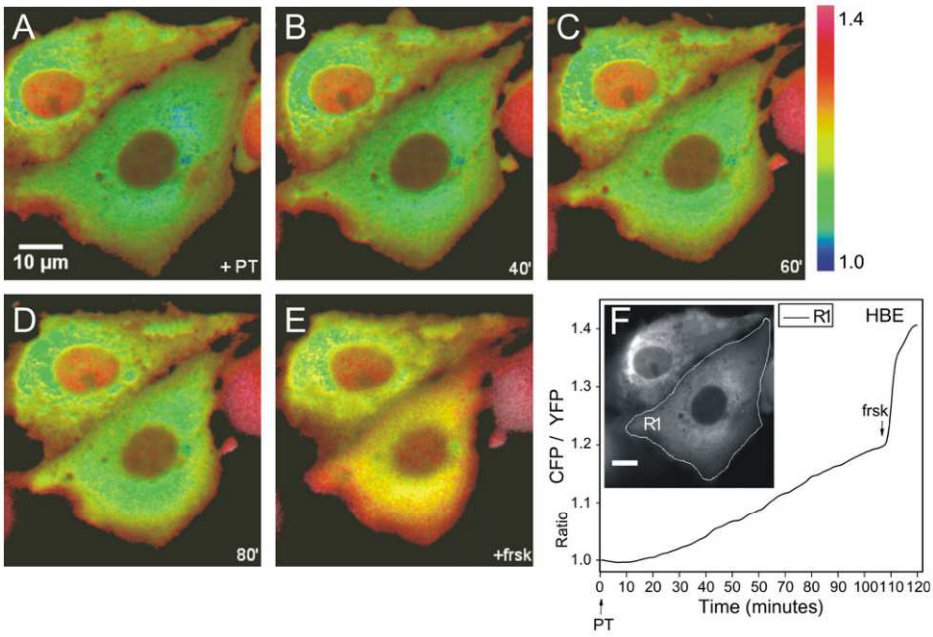

Fig. 1. Imaging of the rise of cAMP induced by pertussis toxin in HBE pulmonary cells transfected with PKA-based fluorescent probes. HBE cells expressing the catalytic PKA subunit-YFP and the regulatory PKA subunit-CFP in the cytosol were imaged after treatment with PT (20 nM). Cells were kept in a micro-incubator at 37 °C and constant 5% CO_2 pressure, under the microscope objective. (A–D) Two cells at the given time periods after toxin addition: the pseudo-colors reflect the increasing cAMP concentration from blue (low cAMP) to red (high cAMP). (E) Effect of the addition of forskolin. (F) Change of cAMP as ratioed in the encircled sub-area indicated in the inset, measured as CFP/YFP ratio. Bars: 10 µm. (For interpretation of the references to color in this figure legend, the reader is referred to the web version of this paper.)

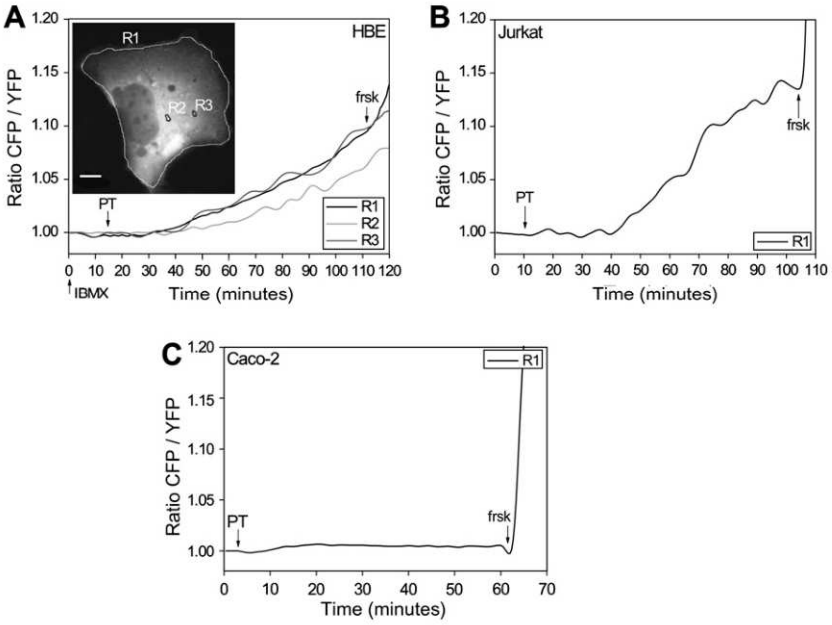

Fig. 2. Time courses of the rise of cAMP as imaged with PKA-based fluorescent probes in HBE, Jurkat cells and Caco-2 treated with pertussis toxin (PT). The three panels show traces of the increase of cytosolic cAMP as detected with the method outlined in Fig. 1 in the indicated cell lines treated with 20 nM PT. (B) Record obtained monitoring the entire cell area, given the reduced dimension of the cytosol of the Jurkat T cells, while three different sub-areas are monitored in the larger HBE cell. The increase in cAMP in the Jurkat T cells and in the pulmonary HBE cells is low, as compared to other toxins (see Figs. 3 and 4), but it is clearly evident after a lag phase of 30–40 min; this gives an *in vivo* indication of the time required for PT to traffic its S1 ADP-ribosyltransferase subunit into the cytosol. In contrast, Caco-2 cells do not rise their cAMP level following the action of PT, though the cells are fully responsive as one can see from the effect of the adenylate cyclase agonist forskolin (abbreviated frsk in A). Bars: 10 µm.

cally active S1 subunit of PT is more rapid than that reported recently [19]. This may be due to the fact that these estimates were based on biochemical modifications of PT subunits or of G proteins, assayed with radioactive tracers. These methods measure the bulk of the phenomenon and can include modification of inactive targets, while the major advantage of the present imaging method

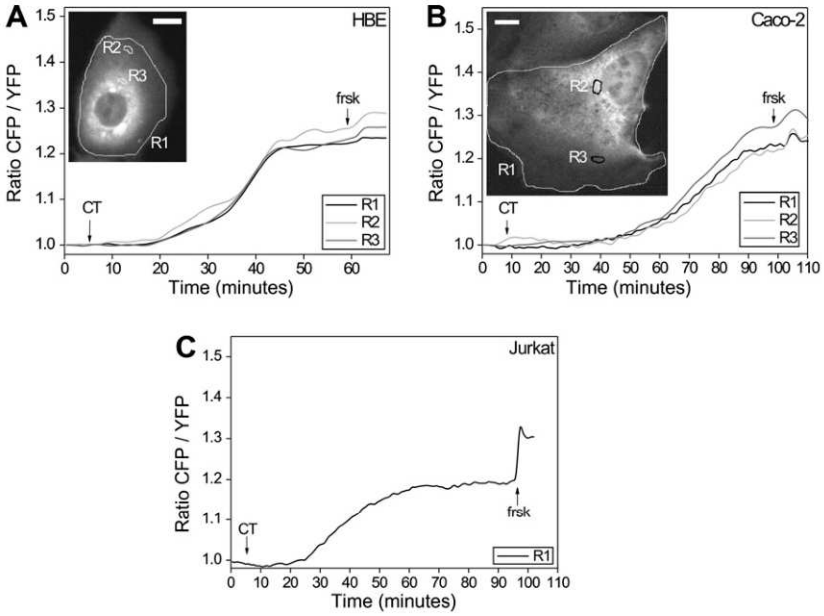

Fig. 3. Time courses of the rise of cAMP as imaged with PKA-based fluorescent probes in HBE, Caco-2 and Jurkat cells treated with cholera toxin (CT). The three cell lines were transfected and imaged as in Figs. 1 and 2, after the exposure to 5 nM CT. The three panels show that all the three cell lines are reactive to CT and that this toxin induces a consistent increase in cAMP cytosolic concentration which begins to rise earlier in Jurkat and HBE than in Caco-2 cells. Bars: 10 μm.

is that it detects the actual functional signal as it is being generated.

Effect of cholera toxin on the dynamics of intracellular cAMP

The first bacterial toxin identified to elevate cytosolic [cAMP] was CT [27]. *In vivo*, CT acts mainly within the intestinal polarized epithelial lining, but it has been used as a molecular tool in a variety of cells. Fig. 3 shows the increase of cytosolic cAMP in the different cells tested here. In all cases, CT induces a strong increase in [cAMP] which begins to rise after a variable lag phase and reaches levels which are only slightly increased by forskolin (except in Jurkat cells). Notwithstanding the fact that the CT-stimulated AC is located on the cytosolic face of the plasma membrane, there appears to be no relevant intracellular cAMP gradients, i.e. this second messenger is rather evenly distributed in the cell cytosol. The profile of the rise of cytosolic cAMP as a function of time differs in the three cell lines tested here. We have no explanation for this difference, but it is likely to be related to different time courses of the entry of the A1 ADP-ribosyltransferase subunit into cells. Though, it is well established that CT reaches the AC via the retrograde transport pathway from the plasma membrane to the ER and the reverse translocon, the exact time course of the process has not been defined, and it may vary from cell to cell type [14,27,28]. The different profiles and time course obtained indicate that this trafficking pathways vary with cell type and this factor should be considered when using CT as a tool in the study of cell physiology.

Anthrax edema toxin induces intracellular concentration gradients of cAMP

At variance from CT and PT, the anthrax ET is itself an AC that reaches the cell cytosol and raises the cytosolic cAMP concentration. ET has been the first bacterial toxin whose intracellular activity has been imaged *in vivo* [16]. Here, we have extended the study to other cell lines to gather more general information on its mode of cell entry.

Fig. 4 shows that ET is poorly active in Caco2 cells, while in HBE cells it causes an increase in cAMP cytosolic concentration similar to the one recorded previously in HeLa cells [16]. Remarkably, also in HBE cells this toxin induces a cAMP concentration gradient

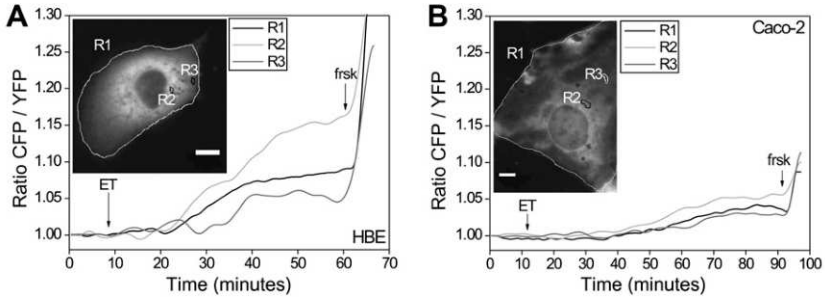

Fig. 4. cAMP imaging in HBE and Caco-2 cells transfected with PKA-based fluorescent probes and treated with the anthrax edema toxin (ET). Caco-2 cells are poorly reactive to the addition of protective antigen (PA, 20 nM) and of edema factor (EF, 10 nM). PA mediates the entry of EF which is an AC causing a modest rise of cAMP in Caco-2 cells, while it is active in HBE cells. Notice that this toxin causes the formation of a gradient of cAMP concentration, higher around the nucleus and lower toward the cell periphery. Bars, 10 μm.

which decreases from the nucleus to the cell periphery which is consistent with the previously suggested localization of EF on late endosomes [16,17]. The low effect of ET on Caco2 cells may be due to the very low expression of both anthrax toxin receptors (TEM8 and CGM2) in these cells (see Fig. 1S). This finding documents that the present method is capable of detecting cAMP intracellular concentration gradients, and that the lack of evidence for such an occurrence in CT- and PT-treated cells is not artifactual.

Discussion

The present study shows the potential of cAMP imaging in the study of cAMP-elevating toxins. The main finding presented here is that the ADP-ribosylating subunit of PT reaches its AC target and causes an increase of cAMP much faster than previously estimated by biochemical methods. The present study brings the value down from hours [19] to 30–40 min and compares well with the value obtained in the same cells with CT, whose pathway of retrograde entry via early endosomes-TGN-Golgi-ER-cytosol is well documented [13,22]. The present finding is therefore compatible with an S1 subunit of PT following the same pathway of entry in the cytosol as the one followed by the A1 subunit of CT.

A second relevant finding is that, notwithstanding the fact that the AC targeted by CT and PT is localized on the cytosolic face of the plasma membrane, there are no gradients of [cAMP] in the cytosol. This is at variance with what previously found for ET and the CyaA adenylate cyclase of *B. pertussis* [16]. Therefore, a given localization of a bacterial toxin within the host cell does not necessarily determine a gradient of effects.

A third point raised by the present work which is relevant to the very large use of CT and PT, and currently also ET, as tools in the study of cell physiology and function, is that it cannot be assumed *a priori* that these toxins necessarily lead to an increase in cytosolic cAMP concentration. In fact, PT and ET do not increase cAMP in Caco2 cells, where CT is very active.

A final consideration that derives from the present results is that different cells have different time courses and extents of cAMP response to the toxins and these parameters are of paramount importance when using these toxins to modulate cAMP to study its role in any given cell function or interaction. The rise of cAMP signals depends on the cellular machinery that controls this second messenger (ACs, phosphodiesterases and anchoring proteins) [20,21,24,28,29] and, therefore, it is almost impossible to make realistic assumptions *a priori* about the action of a cAMP-elevating toxin. cAMP imaging is a very appropriate way of testing the action of any bacterial toxin which induces, either directly or indirectly, a rise in cAMP. The method is applicable to almost any cell which can be transfected and observed without major changes of cell shape and focus under the fluorescence microscope.

Acknowledgments

This work has been supported by grants from MIUR COFIN 2005060371_004 and FIRB-Internalizzazione RBIN04H442 and from the ISS Italy-USA protocol on "Meccanismi tossinogenici e preparazione di antigeni vaccinali" to C.M. and from HFSPO (RGP0001/2005-C), the Fondation Leducq (06 CVD 02) and the EC (LSHB-CT-2006-037189) to M.Z.

Appendix A. Supplementary data

Supplementary data associated with this article can be found, in the online version, at doi:10.1016/j.bbrc.2008.09.012.

References

[1] K.P. Holbourn, C.C. Shone, K.R. Acharya, A family of killer toxins. Exploring the mechanism of ADP-ribosylating toxins, FEBS J. 273 (2006) 4579–4593.
[2] B.E. Turk, Manipulation of host signalling pathways by anthrax toxins, Biochem. J. 402 (2007) 405–417.
[3] N.H. Carbonetti, Immunomodulation in the pathogenesis of *Bordetella pertussis* infection and disease, Curr. Opin. Pharmacol. 7 (2007) 272–278.
[4] C.T. Baldari, F. Tonello, S.R. Paccani, C. Montecucco, Anthrax toxins: a paradigm of bacterial immune suppression, Trends Immunol. 27 (2006) 434–440.
[5] K.J.F. Satchell, Activation and suppression of the proinflammatory immune response by *Vibrio cholerae* toxins, Microbes Infect. 5 (2003) 1241–1247.
[6] M. Ui, Pertussis toxin as a valuable probe for G-protein involvement in signal transduction, in: M. Vaugham, J. Moss (Eds.), ADP-Ribosylating Toxins and G-Proteins. Insights into Signal Transduction, American Society for Microbiology, Washington, DC, 1990, pp. 45–77.
[7] L. De Haan, T.R. Hirst, Cholera toxin: a paradigm for multi-functional engagement of cellular mechanisms (review), Mol. Membr. Biol. 21 (2004) 77–92.
[8] Y. Shen, N.L. Zhukovskaya, Q. Guo, J. Florián, W. Tang, Calcium-independent calmodulin binding and two-metal-ion catalytic mechanism of anthrax edema factor, EMBO J. 24 (2005) 929–941.
[9] M. Domenighini, C. Montecucco, W.C. Ripka, R. Rappuoli, Computer modelling of the NAD binding site of ADP-ribosylating toxins: active-site structure and mechanism of NAD binding, Mol. Microbiol. 5 (1991) 23–31.
[10] A. el Bayâ, R. Linnermann, L. von Olleschik-Elbheim, M.A. Schmidt, Pertussis toxin entry into cells and enzymatic activity, Adv. Exp. Med. Biol. 419 (1997) 83–86.
[11] E.L. Hewlett, K.T. Sauer, G.A. Myers, J.L. Cowell, R.L. Guerrant, Induction of a novel morphological response in Chinese hamster ovary cells by pertussis toxin, Infect. Immun. 40 (1983) 1198–1203.
[12] Y. Xu, J.T. Barbieri, Pertussis toxin-mediated ADP-ribosylation of target proteins in Chinese hamster ovary cells involves a vesicle trafficking mechanism, Infect. Immun. 63 (1995) 825–832.
[13] D.J. Chinnapen, H. Chinnapen, D. Saslowsky, W.I. Lencer, Rafting with cholera toxin: endocytosis and trafficking from plasma membrane to ER, FEMS Microbiol. Lett. 266 (2007) 129–137.
[14] J.A.T. Young, R.J. Collier, Anthrax toxin: receptor binding, internalization, pore formation, and translocation, Annu. Rev. Biochem. 76 (2007) 243–265.
[15] L. Abrami, M. Lindsay, R.G. Parton, S.H. Leppla, F.G. van dar Goot, Membrane insertion of anthrax protective antigen and cytoplasmic delivery of lethal factor occur at different stages of the endocytic pathway, J. Cell Biol. 166 (2004) 645–651.
[16] F. Dal Molin, F. Tonello, D. Ladant, I. Zornetta, I. Zamparo, G. Di Benedetto, M. Zaccolo, C. Montecucco, Cell entry and cAMP imaging of anthrax edema toxin, EMBO J. 25 (2006) 5405–5413.
[17] A. Puhar, C. Montecucco, Where and how do anthrax toxins exit endosomes to intoxicate host cells?, Trends Microbiol 15 (2007) 477–482.
[18] Y. Xu, J.T. Barbieri, Pertussis toxin-catalyzed ADP-ribosylation of Gi-2 and Gi-3 in CHO cells is modulated by inhibitors of intracellular trafficking, Infect. Immun. 64 (1996) 593–599.
[19] R.D. Plaut, N.H. Carbonetti, Retrograde transport of pertussis toxin in the mammalian cell, Cell. Microbiol. 10 (2008) 1130–1139.
[20] D.M.F. Cooper, Compartmentalization of adenylate cyclase and cAMP signalling, Biochem. Soc. Trans. 33 (2005) 1319–1322.
[21] G.S. Baillie, J.D. Scott, M.D. Houslay, Compartmentalisation of phosphodiesterases and protein kinase a: opposites attract, FEBS Lett. 579 (2005) 3264–3270.
[22] K. Sandvig, B. Spilsberg, S.U. Lauvrak, M.L. Torgersen, T. Iversen, B. van Deurs, Pathways followed by protein toxins into cells, Int. J. Med. Microbiol. 293 (2004) 483–490.
[23] M. Zaccolo, F. De Giorgi, C.Y. Cho, L. Feng, T. Knapp, P.A. Negulescu, S.S. Taylor, R.Y. Tsien, T. Pozzan, A genetically encoded, fluorescent indicator for cAMP in living cells, Nat. Cell Biol. 2 (2000) 25–29.
[24] M. Zaccolo, T. Pozzan, Discrete microdomains with high concentration of cAMP in stimulated rat neonatal cardiac myocytes, Science 295 (2002) 1711–1715.
[25] V. Lissandron, A. Terrin, M. Collini, L. D'alfonso, G. Chirico, S. Pantano, M. Zaccolo, Improvement of a fret-based indicator for cAMP by linker design and stabilization of donor-acceptor interaction, J. Mol. Biol. 354 (2005) 546–555.
[26] F. Tonello, L. Naletto, V. Romanello, F. Dal Molin, C. Montecucco, Tyrosine-728 and glutamic acid-735 are essential for the metalloproteolytic activity of the lethal factor of *Bacillus anthracis*, Biochem. Biophys. Res. Commun. 313 (2004) 496–502.
[27] J. Moss, M. Vaughan, Activation of adenylate cyclase by choleragen, Annu. Rev. Biochem. 48 (1979) 581–600.
[28] W. Wong, J.D. Scott, Akap signalling complexes: focal points in space and time, Nat. Rev. Mol. Cell Biol. 5 (2004) 959–970.
[29] M. Zaccolo, G. Di Benedetto, V. Lissandron, L. Mancuso, A. Terrin, I. Zamparo, Restricted diffusion of a freely diffusible second messenger: mechanisms underlying compartmentalized cAMP signalling, Biochem. Soc. Trans. 34 (2006) 495–497.

Supplementary Methods and Results

Real time PCR analysis of the PA receptors in cells

Total RNA was isolated form 7×10^5 cells with RNAspin mini Isolation Kit (GE Healthcare) according to the manufacture protocol. Purified RNA was quantitated using a spectrophotometer (Eppendorf BioPhotometer plus) and optical density 260/280 ratios were determined. Complementary DNA was reverse transcribed from 1 µg of total RNA using SuperScript III first-strand synthesis system for RT-PCR (Invitrogen).

Real time quantitative PCR was performed using iCycler® thermal cycler (Bio-Rad). All amplifications were carried out in a reaction mixture containing 15 ng cDNA, 0.5 µmol/L of each primer and SYBR® Green PCR Master Mix (Applied Biosystem). Human TEM8 and CMG2 amplification primers were as follows: 5'-TCCACCATATGTGCAGGAGA-3' and 5'-AGATAGGCGCTGGACACAGT-3', 5'-AGGTTCGTTGGGGTGATAAA-3' and 5'-TTGTCTGAGGAGGCTGGTG-3', respectively. To amplify the housekeeping gene GAPDH used as internal control, the following primers were used: 5'-ATTTCCTGGTATGACAACGAAT-3' and 5'-GTGTGGTGGGGGACTGAG-3'. Amplification conditions were: 10 minutes at 95°C, 40 cycles: 10 seconds at 95°C, 30 seconds at 59.5°C. A melting curve analysis, consisting of an initial step at 65°C for 10 seconds and a slow elevation of temperature (0.5°C/s) to 95°C, was performed at the end of the amplification cycles to check for the absence of primer dimers and non-specific products. Results were normalized against glyceraldehyde-3-phoshate deydrogenase (GAPDH) as stated and compared by relative expression.

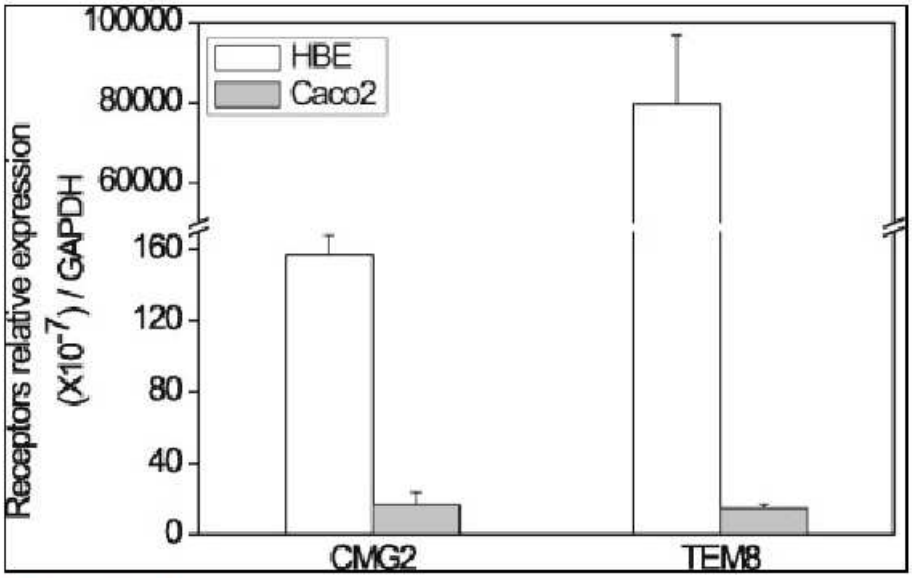

Supplementary Fig. S1.

Chapter IV: The adenylate cyclase toxins of *Bacillus anthracis* and *Bordetella pertussis* promote Th2 cell development by shaping T cell antigen receptor signaling

OPEN ACCESS Freely available online

PLoS PATHOGENS

The Adenylate Cyclase Toxins of *Bacillus anthracis* and *Bordetella pertussis* Promote Th2 Cell Development by Shaping T Cell Antigen Receptor Signaling

Silvia Rossi Paccani[1], Marisa Benagiano[2], Nagaja Capitani[1], Irene Zornetta[3], Daniel Ladant[4], Cesare Montecucco[3], Mario M. D'Elios[2], Cosima T. Baldari[1]*

1 Department of Evolutionary Biology, University of Siena, Siena, Italy, **2** Department of Internal Medicine and Immunoallergology, University of Florence, Florence, Italy, **3** Department of Biomedical Sciences, University of Padua, Padua, Italy, **4** Unité de Biochimie des Interactions Macromoléculaires, CNRS URA 2185, Institut Pasteur, Paris, France

Abstract

The adjuvanticity of bacterial adenylate cyclase toxins has been ascribed to their capacity, largely mediated by cAMP, to modulate APC activation, resulting in the expression of Th2–driving cytokines. On the other hand, cAMP has been demonstrated to induce a Th2 bias when present during T cell priming, suggesting that bacterial cAMP elevating toxins may directly affect the Th1/Th2 balance. Here we have investigated the effects on human $CD4^+$ T cell differentiation of two adenylate cyclase toxins, *Bacillus anthracis* edema toxin (ET) and *Bordetella pertussis* CyaA, which differ in structure, mode of cell entry, and subcellular localization. We show that low concentrations of ET and CyaA, but not of their genetically detoxified adenylate cyclase defective counterparts, potently promote Th2 cell differentiation by inducing expression of the master Th2 transcription factors, c-maf and GATA-3. We also present evidence that the Th2–polarizing concentrations of ET and CyaA selectively inhibit TCR–dependent activation of Akt1, which is required for Th1 cell differentiation, while enhancing the activation of two TCR–signaling mediators, Vav1 and p38, implicated in Th2 cell differentiation. This is at variance from the immunosuppressive toxin concentrations, which interfere with the earliest step in TCR signaling, activation of the tyrosine kinase Lck, resulting in impaired CD3ζ phosphorylation and inhibition of TCR coupling to ZAP-70 and Erk activation. These results demonstrate that, notwithstanding their differences in their intracellular localization, which result in focalized cAMP production, both toxins directly affect the Th1/Th2 balance by interfering with the same steps in TCR signaling, and suggest that their adjuvanticity is likely to result from their combined effects on APC and $CD4^+$ T cells. Furthermore, our results strongly support the key role of cAMP in the adjuvanticity of these toxins.

Citation: Rossi Paccani S, Benagiano M, Capitani N, Zornetta I, Ladant D, et al. (2009) The Adenylate Cyclase Toxins of *Bacillus anthracis* and *Bordetella pertussis* Promote Th2 Cell Development by Shaping T Cell Antigen Receptor Signaling. PLoS Pathog 5(3): e1000325. doi:10.1371/journal.ppat.1000325

Editor: William Bishai, Johns Hopkins School of Medicine, United States of America

Received November 7, 2008; **Accepted** February 3, 2009; **Published** March 6, 2009

Funding: This work was carried out with the financial support of FIRB to CTB and CM, the University of Florence to MMDE, the Istituto Superiore di Sanita within the Italy-USA protocol on "Programmi di Ricerca sulle Malattie di Grande Rilievo Sociale - Meccanismi tossinogenici e preparazione di antigeni vaccinali" to CM, and the EU 6th Framework Programme Contract LSHB-CT-2004-503582 to DL. The contribution of the University of Siena (PAR) is also acknowledged. The sponsors had no role in the design and conduct of the study, in the collection, analysis, and interpretation of the data, and in the preparation, review, or approval of the manuscript.

Competing Interests: The authors have declared that no competing interests exist.

* E-mail: baldari@unisi.it

Introduction

Development of an effective humoral immune response is crucially dependent on T cell help. The last step of B cell differentiation, involving immunoglobulin affinity maturation and isotype switching, occurs in peripheral lymphoid organs under the guidance of a specialized $CD4^+$ T cell subset, known as T helper 2 (Th2). These cells provide both soluble (IL-4) and membrane-bound (CD40L) factors essential for terminal differentiation of antigen specific B cells [1]. Th2 cells are characterized by expression of a unique complement of cytokines, including IL-4, IL-5, IL-10 and IL-13, which are expressed through a complex transcriptional program involving chromatin remodelling at the Th2 cytokine locus control region and *de novo* expression of the lineage specific transcription factors c-maf and GATA-3 [2].

Priming the Th2 differentiation program in naive $CD4^+$ T cells requires essential cues which are provided by antigen presenting cells (APC) in the form of cytokines. Engagement of the T cell antigen receptor (TCR) on naive T cells in the presence of IL-4 promotes their differentiation to Th2 effector cells, whilst simultaneously antagonising committment to the alternative Th1 lineage, which controls cell mediated immunity [1,2]. Additional factors present during T cell priming may profoundly affect the developmental program of helper T cells. Among these, of paramount importance is the second messenger cAMP, which is produced by cellular adenylate cyclases in response to heterotrimeric G-protein coupled surface receptors, such as the receptors for prostaglandin E_2, a proinflammatory prostanoid produced by activated APC [3]. cAMP has been shown to favour Th2 cell differentiation and GATA-3 dependent production of IL-4 and IL-5 through a pathway regulated by phosphoinositide-dependent kinase 1 (PDK1) and protein kinase A (PKA) [4–9].

Suppression of both innate and adaptive immune responses through elevation of intracellular cAMP to supraphysiological

Author Summary

Colonization by pathogens requires keeping at bay the host immune defenses, at least at the onset of infection. The adenylate cyclase (AC) toxins produced by many pathogenic bacteria assist in this crucial function by catalyzing the production of cAMP, which acts as a potent immunosuppressant. Nevertheless, at low concentrations, these toxins act as adjuvants, enhancing antibody responses to vaccination. We have investigated the molecular basis of the immunomodulatory activities of two AC toxins, *Bacillus anthracis* edema toxin and *Bordetella pertussis* CyaA. We show that high toxin concentrations inhibit activation of T lymphocytes, which orchestrate the adaptive immune response against pathogens, whereas low toxin concentrations promote differentiation of helper T lymphocytes to Th2 effectors, which are required for development of antibody-producing cells. Both the immunosuppressant and Th2–driving activities of the toxins are dependent on cAMP. The results demonstrate that, dependent on their concentration, the AC toxins of *B. anthracis* and *B. pertussis* evoke distinct responses on target T lymphocytes by differentially modulating antigen receptor signaling, resulting either in suppression of T cell activation or Th2 cell differentiation. These results are of relevance to the evolution of disease in infected individuals and provide novel mechanistic insight into the adjuvanticity of these toxins.

levels represents a powerful strategy of immune evasion by many bacterial pathogens. This can be achieved indirectly, as for the bacterial enterotoxins, cholera toxin (CT) and *E. coli* heat-labile enterotoxin (LT), which enhance intracellular cAMP production by activating the Gsα subunit of heterotrimeric G-proteins coupled to cellular adenylate cyclases [10]. Alternatively, bacteria such as *B. anthracis* or *B. pertussis* produce and deliver into target cells an adenylate cyclase toxin, the edema factor (EF) and CyaA respectively, respectively, which are themselves adenylate cyclases that catalyze the production of large amounts of cAMP [11,12]. Notwithstanding their immmunosuppressive activity, when administered to mice at subtoxic concentrations together with antigen these toxins potentiate antibody responses, an effect associated with enhanced generation of antigen specific Th2 cells [13–17]. The adjuvanticity of cAMP elevating toxins is believed to result from their capacity to modulate APC differentiation and function. This is exemplified by ET and CyaA, which have been reported to selectively inhibit the production by macrophages and dendritic cells of the master Th1 polarizing cytokine, IL-12, while upregulating IL-4 and IL-10 production, thereby enhancing the induction of Th2 cells [13–15,17–19]. The finding that both non-hydrolysable cAMP analogues and PGE_2 evoke similar effects on APC [18–21] strongly supports the notion that the cAMP elevating activity of these toxins largely accounts for their capacity to differentially affect cytokine production by APC.

We and others have demonstrated that ET and CyaA potently suppress T cell activation [22–24]. This activity results from their capacity to uncouple TCR engagement from activation of the MAP kinase cascade, which is essential for the initiation of the transcriptional program governing T cell activation, proliferation and subsequent differentiation to armed effector cells. Here we have investigated the additional possibility, suggested by the instructive role of the cAMP/PKA axis in Th2 cell differentiation [4–9], that these bacterial toxins might alter TCR signaling to promote naive T cell committment to the Th2 lineage when used at low concentrations. The results show that both ET and CyaA, but not their enzymatically deficient counterparts, directly affect the Th1/Th2 balance by selectively inhibiting TCR dependent activation of the Th1 driving kinase Akt1 while enhancing activation of two essential components of the TCR signaling cascade selectively implicated in human Th2 cell differentiation, the guanine nucleotide exchanger Vav1 and the stress kinase p38. These data support the notion that the adjuvanticity of these cAMP elevating toxins results from their combined effects on APC and $CD4^+$ T cells.

Results

Low concentrations of ET and CyaA catalyze sustained production of cAMP and induce PKA activation in T cells

Both *B. anthracis* ET and *B. pertussis* CyaA potently suppress T cell activation through their cAMP elevating activity [22–24]. To assess the potential effect of these toxins on $CD4^+$ T cell differentiation, a permissive concentration of ET or CyaA was identified in a T cell proliferation assay. Genetically inactivated mutants of ET and CyaA, EL1 [25] and CyaA-E5 [26] respectively, were included as controls. Both ET and CyaA inhibited T cell proliferation in a concentration-dependent manner (Figure 1A). Conversely, neither EL1 or CyaA-E5 affected T cell proliferation (Figure 1B). The toxin concentration selected for the polarization experiments, 0.11 nM and 0.28 nM for ET and CyaA respectively, resulted in ~40% inhibition in the proliferation assays (see arrow in Figure 1A).

A time course analysis of intracellular cAMP production in purified peripheral blood T cells showed that these concentrations of ET and CyaA induced a detectable accumulation of intracellular cAMP, albeit at much lower levels as compared to that obtained with high toxin concentrations (Figure 2A, top). The kinetics of cAMP production by ET and CyaA were significantly different. A fully immunosuppressive ET concentration resulted in a slow increase in intracellular cAMP beginning from 2 h, with a further progressive rise up to 8 h (Figure 2A, top left). On the other hand, a fully immunosuppressive concentration of CyaA evoked a rapid rise of cAMP to plateau levels beginning from the earliest time point analyzed, and the levels of cAMP remained high up to 8 h (Figure 2A, top left). High cAMP concentrations were still measurable after 24 h (data not shown). The kinetics of cAMP production by immunosuppressive concentrations of ET and CyaA were largely reproduced by the low toxin concentrations selected for the studies on T cell polarization (Figure 2A, top right, and data not shown for 24 h). No increase in cAMP was elicited by EL1 and CyaA-E5, even at the highest concentration used (Figure 2A, bottom left).

To understand whether the modest increase in the levels of cAMP catalyzed by low concentrations of ET or CyaA was sufficient to elicit a biological response, we measured the activity of PKA, one of the major cellular targets of cAMP. As a readout of PKA activation we used an antibody specific for the phosphorylated PKA consensus, R-X-X-pT-X-X/R-R-X-pS-X-X, which recognizes phosphorylated PKA substrates. The increase in intracellular cAMP following T cell treatment with high concentrations of ET or CyaA resulted in a strong potentiation of PKA activity, as shown by the qualitative and quantitative changes in the phosphoprotein pattern in lysates from toxin-treated cells compared to untreated cells (Figure 2B, top panel). A similar enhancement in PKA activity was also observed in cells treated with low concentrations of ET or CyaA, despite the smaller increase in intracellular cAMP measured under these conditions (Figure 2B, top panel). Interestingly, notwithstanding the different interacellular localization of the two adenylate cyclase toxins, there

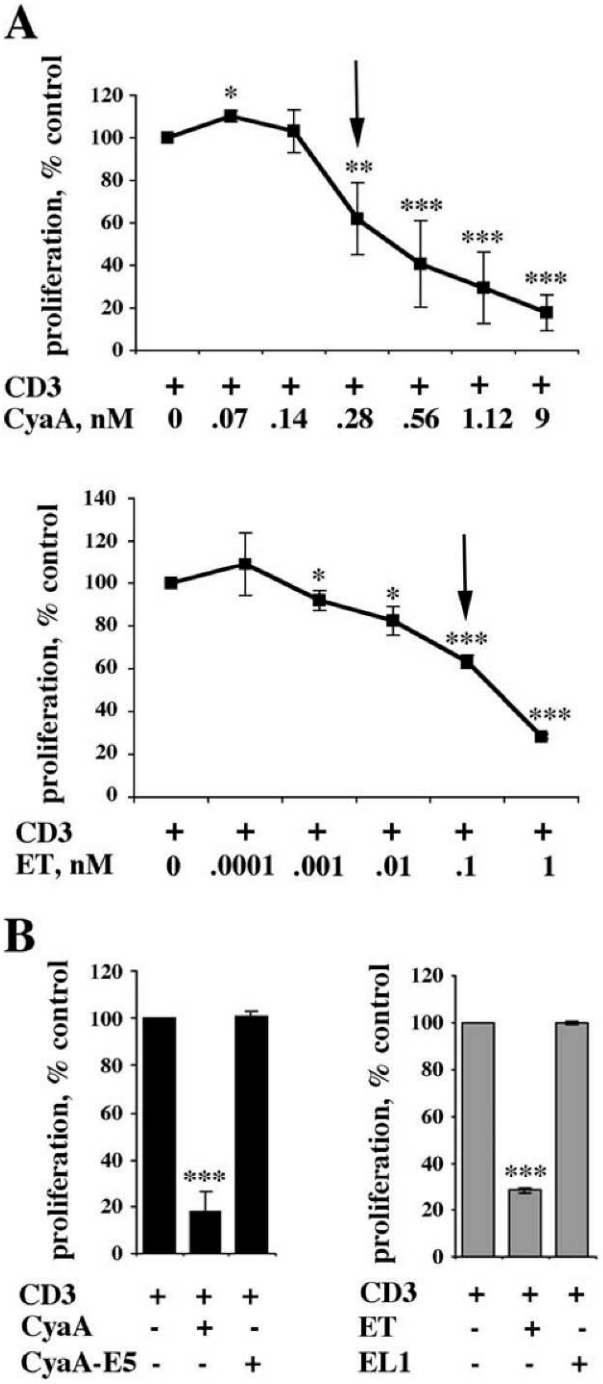

Figure 1. Concentration dependent suppression of T cell proliferation by CyaA and ET. (A) [^{3}H]-thymidine uptake by PBL stimulated for 48 h by CD3 cross-linking in the presence or absence of the indicated concentrations of CyaA (*top*) or ET (*bottom*). The results, obtained on triplicate samples of PBL from 5 independent donors, are expressed as % [^{3}H]-thymidine uptake (cpm) by CyaA or ET treated cells compared to control cells stimulated in the absence of either toxin (taken as 100%). The arrow shows the toxin concentration selected for the polarization experiments (CyaA, 0.28 nM; ET, 0.11 nM). (B) [^{3}H]-thymidine uptake by PBL stimulated for 48 h by CD3 cross-linking in the presence or absence of either CyaA and ET or the respective adenylase deficient mutants (45 nM CyaA/CyaA-E5, 110 nM ET/EL1). The results are expressed as in A. ***$P \leq 0.001$; **$P \leq 0.01$; *$P \leq 0.05$. Error bars, SD.
doi:10.1371/journal.ppat.1000325.g001

was a general overlap in the phosphoprotein pattern observed in cells treated with ET or CyaA. Consistent with the agonistic activity of ET and CyaA on PKA, analysis of the phosphorylation state of the transcriptional activator CREB, a specific PKA substrate, showed that low toxin concentrations induced CREB phosphorylation, albeit to a lesser extent compared to high toxin concentrations (Figure 2B, middle panel). The agonistic effect of the toxins was abrogated to a significant extent when cells were pretreated with pharmacological PKA inhibitors (H89 or KT5720) (Figure 2C and data not shown). Moroever, no CREB phosphorylation was observed in T cells treated with the adenylate cyclase defective ET or CyaA mutant (Figure 2C), supporting the notion that the effects of the toxins are mediated by the cAMP/PKA axis. Of note, maximal activation of both PKA and CREB was observed in cells stimulated by TCR/CD3 cross-linking (Figure 2B), consistent with the potent agonistic activity of the receptor on cAMP production (Figure 2A, bottom right). However, as opposed to the long-lasting increase in cAMP elicited by the toxins, TCR engagement resulted in a transient increase in intracellular cAMP (Figure 2A, bottom right). No further significant enhancement in TCR-dependent PKA or CREB activation was observed in T cells treated with ET or CyaA (Figure 2B and respective legend), despite the increase in cAMP production observed under these conditions (Figure 2D), indicating that PKA and CREB activation reaches plateau levels in response to the cAMP burst elicited by the TCR.

ET and CyaA promote Th2 cell differentiation

To assess the impact of low concentrations of ET and CyaA on human helper T cell polarization, enriched human CD4$^+$ T cells from healthy donors were exposed to ET or CyaA and subsequently primed by TCR/CD3 cross-linking using immobilized anti-CD3 mAb. After 10 days, cells were washed, and restimulated for 24 h or 48 h using the same anti-CD3 mAb. The identity of the Th subset into which cells had differentiated was determined by ELISPOT analysis of cytokine production. As shown in Figure 3A, priming of cells that had been exposed to low concentrations of ET or CyaA resulted in a dramatic increase in production of the Th2 cytokines, IL-4 and IL-13, to levels close to those measured in cells primed to differentiate to the Th2 subset (TCR/CD3 cross-linking in the presence of IL-4). Conversely, consistent with the mutual antagonism of the Th1/Th2 differentiation programs, ET or CyaA had a modest inhibitory effect on production of the Th1 cytokines IFNγ and TNF-α (Figure 3B). No significant enhancement in Th2 cytokines above the levels produced by T cells primed in neutral conditions (TCR/CD3 cross-linking alone) was observed when cells were pretreated with the adenylate cyclase defective EL1 or CyaA-E5 mutants (Figure 3A), indicating that the Th2 driving activity of ET and CyaA is dependent on their capacity to produce cAMP.

Differentiation of helper T cells to the Th2 subset is crucially dependent on expression of the lineage specific transcription factors c-maf and GATA-3, which are essential for transcriptional regulation of the Th2 cytokine control locus [2]. To understand whether ET and CyaA promote production of IL-4 and IL-13 by shaping the transcriptional program triggered by the TCR in naive T cells, resulting in expression of lineage specific transcription factors, the levels of c-maf and GATA-3 mRNA in T cells primed in the presence of either toxin were measured by real-time RT-PCR. Both ET and CyaA potently upregulated expression of c-maf and GATA-3 to levels comparable or higher than those detectable in T cells primed in the presence of IL-4 (Figure 4A). Conversely, expression of the Th1 lineage specific

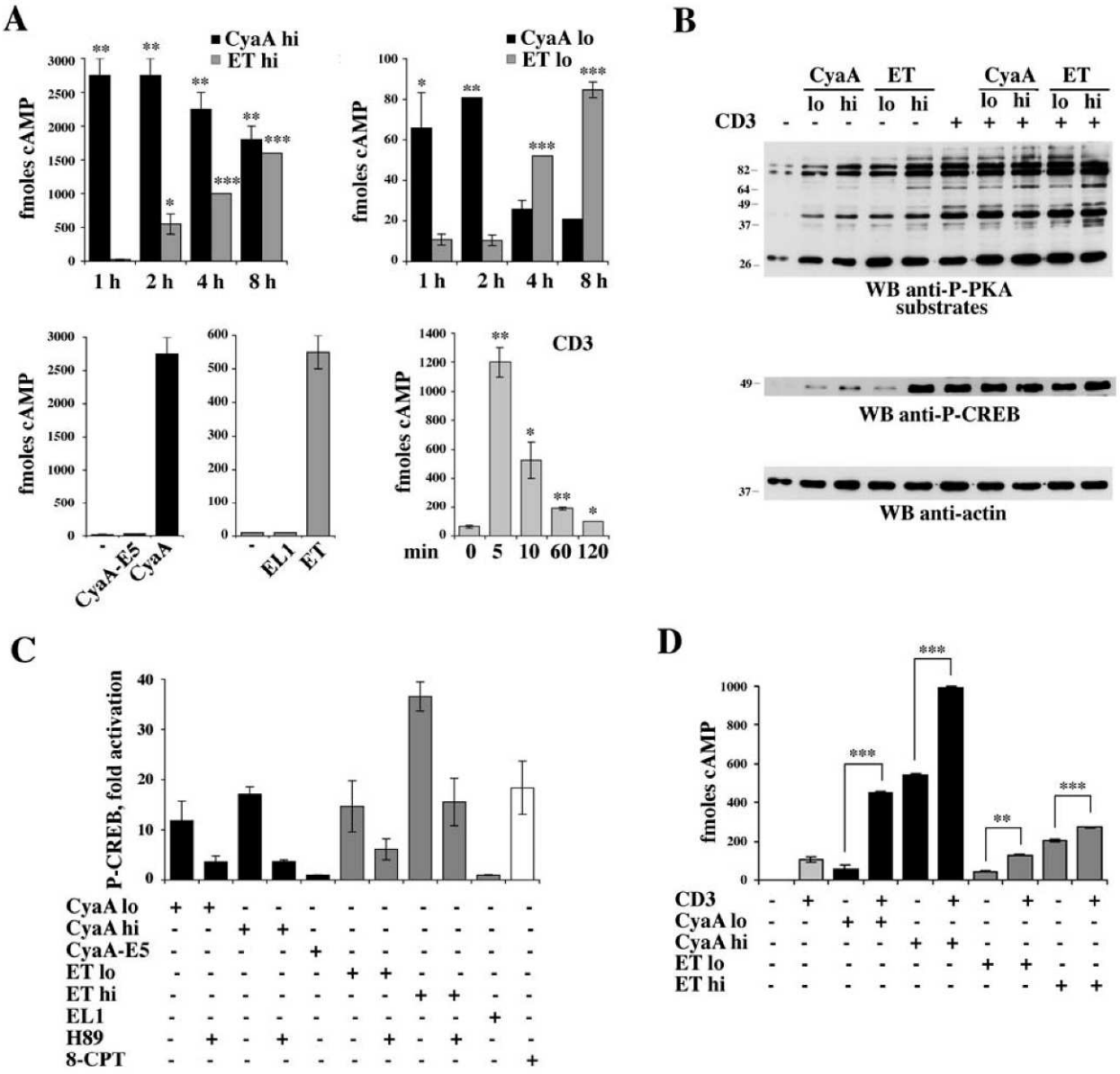

Figure 2. cAMP production and PKA activation in T cells treated with high and low concentrations of CyaA and ET. (A) Time course analysis of cAMP production in purified peripheral blood T lymphocytes treated with high (CyaA hi, 45 nM ; ET hi, 110 nM) (*top left*) or low (CyaA lo, 0.28 nM; ET lo, 0.11 nM) (*top right*) concentrations of CyaA or ET, or activated by TCR/CD3 cross-linking (*bottom right*). The histogram on the bottom left panel also includes the quantification of cAMP in lysates of T cells treated with the adenylase cyclase deficient CyaA and ET mutants (45 nM CyaA-E5, 110 nM EL1) for 2 h or 6 h, respectively. The results, which show the levels of cAMP measured in T cell lysates, are expressed as fmoles/10^6 cells. Representative experiments, each carried out on duplicate samples from individual healthy donors, are shown ($n \geq 4$). (B) *Top*, Immunoblot analysis of the phosphorylation state of PKA substrates in post-nuclear supernatants of T cells treated with 45 nM CyaA (CyaA hi) or 0.28 nM CyaA (CyaA lo), or 110 nM ET (ET hi) or 0.11 nM ET (ET lo), for 2 h (CyaA) or 6 h (ET), and then lysed as such or after stimulation for 1 min with anti-CD3 mAb (CD3). A sample stimulated with anti-CD3 mAb alone was also included. The immunoblot was carried out using an antibody which recognizes a phosphorylated PKA consensus sequence (see Materials and Methods). The stripped filter was reprobed with a phosphospecific antibody which recognizes the active form of CREB *(middle)*. The fold activation of CREB in CyaA/ET treated samples *vs* untreated control in the experiment shown was the following: CyaA low, 8.3; CyaA high, 19.0; ET low, 8.7; ET high, 79.9. The levels of phospho-CREB in the samples treated with CyaA or ET in combination with anti-CD3 mAb *vs* samples treated with anti-CD3 mAb alone (taken as 100%) were the following: CyaA low+CD3, 98.1±4.8%; CyaA high+CD3, 103.4±8.7%; ET low+CD3, 102.1±3.2%; ET high+CD3, 112.1±8.1% ($n = 3$). A control anti-actin blot is shown below. None of the treatments modified the expression levels of CREB (data not shown). Representative experiments are presented ($n \geq 3$). The migration of molecular mass markers is indicated. (C) Quantification of CREB phosphorylation in post-nuclear supernatants of T cells treated with 45 nM CyaA (CyaA hi)/CyaA-E5 or 0.28 nM CyaA (CyaA lo), or 110 nM ET (ET hi) /EL1 or 0.11 nM ET (ET lo), for 2 h (CyaA) or 6 h (ET). Where indicated, cells were pretreated for 1 h with 20 μM H89. A sample stimulated for 30 min with 100 μM 8-CPT was included as positive control. The data were obtained by laser densitometry of anti-phospho-CREB immunoblots. The results are expressed as relative CREB phosphorylation (fold activation *vs* untreated controls) ($n = 2$). (D) Quantification of cAMP in lysates of T cells treated as in B. The results, which show the levels of cAMP measured in T cell lysates, are expressed as fmoles/10^6 cells. A representative experiment, carried out on duplicate samples from an individual healthy donor, is shown ($n = 3$). ***$P \leq 0.001$; **$P \leq 0.01$; *$P \leq 0.05$. Error bars, SD.

doi:10.1371/journal.ppat.1000325.g002

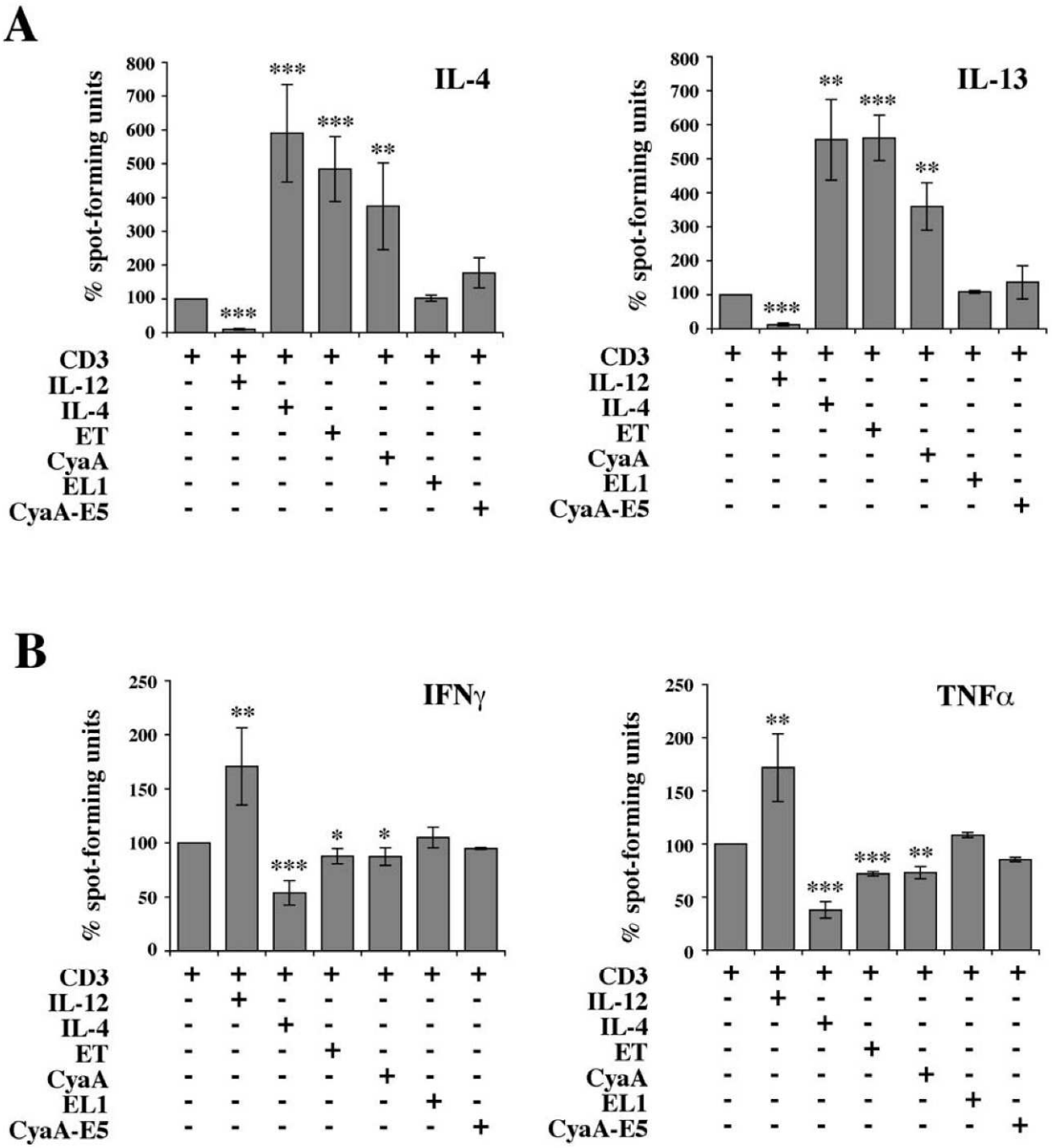

Figure 3. CyaA and ET promote Th2 cell differentiation through their cAMP elevating activity. Enriched $CD4^+$ T cells from 6 healthy donors were primed with anti-CD3 mAb, as such or following pretreatment for 2 h with 0.28 nM CyaA/CyaA-E5, or with 0.11 nM ET/EL1. Cells primed in Th2- (IL-4) or Th1- (IL-12) inducing conditions were included as controls. After 10 days cells were washed and restimulated with anti-CD3 mAb for 48 and 24 h respectively, and the levels of IL-4 and IL-13 (A) and IFN-γ and TNF-α (B) were quantified by ELISPOT. The results, obtained on duplicate samples, are expressed as % spot-forming units by CyaA or ET treated cells compared to control cells primed in the absence of either toxin (taken as 100%). ***$P \leq 0.0001$; **$P \leq 0.001$; *$P \leq 0.01$. Error bars, SD.
doi:10.1371/journal.ppat.1000325.g003

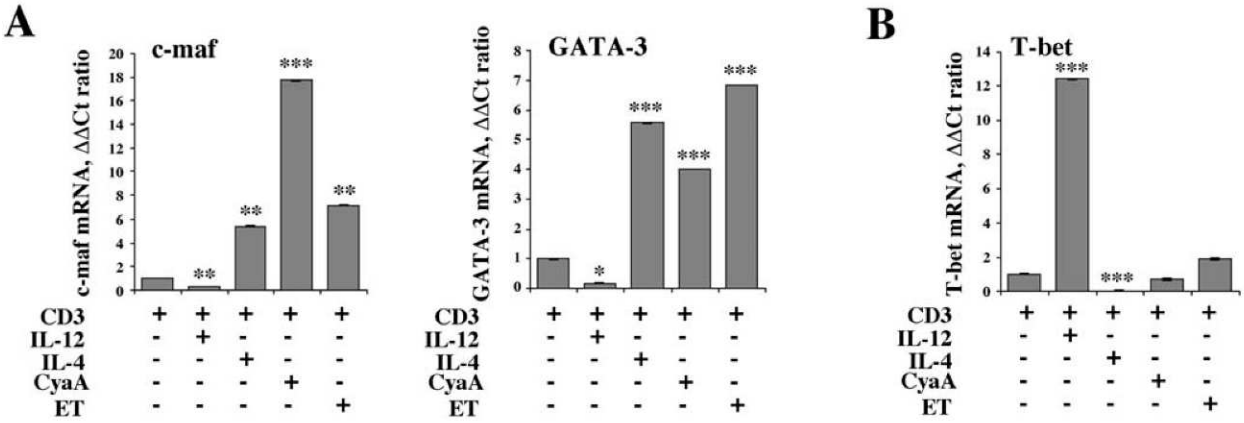

Figure 4. CyaA and ET promote c-maf and GATA-3 expression in primed T cells. Enriched $CD4^+$ T cells from 3 healthy donors were primed with anti-CD3 mAb, as such or following pretreatment for 2 h with 0.28 nM CyaA or 0.11 nM ET. Cells primed in Th2- (IL-4) or Th1- (IL-12) inducing conditions were included as controls. After 10 days cells were restimulated with anti-CD3 mAb for 24 h. The levels of mRNA encoding c-maf and GATA-3 (A) and T-bet (B) were quantified by real-time RT–PCR. Transcript levels were normalized to the expression level of GAPDH. Syber green runs were performed with cDNAs from the same reverse transcription reaction from 400 ng of total RNA. The $\Delta\Delta C_T$ method was applied as a comparative method of quantification, using cells primed in neutral conditions (anti-CD3 mAb) as reference. The data are representative of 3 independent experiments, each in duplicate. ***$P \leq 0.00001$; **$P \leq 0.0001$; *$P \leq 0.001$. Error bars, SD.
doi:10.1371/journal.ppat.1000325.g004

transcription factor T-bet was not significantly affected in T cells primed in the presence of either CyaA or ET (Figure 4B).

Low concentrations of ET and CyaA selectively impair TCR–dependent activation of Akt1, while potentiating activation of Vav1 and p38

TCR signaling is initiated by Lck, a T cell specific Src family protein tyrosine kinase which is responsible for phosphorylation of the ITAMs within the ζ chain of the CD3 complex. As all Src kinases, Lck is negatively regulated by a C-terminal tyrosine residue, Y505, which, when phosphorylated, establishes an intramolecular interaction with the SH2 domain, resulting in a close, inactive conformation. The inhibitory tyrosine residue is phosphorylated by Csk, which in resting cells is maintained close to Lck in lipid rafts through interaction with the PAG adaptor and whose activity is potentiated by PKA dependent phosphorylation of a serine residue at position 364 [27]. By elevating intracellular cAMP, ET and CyaA have therefore the potential to antagonize TCR signaling beginning from the earliest step. Analysis of the phosphorylation state of Y505 on Lck using a phosphospecific antibody revealed that high concentrations of ET or CyaA effectively block TCR dependent dephosphorylation of Lck (Figure 5A and 5B). This activity was not reproduced by the respective adenylate cyclase defective mutants (Figure 5B), supporting the notion that the suppressive effect of ET and CyaA on TCR dependent Lck activation is mediated by cAMP. No enhancement in Lck kinase activity in response to TCR engagement was moreover observed when cells were pretreated with high concentrations of ET or CyaA, as assessed by measuring Lck autophosphorylation in *in vitro* kinase assays (data not shown). Consistent with the failure of the TCR to trigger activation of Lck in the presence of either toxin, both TCR dependent CD3ζ phosphorylation and activation of the effector kinase ZAP-70, which occurs following recruitment to the phosphorylated ITAMs of CD3ζ, were found to be inhibited by ET or CyaA (Figure 5A and 5B). In agreement with previous reports [22–24], activation of the MAP kinase cascade, which couples these early signaling events to gene transcription, was found to be impaired by immunosuppressive concentrations of ET or CyaA, as assessed using as a readout phosphorylation of Erk1/2 (Figure 5A and 5B). Conversely, neither CD3ζ and ZAP-70 phosphorylation, nor Erk1/2 phosphorylation, were affected when the TCR was stimulated in cells exposed to low, Th2 polarizing concentrations of ET or CyaA (Figure 6A and 6B).

To understand whether Th2 polarizing concentrations of ET and CyaA could selectively affect downstream components of TCR signaling specifically implicated in Th lineage committment, we focused on two molecules in the TCR signaling cascade, the Rac/Cdc42 specific guanine nucleotide exchanger Vav1 and the stress-activated kinase p38, which have been implicated in human Th2 cell differentiation [28–32]. Furthermore, we assessed the effect of the toxins on the serine/threonine kinase Akt1, which has been associated to Th1 cell differentiation [9]. Strikingly, analysis of Akt1 activation using phosphospecific antibodies which recognize two critical residues, T308 and S473, showed that low, Th2 polarizing concentrations of ET or CyaA were sufficient to potently impair TCR dependent Akt phosphorylation (Figure 7A and data not shown). Conversely, both basal and TCR dependent Vav1 phosphorylation on Y174, which positively regulates Vav1 activity, was potentiated by low concentrations of ET or CyaA (Figure 7B). A similar enhancement was observed for p38 (Figure 7B), consistent with the capacity of PKA to act as an agonist of this kinase [31,33]. The phosphodiesterase inhibitor, IBMX, further potentiated the agonistic activity of the toxins on p38 activation (data not shown), further supporting the notion that the effects of the toxins are mediated by cAMP. Hence ET and CyaA alter the Th1/Th2 balance at least in part by antagonizing the Akt1 dependent pathway leading to Th1 cell differentiation and by potentiating the Vav1 and p38 dependent pathway(s) leading to Th2 cell differentiation. Of note, TCR dependent Vav1 and p38 activation was not impaired, but actually enhanced, when cells were pretreated with high concentrations of ET or CyaA (Figure 7B), despite their potent inhibitory activity on initiation of TCR signaling, suggesting that an Lck independent pathway triggered by the TCR, which can be potentiated by cAMP, may contribute to a significant extent to their activation.

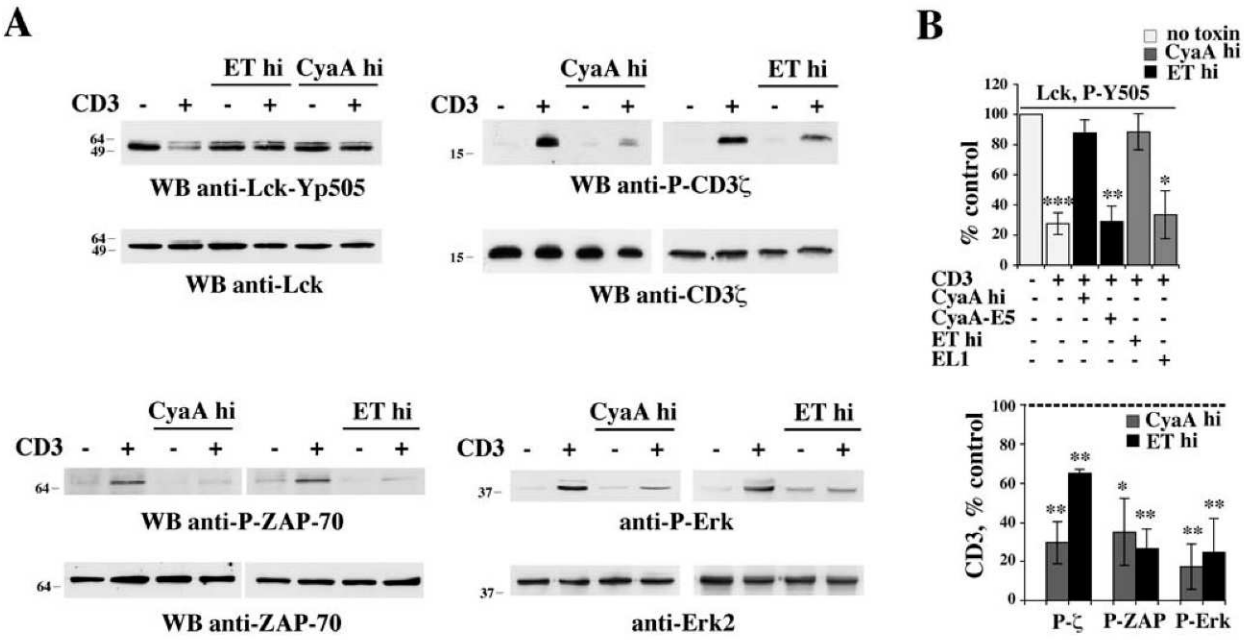

Figure 5. Immunosuppressive concentrations of CyaA or ET prevent initiation of TCR signaling. (A) *Top left*, Immunoblot analysis, using a phosphospecific antibody, of Lck phosphorylation on the inhibitory C-terminal tyrosine residue (Y505) in postnuclear supernatants from PBL activated for 1 min by CD3 cross-linking in the presence or absence of either 45 nM CyaA or 110 nM ET (CyaA hi, ET hi). *Top right*, Immunoblot analysis, using an anti-phosphotyrosine antibody, of CD3ζ specific immunoprecipitates from PBL treated as above. *Bottom*, Immunoblot analysis, using phosphospecific antibodies, of ZAP-70 (left) and Erk1/2 (right) phosphorylation in postnuclear supernatants from PBL activated for 1 min (ZAP-70) or 5 min (Erk1/2) by CD3 cross-linking in the presence or absence of 45 nM CyaA or 110 nM ET (CyaA hi, ET hi). (B) Quantification by laser densitometry of the relative levels of Lck (phosphorylation in unstimulated cells taken as 100%), or CD3ζ, ZAP-70 and Erk1/2 phosphorylation (phosphorylation in anti-CD3 stimulated cells taken as 100%, indicated as a dotted line) in PBL activated by CD3 cross-linking in the presence of 45 nM CyaA or 110 nM ET (CyaA hi, ET hi) ($n \geq 3$). Where indicated, cells were activated in the presence of the adenylase cyclase deficient CyaA and ET mutants (45 nM CyaA-E5, 110 nM EL1) for 2 h or 6 h, respectively ($n = 2$). ***$P \leq 0.001$; **$P \leq 0.01$; *$P \leq 0.05$. Error bars, SD.
doi:10.1371/journal.ppat.1000325.g005

Discussion

The *B. anthracis* ET and *B. pertussis* CyaA adenylate cyclase toxins act as potent suppressors of T cell activation and proliferation in the 10^{-9}–10^{-6} molar range of concentrations [22–24]. In the absence of systemic intoxication, these high concentrations are likely to be reached only locally through accumulation of the toxins at the primary site of infection. However, there are anatomical districts and localized infections (*e.g.* cutaneous anthrax) where low amount of toxins may be released and might modulate the host immune response. We found that both ET and CyaA are potent promoters of naive $CD4^+$ T cell differentiation to Th2 effectors when used at subnanomolar concentrations (0.1–0.3 nM). Interestingly, distinct effects of high *vs* low concentrations of CyaA have also been observed in neutrophils and other phagocytes, ranging from cytolysis to apoptosis to impairment of effector functions [34], suggesting the biological outcome of host cell exposure to the toxin is likely to be dictated by its proximity to the bacterium. The sensitivity of T cells to such low ET concentration can be accounted for by the fact that human leukocytes express the high affinity CMG2 receptor for protective antigen (PA), the receptor binding subunit of ET [35]. Furthermore, although T cells lack CD11b/CD18, the only known CyaA receptor, CyaA can effectively insert into cell membranes or artificial lipid bilayers in the absence of CD11b/CD18, albeit with a reduced efficacy [36]. The presence on T cells of a putative alternative CyaA receptor cannot however be ruled out.

The immunosuppressant activity of high concentrations of ET and CyaA is fully consistent with the known inhibitory effects of cAMP on T cell activation. In physiological conditions cAMP production by a TCR-coupled adenylate cyclase is part of a negative feed-back loop which ensures extinction of TCR signaling through PKA dependent activation of Csk, a kinase that inhibits Lck by phosphorylating its C-terminal tyrosine residue [27]. This feed-back loop does not become immediately operational because cAMP production is counterbalanced by TCR dependent recruitment of PDE-4 to lipid rafts, where also the activated TCR localizes, thereby allowing the protein tyrosine kinase cascade to start [37]. Once PDE-4 dissociates from lipid rafts, the feed-back loop can terminate the signal. Since cAMP production and PKA activation are TCR-dependent, cAMP returns to basal levels after signal extinction. Alterations in this finely regulated cAMP balance by adenylate cyclase agonists, such as PGE_2 receptors, result in impaired TCR signaling and T cell activation [27]. The inhibitory activity of high concentrations of ET and CyaA on Lck activation and CD3ζ phosphorylation indicates that these toxins preventing firing of the TCR signaling cascade by altering the cAMP balance through the massive and sustained production of cAMP. In this context, it should be underlined that TCR engagement results in a rapid elevation in the levels of cAMP, which elicit a potent enhancement in PKA activation, comparable to the one observed in cells exposed to high toxin concentrations. Nevertheless, under these conditions the TCR triggers a productive signaling cascade, as opposed to cells pre-exposed to high concentrations of ET or CyaA, supporting the

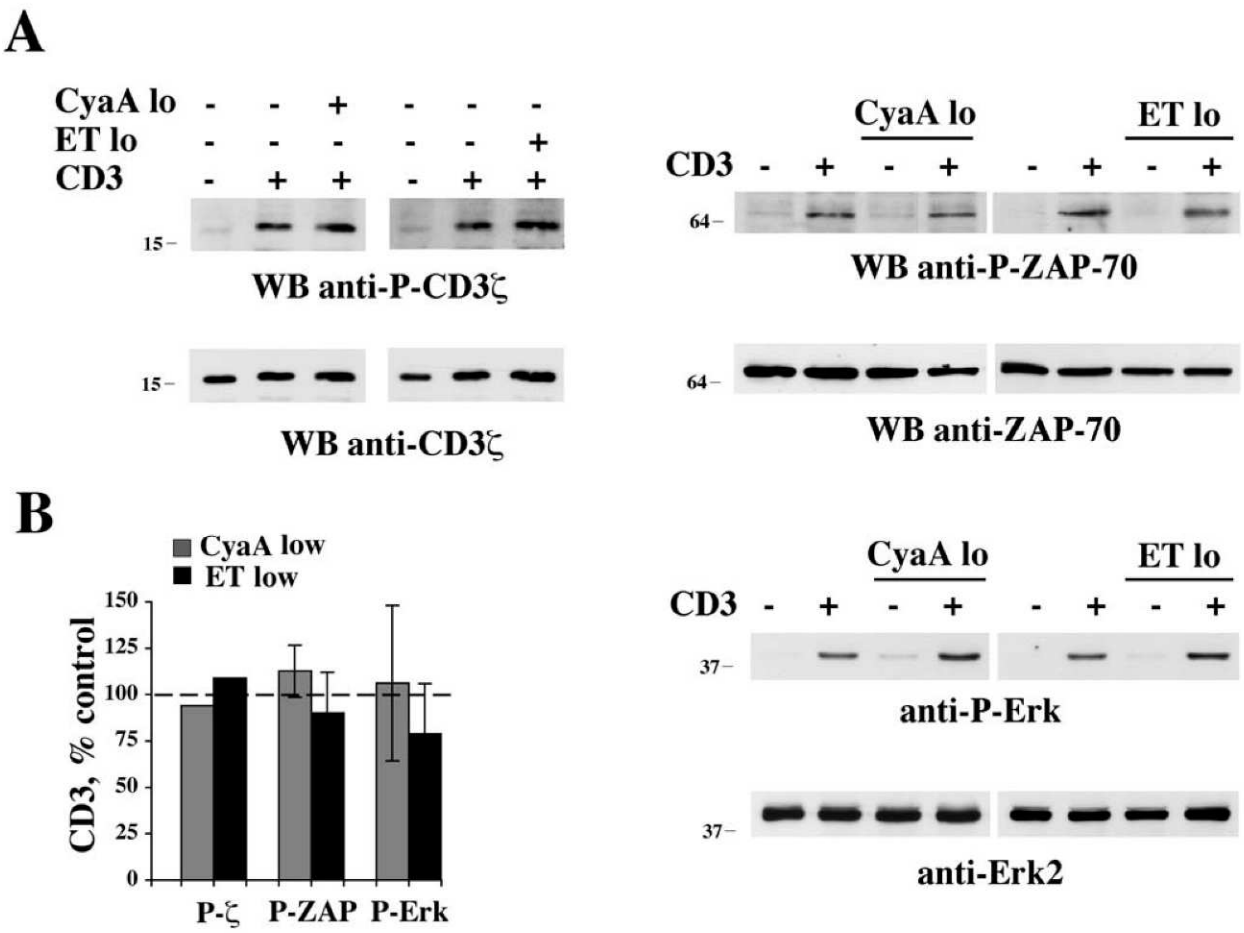

Figure 6. Low CyaA or ET concentrations do not affect initiation of TCR signaling. (A) Immunoblot analysis, using phosphospecific antibodies, of CD3ζ, ZAP-70, or Erk1/2 phosphorylation in postnuclear supernatants of cells activated as above in the presence or absence of either 0.28 nM CyaA or 0.11 nM ET (CyaA lo, ET lo). Filters were stripped and re-probed with control antibodies. Representative experiments are shown ($n \geq 3$). The migration of molecular mass markers is indicated. (B) Quantification by laser densitometry of the relative levels of CD3ζ, ZAP-70, and Erk1/2 phosphorylation (phosphorylation in anti-CD3 stimulated cells taken as 100%, indicated as a dotted line) in PBL activated by CD3 cross-linking in the presence or absence of either 0.28 nM CyaA or 0.11 nM ET (CyaA lo, ET lo) ($n \geq 3$). Error bars, SD.
doi:10.1371/journal.ppat.1000325.g006

importance of the spatiotemporal regulation of cAMP in TCR signaling. Low toxin concentrations on the other hand, do not inhibit initiation of TCR signaling. The intracellular concentration of cAMP measured under these conditions, which is very modest compared to the burst of cAMP evoked by the TCR, may be locally and transiently neutralized by PDE-4.

At variance with their inability to impair initiation of TCR signaling, low concentrations of ET or CyaA were found to selectively affect specific downstream nodes -Akt1, Vav1 and p38 activation- crucial to Th1/Th2 lineage committment. This activity is likely to result from their PKA dependent modulation of intracellular signaling mediators implicated in Th2 cell differentiation downstream of signal initiation. Akt1 has been reported to favour Th1 cell differentiation by providing the CD28 costimulatory signal required for expression of the Th1 cytokines IL-2 and IFN-γ [9]. Although our study was carried out on T cells stimulated by TCR/CD3 cross-linking in the absence of CD28 costimulation, the results show that Akt1 is effectively phosphorylated in response to TCR engagement and that this event is potently inhibited by low concentrations of ET or CyaA. The negative regulation of Akt by PKA [38,39] is likely to underlie this inhibitory, TCR-distal effect of the two toxins, which would moreover favour differentiation to the Th2 lineage by potentiating the PDK1/PKA pathway coupling the TCR to IL-4 gene transcription [9].

Under the same conditions, both toxins enhance TCR dependent phosphorylation of the guanine nucleotide exchanger Vav1 and activation of the stress kinase p38, which participate in Th2 lineage commitment. A skewing of the Th1/Th2 balance to Th1, as well as defects in Th2 dependent B cell responses, have been indeed observed in $Vav1^{-/-}$ mice [28,40]. Furthermore, p38 has been implicated in human Th2 cell differentiation, at least in part through its capacity to promote activation of GATA-3 [29–32]. The similar enhancement of TCR-dependent Vav and p38 activation in the presence of high toxin concentrations, which block signal initiation, supports a local effect on a specific signaling module independent of the TCR proximal, Lck-dependent signaling cascade. While there is evidence for an agonistic role of cAMP in p38 activation [31], the potential function of cAMP in the modulation of Vav1 activity has not been directly addressed.

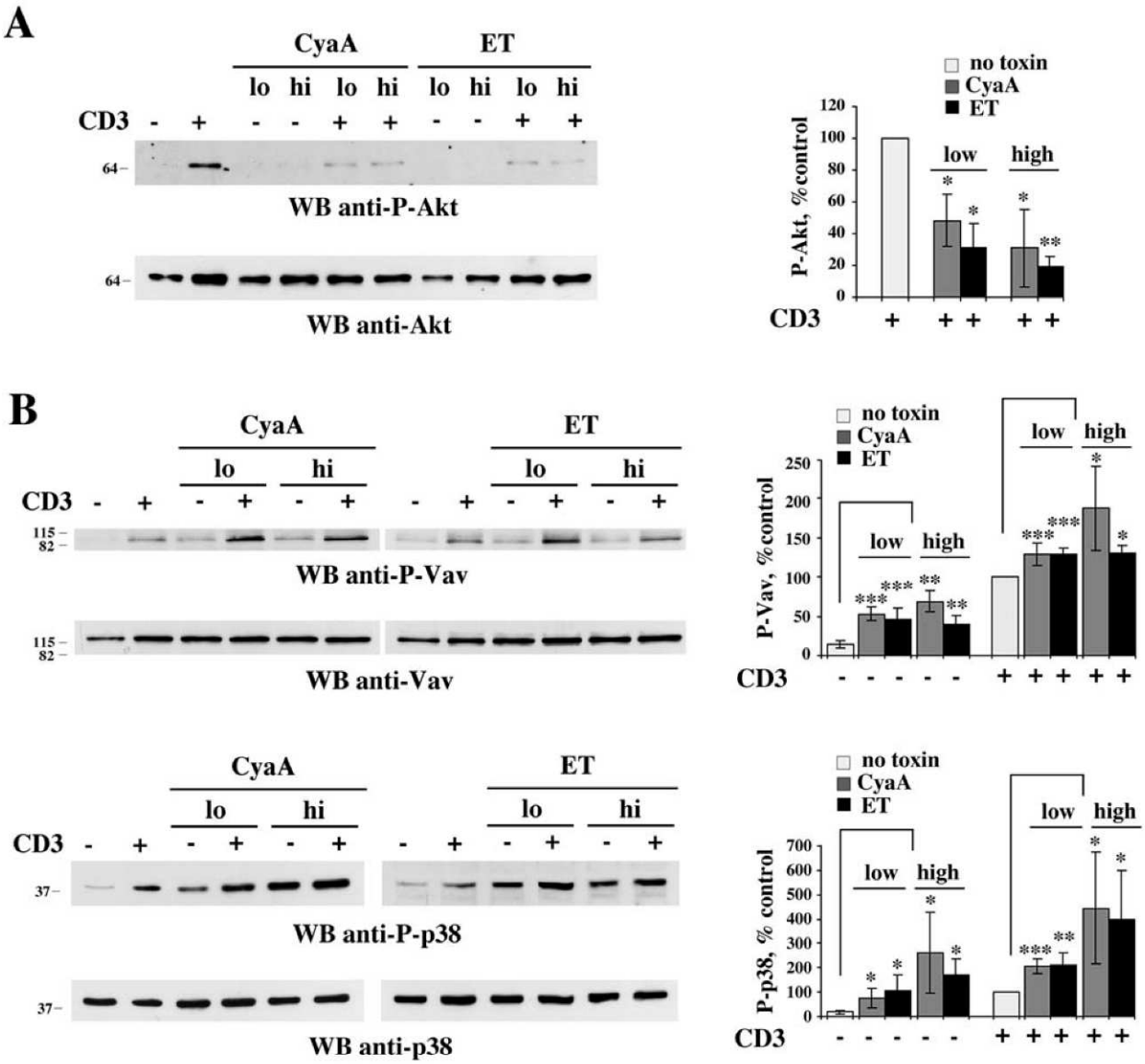

Figure 7. Low CyaA or ET concentrations impair TCR–dependent Akt1 phosphorylation while enhancing Vav1 and p38 phosphorylation. (A) Immunoblot analysis, using a phosphospecific antibody, of Akt1 activation in postnuclear supernatants from PBL activated for 5 min by CD3 cross-linking in the presence or absence of 45 nM CyaA or 110 nM ET (CyaA hi, ET hi) or alternatively in the presence or absence of 0.28 nM CyaA or 0.11 nM ET (CyaA lo, ET lo). A representative experiment is shown ($n = 3$). (B) Immunoblot analysis, using phosphospecific antibodies, of Vav1 (*top*) or p38 (*bottom*) activation in postnuclear supernatants from PBL activated for 1 min (Vav) or 5 min (p38) by CD3 cross-linking in the presence or absence of 45 nM CyaA or 110 nM ET (CyaA hi, ET hi) or alternatively in the presence or absence of 0.28 nM CyaA or 0.11 nM ET (CyaA lo, ET lo). Filters were stripped and re-probed with control antibodies. Representative experiments are shown ($n \geq 4$). The migration of molecular mass markers is indicated. The graphs on the right of the immunoblots show the quantification by laser densitometry of the relative levels of Akt1, Vav1, and p38 phosphorylation (phosphorylation in anti-CD3 stimulated cells taken as 100%) in PBL activated by CD3 cross-linking in the presence or absence of 45 nM CyaA or 110 nM ET (CyaA hi, ET hi) or alternatively in the presence or absence of 0.28 nM CyaA or 0.11 nM ET (CyaA lo, ET lo). ***$P \leq 0.001$ **$P \leq 0.01$; *$P \leq 0.05$. Error bars, SD.
doi:10.1371/journal.ppat.1000325.g007

We have previously characterized a Fyn dependent, Lck independent pathway linking the TCR to Vav1 phosphorylation and p38 activation which could be potentiated by PGE_2 [41]. Together with the evidence implicating Vav1 and p38 in Th2 cell differentiation, the Th1 bias observed in $Fyn^{-/-}$ mice [42,43] may suggest a potential involvement of this cAMP sensitive pathway in the Th2 promoting activity of ET and CyaA.

It is noteworthy that the effects of ET and CyaA are almost undistinguishable, notwithstanding their differences in stucture, mode of cell entry and intracellular localization. ET is an A–B type toxin, consisting of a cell binding component, PA, which targets cells *via* the receptors TEM8 or CMG2, and a toxin component, EF. ET enters the cell by receptor mediated internalization and is transported to the endosomes, wherefrom it is released into the

cytosol [11]. CyaA is a single polypeptide which binds to target cells both directly and through a membrane receptor, which in macrophages and other APC is the integrin CD11b/CD18 [44]. Following binding, the adenylate cyclase N-terminal domain is translocated accross the plasma membrane of target cells [12]. Hence EF and CyaA produce cAMP not only with different kinetics, which is delayed for ET probably due to the multistep mechanism of delivery into host cells, but also at different subcellular locations, in the cytosol with a prevalent perinuclear localization, and close to the plasma membrane, respectively [45–47]. The role of AKAPs in segregation of PKA pools at specific subcellular localizations and dynamic recruitment of phosphodiesterases underscores the importance of the spatiotemporal control of cAMP signaling [48]. By focalizing cAMP production at distinct sites within the cell, EF and CyaA could differentially affect early and late events in TCR signaling. Our findings indicate that the critical targets of the cAMP dependent Th2 polarizing activities of ET and CyaA can be activated independently of the subcellular site of cAMP production. It is likely that the sustained cAMP production overrides the negative local feedback mechanisms, resulting in loss of compartmentalization of cAMP dependent signaling. It should be however underlined that low ET concentrations are almost as effective as high concentrations in triggering PKA activation, suggesting that ET may modulate other functions, such as CREB mediated gene expression [45,47], through activation of specific PKA pools.

Both ET and CyaA have been reported to potentiate antibody responses and development of antigen specific Th2 cells in mice when coadministered with antigen [13–17]. This adjuvant activity had been related to their capacity to modulate cytokine production by dendritic cells and macrophages *in vitro*, resulting in reduction in IL-12 and enhancement in IL-10 and IL-4 expression [13–16,18,19]. Our finding that ET and CyaA directly affect the Th1/Th2 balance by favouring Th2 cell development suggests that their adjuvanticity is also due to their effects on $CD4^+$ T cells. This activity appears mediated by cAMP, as it cannot be reproduced by the respective enzymatically deficient mutants. The Th2 polarizing effects of these toxins resulting from their modulation of cytokine expression by APC have also been related to their cAMP elevating activity [15,18,19,49]. Consistent with these findings, both non-hydrolysable cAMP analogues and PGE_2 have been reported to favour Th2 cell development both by directly affecting $CD4^+$ T cell differentiation [4,6,8] and by shaping the pattern of cytokine production by APC [19–21]. The Th2 driving activity of ET may be very relevant to cutaneous anthrax, where there is a limited toxin production and where resolution of infection has been causally linked to the development of an antibody response against the toxin [50,51].

As opposed to the clear-cut role of cAMP in both the direct and the APC dependent Th2 driving activity of ET or CyaA *in vitro*, the role of cAMP in the adjuvanticity of the toxins *in vivo* is more controvertial. While the adjuvant activity of adenylate cyclase deficient ET mutants has as yet not been tested *in vivo*, there are discrepancies as to the adjuvanticity of catalytically inactive CyaA mutants, which have been proposed to result from a number of factors, including the genetic background of the mouse strain, the route of antigen delivery, the dose of CyaA mutant and the vaccination schedule [14,15,52,53]. Genetically detoxified mutants of other cAMP elevating toxins such as CT or LT-I, or their individual B (binding) subunits, have been demonstrated to retain adjuvant activity [10], indicating that both cAMP production and toxin binding to specific receptors contribute to their adjuvanticity. This possibility has been ruled out for ET, as PA does not harbour any activity either on APC or T cells *in vitro* nor acts as an adjuvant *in vivo* [16]. On the other hand, at variance with other reports [15,53], an enzymatically deficient CyaA mutant, highly purified to rule out a contamination by LPS, has been reported to display adjuvant properties comparable or even superior to wild-type CyaA [14,52]. A potential implication of CD11b/CD18 in the adjuvanticity of CyaA appears unlikely, as this integrin suppresses cytokine production by dendritic cells [54,55], and moreover does not account either for the immunodeviating activity of CyaA on APC *in vitro*, which is cAMP dependent [15,18,19], or for the conflicting results obtained by different groups *in vivo* [14,15,52,53]. An integrated and detailed analysis of the structural and functional interaction of adenylate cyclase toxins with the different cellular components which together orchestrate the immune response is expected not only to clarify their mechanism of adjuvanticity but also to lead to the development of more specific and effective adjuvants.

Materials and Methods

Cells, antibodies, reagents, and toxins

Peripheral blood mononuclear cells were purified from buffy coats from anonymous healthy donors (collectively ~30, available from authorised blood banks) by density gradient centrifugation on Ficoll-Paque (Amersham Biosciences, Buckinghamshire, UK), using a Beckman GS-6R tabletop centrifuge (Beckman Coulter SpA, Milan, Italy). Cells were washed 2× in phosphate buffered saline (PBS), resuspended in RPMI 1640 (Invitrogen Ltd, Paisley, UK) (buffered with sodium bicarbonate to pH 7.2) supplemented with 7.5% fetal calf serum (FCS) (Hyclone, Thermofischer Scientific Inc, SouthLogan, UT), plated in plastic flasks (Sarstedt AG, Numbrecht, Germany) and incubated overnight at 37°C in a humidified atmosphere with 5% CO_2. Non-adherent cells, which consisted principally of peripheral blood lymphocytes (PBL) and of which >90% were T cells ($CD3^+$), were centrifuged at 800×*g* for 5 min at room temperature in Beckman GS-6R tabletop centrifuge and resuspended in fresh RPMI 1640 supplemented with 7.5% FCS.

For cAMP measurement, T cells were purified from peripheral blood mononuclear cell suspensions using the StemSep Human T cell enrichment kit (Voden Medical Instruments SpA, Milan, Italy).

Phosphospecific antibodies recognizing the phosphorylated active forms of CD3ζ, ZAP-70 (Y493), Vav1 (Y160), Akt1 (T308/S473), Erk1/2 (T202/Y204), p38 (T180/Y182) and CREB (S133), as well as an antibody recognizing phosphorylated Y505 on Lck, were from Cell Signaling Technology (Beverly, MA), Santa Cruz Biotechnology (Santa Cruz, CA) and Biosource Europe SA (Nivelles, Belgium). An antibody against the phosphorylated PKA consensus phosphorylation site, R-X-X-pT-X-X/R-R-X-pS-X-X, was purchased from Cell Signaling Technology. Anti-CD3ζ, -Lck, ZAP-70, -Vav, -Erk2, -p38, -CREB and anti-actin antibodies were from Santa Cruz Biotechnology, Upstate Biotechnology (Dundee, UK) and Cell Signaling Technology. A mAb suitable for immunoprecipitation of tyrosine phosphorylated CD3ζ was kindly provided by M. Banyiash. Fluorochrome-labeled anti-CD3 mAb were obtained from Becton Dickinson Biosciences (Milan, Italy). Unlabeled secondary antibodies were purchased from Cappel (ICN Pharmaceuticals Inc, CA) and peroxidase labeled antibodies from Amersham Biosciences. IgG antibodies from OKT3 (anti-CD3; American Type Culture Collection, Manassas, VA) hybridoma supernatants were purified on Mabtrap (Amersham Biosciences, Inc) and titrated by flow cytometry.

CyaA and the enzymatically inactive variant CyaA-E5 (resulting from a Leu-Gln dipeptide insertion between D188 and I189 in the

catalytic core of the enzyme) were expressed in *E. coli* and purified to near homogeneity by previously established procedures modified as described [56] in order to eliminate most of the contaminating endotoxin. The specific activity of CyaA, measured as described in Ladant *et al.* [26] was higher than 500 μmol cAMP/min.mg whereas CyaA-E5 had no detectable enzymatic activity. In both preparations the endotoxin content, determined using a LAL assay (QCL-1000 kit from Lonza), was below 0.5 EU/μg protein. PA, LF and EL1 were expressed in *E. coli* and purified as described [25,45,57]. H89, KT5720, IBMX and 8-CPT were purchased from Sigma-Aldrich (Milan, Italy) and Calbiochem (Merck Biosciences GmbH, Schwalboch, Germany).

Cell activations and lysis, immunoblots

For immunoblot analyses cells were plated at 5×10^6 cells/ml in plastic flasks in RPMI 1640 supplemented with 7.5% FCS and 2 mM $CaCl_2$ (required for CyaA entry into the cells), added with CyaA/CyaA-E5, and incubated at 37°C in a humidified atmosphere with 5% CO_2 for 2 h before activation. Alternatively, cells were plated as above, added with ET (ratio PA:EF 1.6), and incubated at 37°C for 6 h before activation. Activations by TCR/CD3 cross-linking were performed by incubating PBL with saturating concentrations of anti-CD3 mAb (as assessed by flow cytometry) and 50 μg ml^{-1} secondary antibodies (goat anti-mouse immunoglobulin Ig) in RPMI 1640 for 1–5 min at 37°C as previously described [58]. None of the above mentioned treatments affected cell viability, as assessed by Trypan blue exclusion (data not shown). When required, cells were pretreated with the PKA inhibitors, H89 (20 μM) and KT5720 (56 nM), or with the PDE inhibitor, IBMX (0.5 mM), for 1 h before addition of ET or CyaA. Alternatively, cells were treated for 30 min with 8-CPT (100 μM).

Cells were recovered by centrifugation at 16,000×*g* for 30 sec at 4°C in an Eppendorf 5415R microcentrifuge (Eppendorf srl, Milan, Italy), washed 2× in PBS and lysed in 1% (v/v) Triton X-100 in 20 mM Tris-HCl pH 8, 150 mM NaCl (in the presence of 0.2 mg/ml Na orthovanadate, 1 μg/ml pepstatin, leupeptin, and aprotinin, and 10 mM phenyl methyl sulfonyl fluoride). To normalize for variations in protein content among samples, equal amounts of proteins from each sample (measured using a kit from Pierce, Rockford, IL) were resolved by 12% SDS-PAGE and transferred to 0.45-μm nitrocellulose filters Whatman GmbH, Dassel, Germany). Prestained molecular mass markers (Invitrogen) were included in each gel.

Immunoblots were carried out using primary antibodies and peroxidase-labeled secondary antibodies according to the manufacturers' instructions and a chemiluminescence detection kit (Pierce). Blots were scanned using a laser densitometer (Duoscan T2500 Agfa, Milan, Italy) and quantified using the ImageQuant 5.0 software (Molecular Dynamics, Sunnyvale, CA). Data were normalized to loading controls.

T cell proliferation assays, cytokine, and cAMP measurements

For proliferation assays, cells (2×10^5/sample) were plated in 96-well plates in RPMI 1640 supplemented with 7.5% FCS (and 2 mM $CaCl_2$ for CyaA treatments and respective controls), added with CyaA/CyaA-E5 (0.07–45 nM) or ET/EL1 (0.01 pM–1.1 nM), and incubated at 37°C in a humidified atmosphere with 5% CO_2 for 2 h (CyaA) or 6 h (ET) before activation. Cells were activated by CD3 cross-linking on secondary antibody-coated plates as described [58] and processed 16–48 h after activation. [^{3}H]-thymidine (1 mCi) was added to each microtiter well (96-well plates) for the last 18 h of culture. After harvesting the cells with an automatic harvester (Micromate 196, Canberra Packard, Meriden, CT), proliferation was determined by measuring the [^{3}H]thymidine (Amersham, Buckinghamshire, UK) incorporation in a β-counter (Matrix 9600, Canberra Packard, Meriden, CT).

To measure Th cell differentiation, enriched human $CD4^+$ T cells were activated by immobilized anti-CD3 mAb (purified from OKT3 hybridoma supernatants on Mabtrap, Amersham Biosciences Europe) as described [59], in the absence or presence of recombinant hIL-12 (2 ng/ml, Sigma-Aldrich Milan, Italy) to promote Th1 differentiation, or recombinant hIL-4 (10 ng/ml, Sigma-Aldrich Milan, Italy) to promote Th2 differentiation. Recombinant hIL-2 (kindly provided by Eurocetus Milan, Italy) was added to the cultures on day 4 and 7. After 10 days, cells (1×10^6) were washed, stimulated for 24 h or 48 h using anti-CD3 mAb and the levels of IL-4, IL-13, IFNγ and TNF-α were measured by ELISPOT as described [59].

Intracellular cAMP was quantitated by enzyme-linked immunoassay kit (Biotrak EIA, Amersham Biosciences) according to the manufacturers' instructions. For these experiments, cells (1×10^6 plated in 96-well plates in 200 μl RPMI 1640/7.5% FCS) were treated with CyaA/CyaA-E5 or ET/EL1 as described above for 30 min to 24 h in a humidified atmosphere with 5% CO_2. At the end of the treatment, cells were washed 2× in PBS and lysed in the lysis reagent included in the kit.

RNA purification and real-time quantitative RT–PCR

Total RNA was extracted from Th cells, polarized as described above, using Tri Reagent (Ambion, Austin, TX). Reverse transcription-polymerase chain reaction (RT-PCR) was carried out on 400 ng total RNA using ImProm-II™ reverse transcriptase and and oligo-dT (Promega Italia srl, Milan, Italy) as first strand primer.

Real-time quantitative PCR was performed using SYBR Green I SensiMix™ dT Kit (Quantace, Watford, UK) according to the manufacturer's instructions, in an Opticon 2 Continuous Fluorescence Detection System (MJ Research, Bio-Rad Laboratories, Waltham, MA). All samples were run in duplicate on 96-well optical PCR plates (Roche Diagnostics, Milan, Italy). The specific primers used to amplify cDNA fragments corresponding to c-maf, GATA-3, T-bet and GAPDH were: 5′-TGGAGTCGGAGAA-GAACCAG-3′ (*sense*), 5′-GCTTCCAAAATGTGGCGTAT-3′ (*antisense*) for c-Maf; 5′-GAAGGAAGGCATCCAGACCAG-3′ (*sense*), 5′-ACCCATGGCGGTGACCATGC-3′ (*antisense*) for GATA-3; 5′-TAATAACCCCTTTGCCAAAGG-3′ (*sense*); and 5′-TCCCCCAAGGAATTGACAGT-3′ (*anti-sense*) for T-bet and 5′-TGCACCACCAACTGCTTAGC-3′ (*sense*) and 5′-GGCATGGACTGTGGTCATGAG-3′ (*anti-sense*) for GAPDH. After an initial denaturation for 10 min at 95°C, denaturation at the subsequent 40 cycles was performed for 15 s at 95°C, followed by 15 s primer annealing at 60°C and a final extension at 72°C for 30 s. The $\Delta\Delta C_T$ method [60] was applied as a comparative quantification method. The specificity of the amplified fragment was demonstrated by the melting curve, where a single peak was observed for each sample amplified with c-maf, GATA-3, T-bet and GAPDH primers. c-maf, GATA-3 and T-bet mRNA levels were normalized to GAPDH, used as a housekeeping gene.

Statistical analyses

Mean values, standard deviation values and Student's *t* test (unpaired) were calculated using the Microsoft Excel application. A level of $P<0.05$ was considered statistically significant.

Acknowledgments

The authors want to thank Sonia Grassini for skilled technical assistance.

Author Contributions

Conceived and designed the experiments: SRP CM MMD CTB. Performed the experiments: SRP MB NC IZ. Analyzed the data: SRP MB NC CM MMD CTB. Contributed reagents/materials/analysis tools: IZ DL. Wrote the paper: DL CM MMD CTB.

References

1. Abbas AK, Murphy KM, Sher A (1996) Functional diversity of helper T lymphocytes. Nature 383: 787–793.
2. Glimcher LH, Murphy KM (2000) Lineage commitment in the immune system: the T helper lymphocyte grows up. Genes Dev 14: 1693–1711.
3. Norgauer J, Ibig Y, Gmeiner D, Herouy Y, Fiebich BL (2003) Prostaglandin E2 synthesis in human monocyte-derived dendritic cells. Int J Mol Med 12: 83–86.
4. Siegel MD, Zhang DH, Ray P, Ray A (1995) Activation of the interleukin-5 promoter by cAMP in murine EL-4 cells requires the GATA-3 and CLE0 elements. J Biol Chem 270: 24548–24555.
5. Lacour M, Arrighi JF, Muller KM, Carlberg C, Saurat JH, et al. (1994) cAMP up-regulates IL-4 and IL-5 production from activated CD4+ T cells while decreasing IL-2 release and NF-AT induction. Int Immunol 6: 1333–1343.
6. van der Pouw Kraan TC, Boeije LC, Smeenk RJ, Wijdenes J, Aarden LA (1995) Prostaglandin-E2 is a potent inhibitor of human interleukin 12 production. J Exp Med 181: 775–779.
7. Klein-Hessling S, Jha MK, Santner-Nanan B, Berberich-Siebelt F, Baumruker T, et al. (2003) Protein kinase A regulates GATA-3-dependent activation of IL-5 gene expression in Th2 cells. J Immunol 170: 2956–2961.
8. Tokoyoda K, Tsujikawa K, Matsushita H, Ono Y, Hayashi T, et al. (2004) Up-regulation of IL-4 production by the activated cAMP/cAMP-dependent protein kinase (protein kinase A) pathway in CD3/CD28-stimulated naive T cells. Int Immunol 16: 643–653.
9. Nirula A, Ho M, Phee H, Roose J, Weiss A (2006) Phosphoinositide-dependent kinase 1 targets protein kinase A in a pathway that regulates interleukin 4. J Exp Med 203: 1733–1744.
10. Freytag LC, Clements JD (1999) Bacterial toxins as mucosal adjuvants. Curr Top Microbiol Immunol 236: 215–236.
11. Young JA, Collier RJ (2007) Anthrax toxin: receptor binding, internalization, pore formation, and translocation. Annu Rev Biochem 76: 243–265.
12. Vojtova J, Kamanova J, Sebo P (2006) Bordetella adenylate cyclase toxin: a swift saboteur of host defense. Curr Opin Microbiol 9: 69–75.
13. Ross PJ, Lavelle EC, Mills KH, Boyd AP (2004) Adenylate cyclase toxin from *Bordetella pertussis* synergizes with lipopolysaccharide to promote innate interleukin-10 production and enhances the induction of Th2 and regulatory T cells. Infect Immun 72: 1568–1579.
14. Cheung GY, Xing D, Prior S, Corbel MJ, Parton R, et al. (2006) Effect of different forms of adenylate cyclase toxin of *Bordetella pertussis* on protection afforded by an acellular pertussis vaccine in a murine model. Infect Immun 74: 6797–6805.
15. Boyd AP, Ross PJ, Conroy H, Mahon N, Lavelle EC, et al. (2005) *Bordetella pertussis* adenylate cyclase toxin modulates innate and adaptive immune responses: distinct roles for acylation and enzymatic activity in immunomodulation and cell death. J Immunol 175: 730–738.
16. Duverger A, Jackson RJ, van Ginkel FW, Fischer R, Tafaro A, et al. (2006) *Bacillus anthracis* edema toxin acts as an adjuvant for mucosal immune responses to nasally administered vaccine antigens. J Immunol 176: 1776–1783.
17. Quesnel-Hellmann A, Cleret A, Vidal DR, Tournier JN (2006) Evidence for adjuvanticity of anthrax edema toxin. Vaccine 24: 699–702.
18. Spensieri F, Fedele G, Fazio C, Nasso M, Stefanelli P, et al. (2006) *Bordetella pertussis* inhibition of interleukin-12 (IL-12) p70 in human monocyte-derived dendritic cells blocks IL-12 p35 through adenylate cyclase toxin-dependent cyclic AMP induction. Infect Immun 74: 2831–2838.
19. Hickey FB, Brereton CF, Mills KH (2008) Adenylate cycalse toxin of *Bordetella pertussis* inhibits TLR-induced IRF-1 and IRF-8 activation and IL-12 production and enhances IL-10 through MAPK activation in dendritic cells. J Leukoc Biol 84: 234–243.
20. Kubo S, Takahashi HK, Takei M, Iwagaki H, Yoshino T, et al. (2004) E-prostanoid (EP)2/EP4 receptor-dependent maturation of human monocyte-derived dendritic cells and induction of helper T2 polarization. J Pharmacol Exp Ther 309: 1213–1220.
21. Bagley KC, Abdelwahab SF, Tuskan RG, Lewis GK (2006) Cholera toxin indirectly activates human monocyte-derived dendritic cells in vitro through the production of soluble factors, including prostaglandin E(2) and nitric oxide. Clin Vaccine Immunol 13: 106–115.
22. Paccani SR, Tonello F, Ghittoni R, Natale M, Muraro L, et al. (2005) Anthrax toxins suppress T lymphocyte activation by disrupting antigen receptor signaling. J Exp Med 201: 325–331.
23. Comer JE, Chopra AK, Peterson JW, Konig R (2005) Direct inhibition of T-lymphocyte activation by anthrax toxins in vivo. Infect Immun 73: 8275–8281.
24. Paccani SR, Dal Molin F, Benagiano M, Ladant D, D'Elios MM, et al. (2008) Suppression of T-lymphocyte activation and chemotaxis by the adenylate cyclase toxin of Bordetella pertussis. Infect Immun 76: 2822–2832.
25. Shen Y, Zhukovskaya NL, Guo Q, Florian J, Tang WJ (2005) Calcium-independent calmodulin binding and two-metal-ion catalytic mechanism of anthrax edema factor. Embo J 24: 929–941.
26. Ladant D, Glaser P, Ullmann A (1992) Insertional mutagenesis of *Bordetella pertussis* adenylate cyclase. J Biol Chem 267: 2244–2250.
27. Tasken K, Stokka AJ (2006) The molecular machinery for cAMP-dependent immunomodulation in T-cells. Biochem Soc Trans 34: 476–479.
28. Tanaka Y, So T, Lebedeva S, Croft M, Altman A (2005) Impaired IL-4 and c-Maf expression and enhanced Th1-cell development in Vav1-deficient mice. Blood 106: 1286–1295.
29. Dodeller F, Skapenko A, Kalden JR, Lipsky PE, Schulze-Koops H (2005) The p38 mitogen-activated protein kinase regulates effector functions of primary human CD4 T cells. Eur J Immunol 35: 3631–3642.
30. Schafer PH, Wadsworth SA, Wang L, Siekierka JJ (1999) p38α mitogen-activated protein kinase is activated by CD28-mediated signaling and is required for IL-4 production by human CD4+CD45RO+ T cells and Th2 effector cells. J Immunol 162: 7110–7119.
31. Chen CH, Zhang DH, LaPorte JM, Ray A (2000) Cyclic AMP activates p38 mitogen-activated protein kinase in Th2 cells: phosphorylation of GATA-3 and stimulation of Th2 cytokine gene expression. J Immunol 165: 5597–5605.
32. Maneechotesuwan K, Xin Y, Ito K, Jazrawi E, Lee KY, et al. (2007) Regulation of Th2 cytokine genes by p38 MAPK-mediated phosphorylation of GATA-3. J Immunol 178: 2491–2498.
33. Yu CT, Shih HM, Lai MZ (2001) Multiple signals required for cyclic AMP-responsive element binding protein (CREB) binding protein interaction induced by CD3/CD28 costimulation. J Immunol 166: 284–292.
34. Hewlett EL, Donato GM, Gray MC (2006) Macrophage cytotoxicity produced by adenylate cyclase toxin from Bordetella pertussis: more than just making cyclic AMP! Mol Microbiol 59: 447–459.
35. Scobie HM, Wigelsworth DJ, Marlett JM, Thomas D, Rainey GJ, et al. (2006) Anthrax toxin receptor 2-dependent lethal toxin killing in vivo. PLoS Pathog 2: e111. doi:10.1371/journal.ppat.0020111.
36. Knapp O, Maier E, Masin J, Sebo P, Benz R (2008) Pore formation by the Bordetella adenylate cyclase toxin in lipid bilayer membranes: role of voltage and pH. Biochim Biophys Acta 1778: 260–269.
37. Abrahamsen H, Baillie G, Ngai J, Vang T, Nika K, et al. (2004) TCR- and CD28-mediated recruitment of phosphodiesterase 4 to lipid rafts potentiates TCR signaling. J Immunol 173: 4847–4858.
38. Wang L, Liu F, Adamo ML (2001) Cyclic AMP inhibits extracellular signal-regulated kinase and phosphatidylinositol 3-kinase/Akt pathways by inhibiting Rap1. J Biol Chem 276: 37242–37249.
39. Lou L, Urbani J, Ribeiro-Neto F, Altschuler DL (2002) cAMP inhibition of Akt is mediated by activated and phosphorylated Rap1b. J Biol Chem 277: 32799–32806.
40. Gulbranson-Judge A, Tybulewicz VL, Walters AE, Toellner KM, MacLennan IC, et al. (1999) Defective immunoglobulin class switching in Vav-deficient mice is attributable to compromised T cell help. Eur J Immunol 29: 477–487.
41. Paccani SR, Patrussi L, Ulivieri C, Masferrer JL, D'Elios MM, et al. (2005) Nonsteroidal anti-inflammatory drugs inhibit a Fyn-dependent pathway coupled to Rac and stress kinase activation in TCR signaling. Blood 105: 2042–2048.
42. Davidson D, Shi X, Zhang S, Wang H, Nemer M, et al. (2004) Genetic evidence linking SAP, the X-linked lymphoproliferative gene product, to Src-related kinase FynT in T(H)2 cytokine regulation. Immunity 21: 707–717.
43. Cannons JL, Yu LJ, Hill B, Mijares LA, Dombroski D, et al. (2004) SAP regulates T(H)2 differentiation and PKC-theta-mediated activation of NF-kappaB1. Immunity 21: 693–706.
44. Guermonprez P, Khelef N, Blouin E, Rieu P, Ricciardi-Castagnoli P, et al. (2001) The adenylate cyclase toxin of Bordetella pertussis binds to target cells via the $\alpha_M\beta_2$ integrin (CD11b/CD18). J Exp Med 193: 1035–1044.
45. Dal Molin F, Tonello F, Ladant D, Zornetta I, Zamparo I, et al. (2006) Cell entry and cAMP imaging of anthrax edema toxin. EMBO J 25: 5405–5413.
46. Dal Molin F, Zornetta I, Puhar A, Tonello F, Zaccolo M, et al. (2008) cAMP imaging of cells treated with pertussis toxin, cholera toxin, and anthrax edema toxin. Biochem Biophys Res Commun 376: 429–433.
47. Puhar A, Dal Molin F, Horvath S, Ladants D, Montecucco C (2008) Anthrax edema toxin modulates PKA- and CREB-dependent signaling in two phases. PLoS ONE 3: e3564. doi:10.1371/journal.pone.0003564.
48. McConnachie G, Langeberg LK, Scott JD (2006) AKAP signaling complexes: getting to the heart of the matter. Trends Mol Med 12: 317–323.
49. Tournier JN, Quesnel-Hellmann A, Mathieu J, Montecucco C, Tang WJ, et al. (2005) Anthrax edema toxin cooperates with lethal toxin to impair cytokine secretion during infection of dendritic cells. J Immunol 174: 4934–4941.
50. Quinn CP, Dull PM, Semenova V, Li H, Crotty S, et al. (2004) Immune responses to *Bacillus anthracis* protective antigen in patients with bioterrorism-related cutaneous or inhalation anthrax. J Infect Dis 190: 1228–1236.
51. Harrison LH, Ezzell JW, Abshire TG, Kidd S, Kaufmann AF (1989) Evaluation of serologic tests for diagnosis of anthrax after an outbreak of cutaneous anthrax in Paraguay. J Infect Dis 160: 706–710.

52. Macdonald-Fyall J, Xing D, Corbel M, Baillie S, Parton R, et al. (2004) Adjuvanticity of native and detoxified adenylate cyclase toxin of *Bordetella pertussis* towards co-administered antigens. Vaccine 22: 4270–4281.
53. Hormozi K, Parton R, Coote J (1999) Adjuvant and protective properties of native and recombinant Bordetella pertussis adenylate cyclase toxin preparations in mice. FEMS Immunol Med Microbiol 23: 273–282.
54. Morelli AE, Larregina AT, Shufesky WJ, Zahorchak AF, Logar AJ, et al. (2003) Internalization of circulating apoptotic cells by splenic marginal zone dendritic cells: dependence on complement receptors and effect on cytokine production. Blood 101: 611–620.
55. Behrens EM, Sriram U, Shivers DK, Gallucci M, Ma Z, et al. (2007) Complement receptor 3 ligation of dendritic cells suppresses their stimulatory capacity. J Immunol 178: 6268–6279.
56. Preville X, Ladant D, Timmerman B, Leclerc C (2005) Eradication of established tumors by vaccination with recombinant *Bordetella pertussis* adenylate cyclase carrying the human papillomavirus 16 E7 oncoprotein. Cancer Res 65: 641–649.
57. Tonello F, Naletto L, Romanello V, Dal Molin F, Montecucco C (2004) Tyrosine-728 and glutamic acid-735 are essential for the metalloproteolytic activity of the lethal factor of *Bacillus anthracis*. Biochem Biophys Res Commun 313: 496–502.
58. Boncristiano M, Paccani SR, Barone S, Ulivieri C, Patrussi L, et al. (2003) The *Helicobacter pylori* vacuolating toxin inhibits T cell activation by two independent mechanisms. J Exp Med 198: 1887–1897.
59. Amedei A, Cappon A, Codolo G, Cabrelle A, Polenghi A, et al. (2006) The neutrophil-activating protein of *Helicobacter pylori* promotes Th1 immune responses. J Clin Invest 116: 1092–1101.
60. Livak KJ, Schmittgen TD (2001) Analysis of relative gene expression data using real-time quantitative PCR and the $2^{-\Delta\Delta CT}$ Method. Methods 25: 402–408.

Chapter V: Imaging the Cell Entry of the Anthrax Edema and Lethal toxins with Fluorescent Protein Chimerae

Summary

To investigate anthrax edema and lethal factors (EF and LF) entry and intracellular trafficking, they were C-terminally fused to the EGFP or mCherry. Both LF and EF chimerae bound to the surface of cells treated with protective antigen (PA) in a patchy mode. Binding was followed by rapid internalization, and the two anthrax factors were found to traffic along the same endocytic route with identical kinetics, indicating that their intracellular path is essentially dictated by PA. Colocalization studies indicated that anthrax toxins enter caveolin-1 containing compartments and then endosomes marked by PI3P and Rab5, but not by EEA1 and transferrin. After 40 minutes, both EF and LF chimerae are inside late compartments marked by LBPA. Eventually the catalytic activities of LF and of EF appear in the cytosol with kinetics consistent with translocation from the late endosomal lumen. Only the EGFP derivatives were active in the cytosol because they translocate through the PA channel, whilst the mCherry derivatives do not. This difference appears to be due to a higher resistance of mCherry to unfolding. After translocation, LF appears to be dispersed in the cytosol with some possible binding to organelles, whilst EF localized on the cytosolic face of late endosomes.

Introduction

Anthrax is a zoonosis, which may also affect humans, caused by infection with toxigenic strains of Bacillus anthracis, a spore-forming Gram positive bacterium largely diffused in the environment (Beyer and Turnbull, 2009; Koehler, 2009). Depending on the site of entry of spores or bacteria, humans may develop three forms of anthrax: cutaneous, gastrointestinal or pulmonary anthrax, the latter form being the most dangerous (Dixon et al., 1999). Virulent B. anthracis strains are characterized by the expression of three major virulence factors: an anti-phagocytic polyglutammic capsule, which largely prevents phagocytosis by neutrophils and macrophages (Fouet, 2009), and two A-B type toxins. The toxins are capable of binding and entering in almost any cell type, where they derange two major cell signalling pathways (Ascenzi et al., 2002, Mohayeri and Leppla, 2009). The two toxins were termed edema toxin because when injected sub-cutaneously it caused edema, and lethal toxin because it caused rapid death in guinea pigs and in the Fischer 344 rats (Smith and Keppie, 1954; Smith et al., 1955; Smith et al., 1956; Beall et

al., 1962). These two toxins share the same B binding component, a protein of 83 kDa, named protective antigen (PA) from the fact that it is an immunogen that provides effective protection against B. anthracis infection in several animal species, including humans (Cybulski et al., 2009). The A part of the lethal toxin is the lethal factor (LF, 90 kDa) and that of the edema toxin is the edema factor (EF, 89 kDa) (Young and Collier, 2007). PA binds to two different cell surface receptors: Tumor Endotelial Marker 8 (TEM8) and Capillary Morphogenesis Protein 2 (CMG2), both of which are widely expressed in different tissues and cell types (Van der Goot and Young, 2009). The removal of a 20 kDa N-terminal domain converts PA into the PA_{63} form, which self-associates into heptamers $(PA_{63})_7$ capable of binding LF and EF (Young and Collier, 2007; Van der Goot and Young, 2009). The $(PA_{63})_7$+LF complex (lethal toxin, LeTx) promotes its own endocytosis by entering surface rafts and inducing specific signalling events on the cytosolic face of the membrane (Abrami et al., 2003, 2006, 2008#1). Similar data are not available for the $(PA_{63})7$ +EF (EdTx) complex, and it remains to be determined if this toxin follows the same binding and intracellular trafficking route followed by LeTx. After entering early endosomal compartments, LeTx reaches late endosomes, wherefrom LF is delivered into the cytosol (Abrami et al., 2004, 2005; Dal Molin et al., 2006; Puhar and Montecucco, 2007).

LF is a zinc metalloprotease that cleaves mitogen-activated protein kinase kinases (MAPKKs or MEKs) (Duesbery et al.,1998; Vitale et al., 1998, 2000; Tonello and Montecucco, 2009), thereby interfering with the MAPK cascade, a major signalling event triggered by surface receptors and controlling cell proliferation and survival (Gaestel et al., 2006). As this signalling plays a major role in the activation of immune cells, this inhibition accounts for the immuno-suppressive activity of LF (Pellizzari et al., 1999; Baldari et al., 2006; Tournier et al., 2009). EF is a calcium/calmodulin-activated adenylate cyclase, which catalyzes the formation of cAMP (Drum et al., 2002; Shen et al., 2005), thus altering cell signalling and tissue ion fluxes; the ensuing edema causes failure of different organs leading to rapid death (Firoved et al., 2005; Moayeri and Leppla, 2009). Another consequence is that EF is a strong inhibitor of the activation of different immune cells (Dal Molin et al., 2006; Puhar et al., 2008; Tournier et al., 2009). It is noteworthy that EF and LF have a strong synergistic action on the activation of dendritic cells and T cells (Paccani Rossi et al., 2005; Tournier et al., 2005).

The process of cell entry of EF and LF has been studied using cell fractionation and electron microscopic methods, and in several cases a construct between the N-terminal of LF and

diphtheria toxin (for recent review see Collier, 2009; Moayeri and Leppla, 2009; Van der Goot and Young, 2009). We have attempted to improve the knowledge of this essential process by producing chimerae consisting of the full length LF and EF molecules fused at their C-termini to different fluorescent proteins: enhanced green fluorescent protein (EGFP) or monomeric Cherry protein (mCherry) (Shaner et al., 2004, 2005). Fusion at the N terminus was avoided because this part of the molecule is essential for membrane translocation (Collier, 2009). We have found that the two toxins follow exactly the same pathway of entry and have similar kinetics. Both EF and LF enter the cytosol from late endosomal compartments only when coupled to EGFP, but not to the mCherry protein. The two toxins reach different cytosolic locations: LF diffuses in the cytosol whilst EF appears to remain bound to the cytosolic face of the limiting membrane of late endosomes.

Results

Fluorescent chimerae of EF and LF

The four chimerae EF-EGFP, EF-mCherry, LF-EGFP and LF-mCherry were produced as recombinant molecules with a N-terminal 6xHis, which allows easier purification (supplementary fig. S1) and was shown to confer to LF an increased capacity to enter and translocate across the $(PA_{63})_7$ transmembrane channel (Neumeyer et al., 2006).

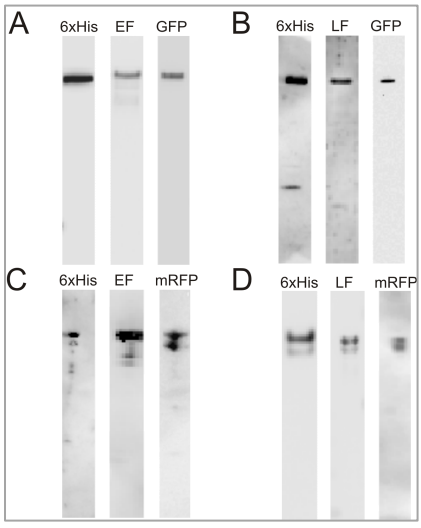

Fig. S1. Immunoblot analysis of EF and LF chimeric derivatives. Immunoblot analysis of SDS-PAGE separated, fluorescent chimeric proteins (0.1 µg) performed with antibodies against the 6xHis, EF or LF, and fluorescent protein mCherry or EGFP. We used an antibody against mRFP that recognizes a conserved epitope on mCherry because no antibody was available for the latter red variant. WB analysis of EGFP derivatives of EF (A) and LF (B) and of EF-mCherry (C) and LF-mCherry (D).

The two LF derivatives and the two EF derivatives were controlled for their ability to perform their respective biochemical activities in cell culture. BHK cells were used because of their flattened shape, which favours fluorescence microscopy, and because they express both PA receptors, as the majority of sensitive animal cells do. Fig. 1 shows that both of the EGFP derivatives of LF and

EF are active in the cell cytoplasm, though with lower levels of activity with respect to their unconjugated counterparts, as if a smaller number of molecules is capable of reaching the cytosol when EGFP is present. However, these chimeric toxins do reach the cytosol and therefore can report on each step of the cell entry process. On the contrary, the two mCherry derivatives displayed no intracellular activity. The most likely explanation was that the two mCherry chimerae were unable to unfold and translocate into the cytosol across the $(PA_{63})_7$ channel (Collier, 2009).

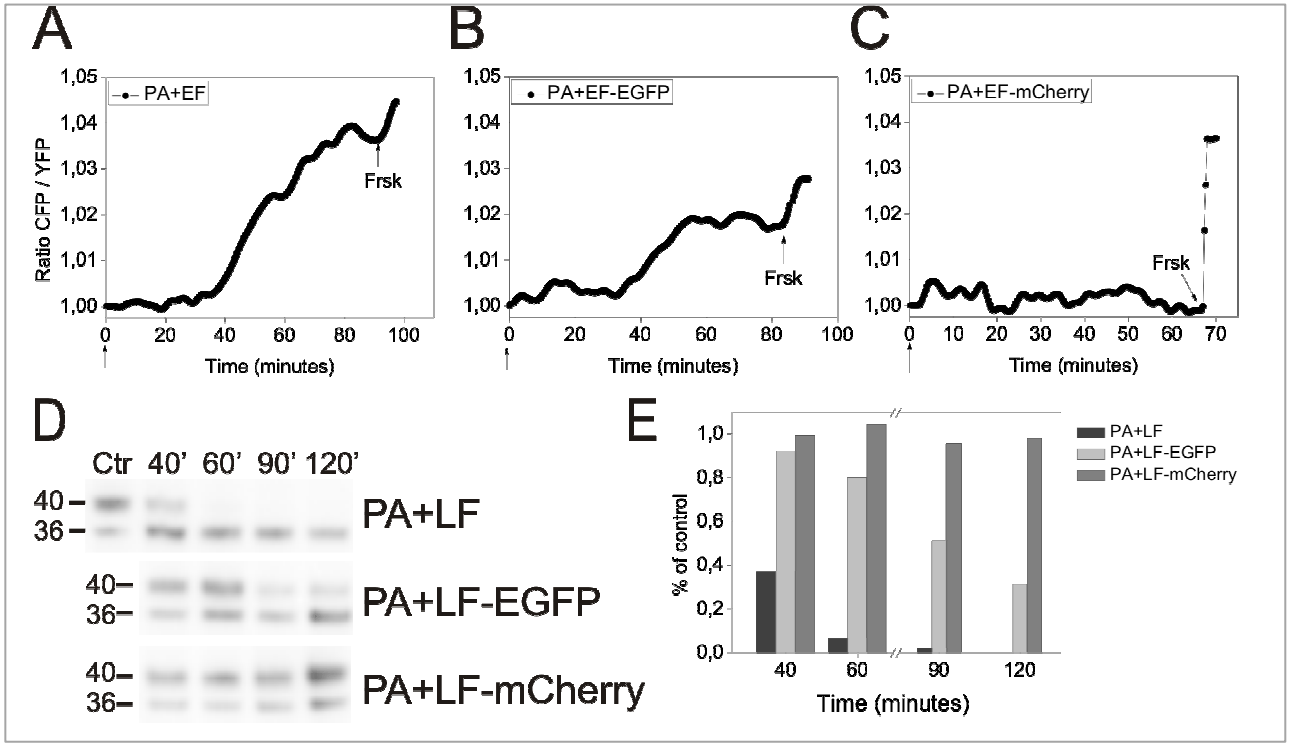

Figure 1. Fluorescent chimeric anthrax edema factor and lethal factor are enzymatically active in the cytosol of cells in culture. cAMP fluorescence resonance energy transfer imaging in transfected cells expressing the catalytic PKA subunit-YFP and the regulatory PKA subunit-CFP in the cytosol. BHK cells were imaged after treatment with PA (400 nM) in combination with 200 nM of EF (A) or EF-EGFP (B) and EF-mCherry (C). Arrows indicate addition of toxins or forskolin (25 µM) as controls at the end of experiments. The time course of the cleavage of MEK 3 in BHK cells treated with PA (400 nM) and LF (200 nM), or LF-EGFP (200 nM) or LF-mCherry (200 nM) is given in panels D and E, and shows the corresponding quantification of the bands normalized with respect to the control. Cell extracts were made at the given time, and after SDS-PAGE, the proteins were blotted onto nitro-cellulose paper and stained with an anti-MEK 3 specific antibody directed versus the COOH-terminal peptide. Arrows indicate the full-length and cleaved forms of MEK 3. Notice that the two mCherry fusion proteins do not display activity.

To test this possibility, we measured translocation of the chimeric proteins through pores formed by PA_{63} in planar phospholipid bilayers (fig. 2). The EGFP derivatives of both LF and EF translocated with slightly lower efficiency and time course than the native proteins, whereas the mCherry derivatives did not translocate at all. We have not investigated in detail the reason for the

difference between mCherry and EGFP, but this is likely to be due to a different energy requirement for their unfolding, as shown by their different resistance to guanidinium induced unfolding (supplementary fig. S2). Protein unfolding has been well documented to be necessary for the translocation across the PA_{63} channel (Collier, 2009). According to these results, only EGFP-EF and EGFP-LF were used in the study of the final stage of cell intoxication.

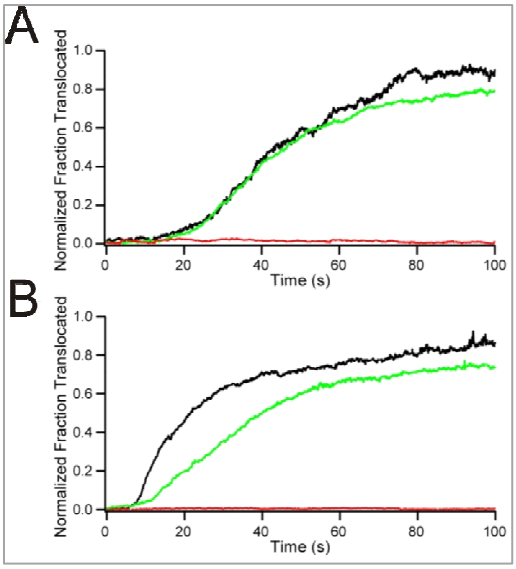

Figure 2. Translocation of chimeric proteins across artificial membranes. At time 0, translocation was initiated by adding 2 M KOH to the trans compartment to raise the pH from 5.5 to 7.2 and by increasing the membrane potential from $\Delta\psi$ = +20 mV to $\Delta\psi$ = +50mV. Under these conditions, with both compartments continuously stirred, there was a ~ 5 s mixing delay. Representative data are shown from n ≥ 3 trials. (A) Translocation of LF (black) versus LF fused with either EGFP (green) or mCherry (red). (B) Translocation of EF (black) versus EF fused with either EGFP (green) or mCherry (red).

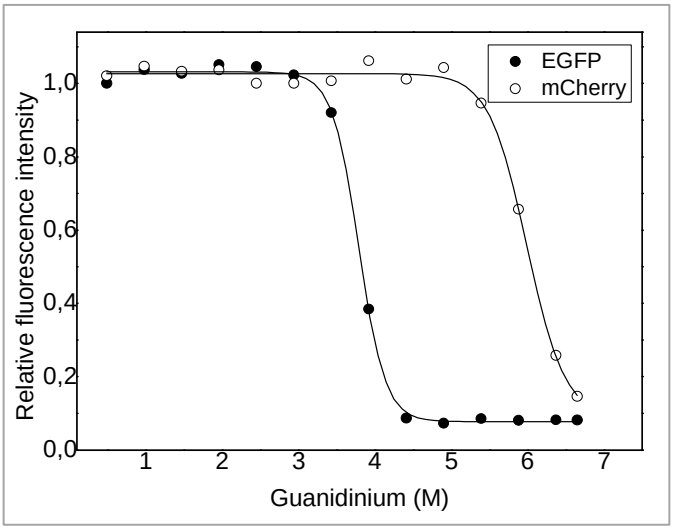

Fig. S2. Fluorescence changes for EGFP and mCherry accompanying protein unfolding in different concentration of guanidine hydrochloride. Protein samples (0.050 mg/ml) were incubated for 20 hours at 25 °C in the presence of various concentrations of guanidine hydrochloride. Unfolding curves were determined by exciting the samples at 365 nm and detecting the emitted fluorescence at appropriate wavelenght for EGFP and mCherry (see supplementary material and methods).

Cell binding of the EGFP derivatives of EF and LF

In the present work, we have attempted to use conditions that mimic the in vivo situation. In particular, we have not used cells transfected with TEM8 or CMG2 in order to avoid the possibility that a high receptor density may distort the picture of toxin cell surface binding by creating arrays

or clusters of PA receptors. In addition, the toxins were added at 37°C, to avoid the cell shape change that takes place when the cells are shifted from the cold (to avoid endocytosis) to 37°C. PA was added and allowed to be processed to PA_{63} for 12 minutes; LF or/and EF were then added and cells were fixed, after 2 minutes, and processed for fluorescence microscopy. Fig. 3 shows that both the LF and EF fluorescent derivatives bind to BHK cell in a spotty manner, consistent with the biochemical findings of Abrami et al. (2003) in CHO cells showing that the binding of LF to $(PA_{63})_7$ oligomers induces the partition of LeTx in plasma membrane rafts. Clearly, the presence of the EGFP did not prevent binding of EF or LF to $(PA_{63})_7$. However, the strength of the fluorescence signal was not optimal and was improved by using anti-GFP antibodies, which was found not to alter the patterns of fluorescence distribution.

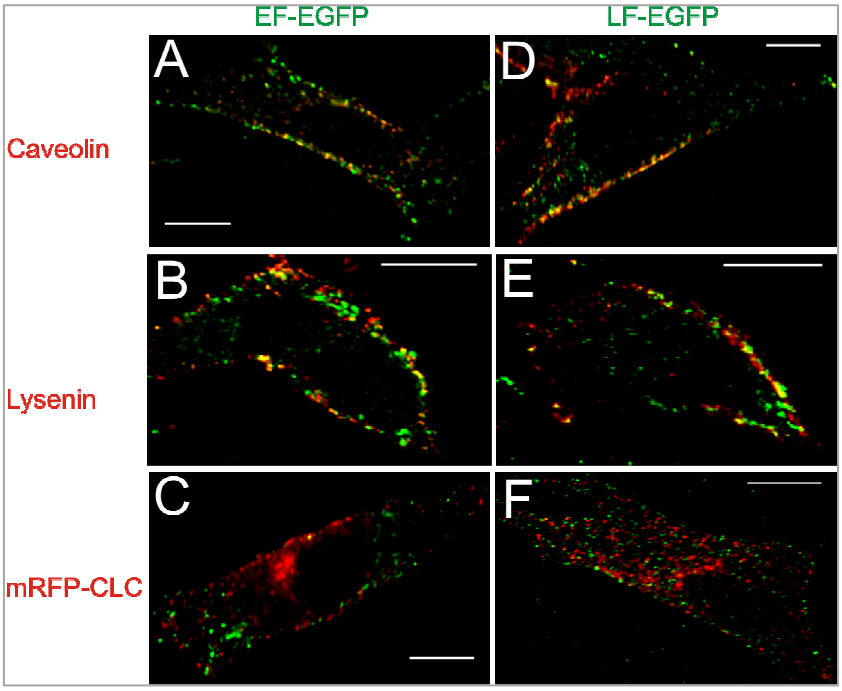

Figure 3. Binding of EF and LF fluorescent chimeric proteins to BHK cells. EF-EGFP (A) and LF-EGFP (D) colocalize with caveolin1 and Lysenin (B and E, respectively) in peripheral punctate structures in cells pre-treated with PA_{83} to allow its binding and processing and for 2 min at 37°C with chimeric subunits, fixed and stained with antibodies to caveolin. Lower or no colocalization with clathrin is seen in cells transfected with mRFP-clathrin light chain (C and F, respectively), intoxicated, stained and fixed. Every image is the 2D projection of a 3D image stack after restoration. The overlap between the two signals is depicted in yellow. Scale bar is equal to 10 µm.

No difference in the spotty binding of LF-EGFP and EF-EGFP was ever noticed in hundreds of cells observed, and the two fluorescent toxins always overlapped, indicating that LF and EF distribute similarly on the cell surface after binding. Partial colocalization of the fluorescence of the two toxins was found with caveolin-1 (~50%) and Lysenin (~35%), a protein that binds specifically to

sphingomyelin enriched in raft membrane domains (Yamaji et al., 1998); there was little colocalization with the clathrin light chain (~3%). This finding is in agreement with the previous report that $(PA_{63})_7$ -LF enters into membrane rafts of the plasma membrane that contain caveolin-1 (Abrami et al., 2003, 2008), and also with the finding that dynamin is involved in the cell entry of LF, as dynamin is essential for the endocytosis of caveolin-1 rafts (Boll et al., 2004). The similar distribution of EGFP fluorescence always seen with EF and LF derivatives indicates also that $(PA_{63})_7$-EF segregates into plasma membrane rafts, as previously found for $(PA_{63})_7$-LF.

Endocytosis of LF-EGFPF and EF-EGFP

Binding of the chimeric fluorescent LF and EF is followed by rapid endocytosis, as only five minutes after EF or LF addition at 37°C a significant amount of EF/LF is found inside cells.

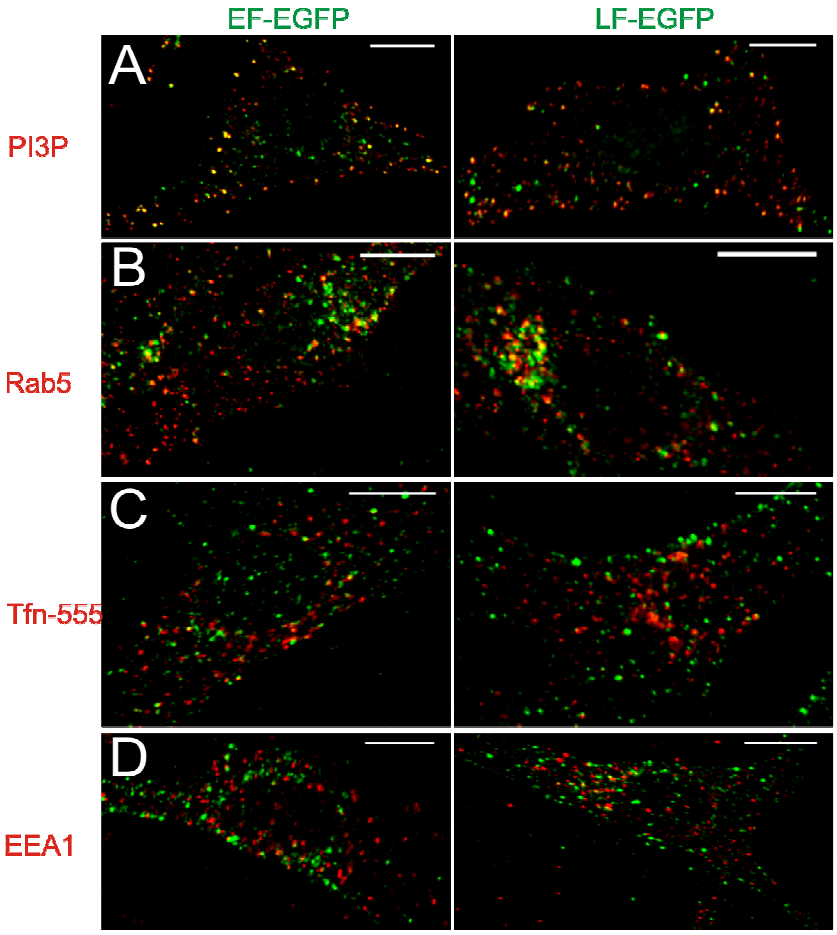

Figure 4. EF and LF fluorescent chimeric proteins enter early endosomes containing phosphatidyl-phosphoinositides. Intracellular distribution of the chimeric toxins in BHK cells treated with PA together with EGFP chimeric subunit for 10 minutes at 37°C show a pattern of spots primarily distributed in the cell periphery. EF-EGFP (A, left panel) and LF-EGFP (A, right panel) colocalize with early endosomes lipid PI3P and Rab5 (B, left and right panels, respectively), but not with Tnf-555 (C) or EEA1 (D). Every image is the 2D maximum intensity projection of z-stack sections after restoration. The overlap between the two signals is depicted in yellow. Scale bar is equal to 10 µm.

Fig. 4 shows the images obtained after addition of PA together with LF/EF, a situation that mimics the in vivo one, with incubation for 10 min at 37°C. The two toxins are inside early endosomal compartments that contain phosphatidylinositol 3-phosphate (PI3P) (~30%) and Rab5 (~40%) but, apparently, not transferrin (Tfn) or the early endosomal antigen 1 (EEA1), 13% and 12%,

respectively. This is not unprecedented, as it has been reported that cholera toxin B- and Simian virus 40-containing organelles are distinct from classical EEA1- and transferrin-positive endosomes, but communicate with early endosomes via a pathway regulated by Rab5 (Pelkmans et al., 2001; Nichols, 2002; Parton and Simons, 2007). These data show that the endocytosis of LF/EF mediated by the binding of PA to its receptors in BHK cells is rapid and efficient, with undetectable LF/EF remaining on the cell surface after 10 minutes. This kinetics reflects the fact that the $(PA_{63})_7$-LF triggers its own endocytosis via a modification of the PA receptor, which takes place on the cytosolic side and includes ubiquitination, palmitoylation and induction of specific phosphorylation of the receptors associated proteins (Abrami et al., 2004; 2008).

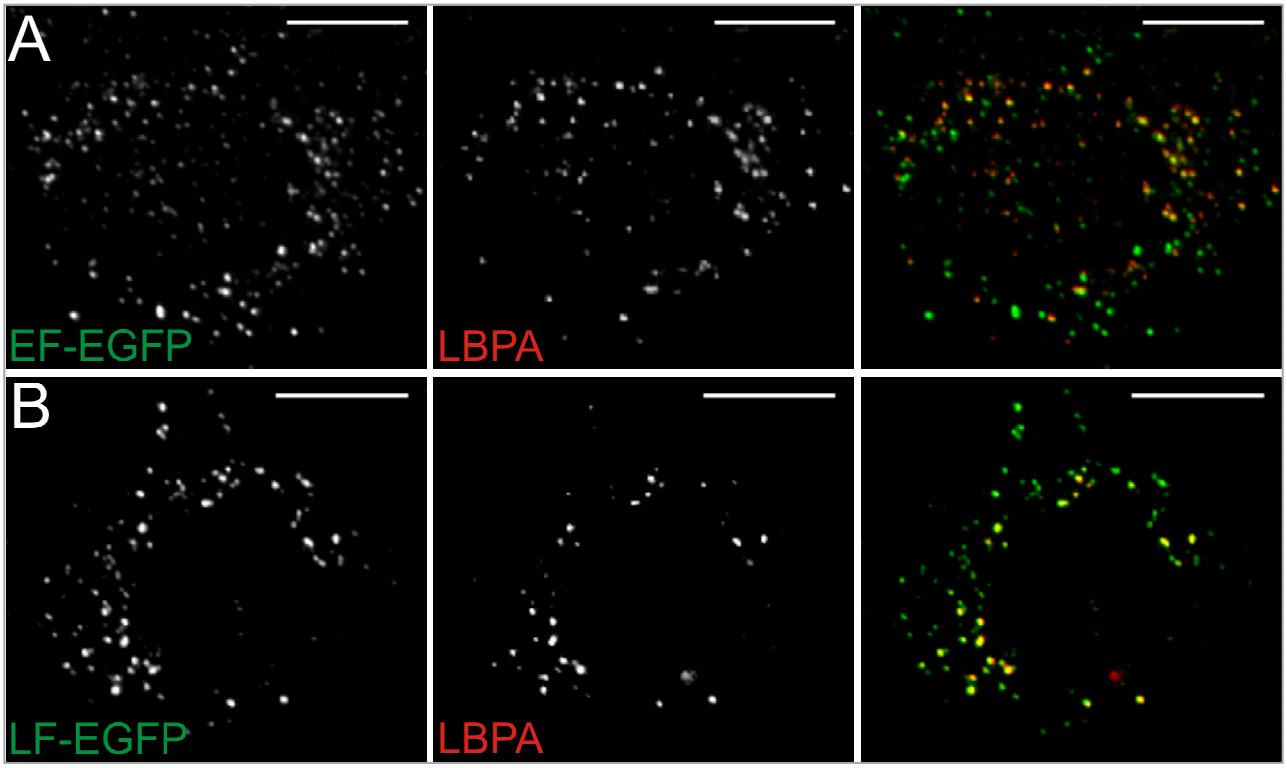

Figure 5. Intracellular distribution of the fluorescent chimeric EF and LF after 40 min of incubation with BHK cells. BHK cells were treated with PA and EGFP catalytic subunits for 40 min at 37°C, fixed and mounted for fluorescence microscopy. As shown by the identical pattern of spots in the cell perinuclear region and the extensive co-localization with the lipid molecule LBPA the chimeric EF-EGFP (A) and LF-EGFP (B) reach the late endosomal compartments. Every image is the 2D projection of a 3D image stack after restoration. The overlap between the two signals is depicted in yellow. Scale bar is equal to 10 µm.

After 40 min, both EF and LF are inside late endosomal compartments, as indicated by the extensive colocalization (~94%) with the lipid molecule LBPA (fig. 5), a marker of late endosomal compartments (Kobayashi et al., 1998).

The patterns of intracellular distribution of the fluorescence of EF-mCherry and LF-EGFP are identical up to this time point (fig. 6). However, it should be recalled that preliminary experiments had indicated that the conjugation with the mCherry protein prevents cell intoxication, by blocking the translocation of EF/LF across the trans-membrane PA channel. Therefore, to study the intracellular distribution of LF and EF at later time points, only the EGFP derivatives were used.

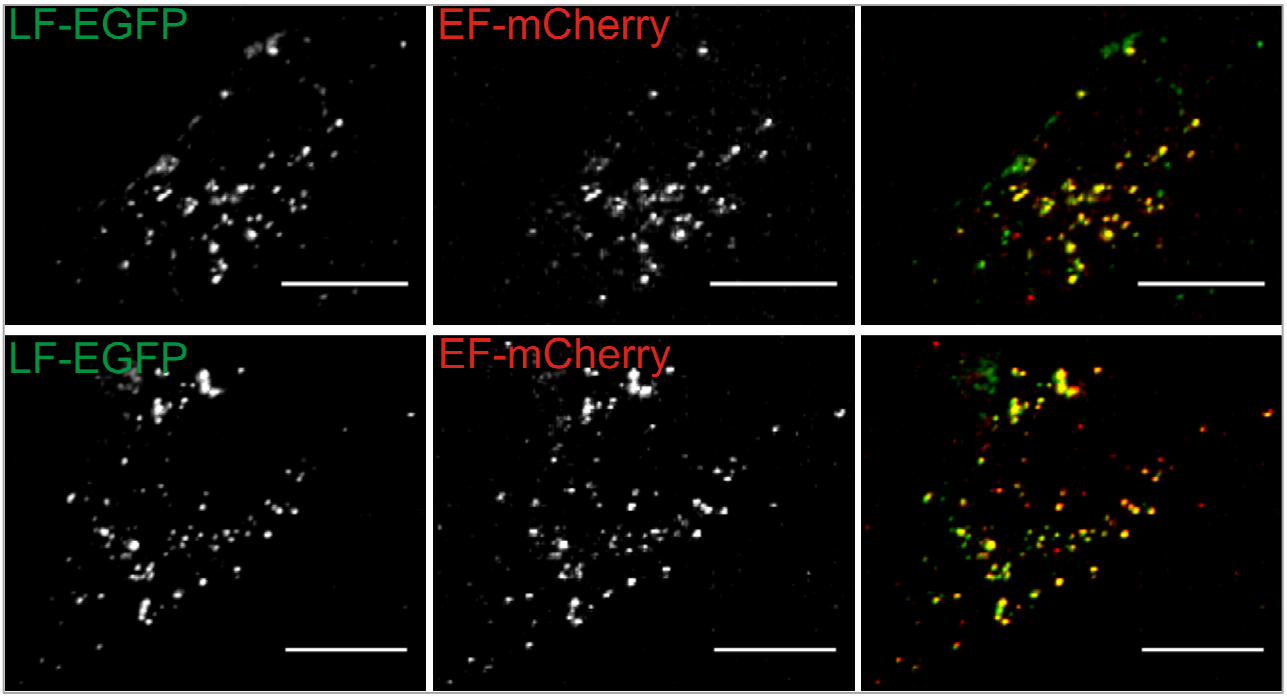

Figure 6. The intracellular distributions of EF-mCherry and LF-EGFP are identical. After internalization of PA in presence of both LF-EGFP and EF-mCherry for 40 minutes at 37°C, BHK cells were fixed and observed in a widefield microscopy. Here, two examples of the co-localization of the two catalytic moieties (in yellow) in the perinuclear region. Every image is the 2D maximum intensity projection of a 3D image stack after restoration. Scale bar, 10 µm.

Different intracellular localization of EF and LF

Fig. 7 shows that, after 90 minutes from their addition, EF and LF have a different intracellular localization, with LF being clearly cytosolic, though its fluorescence signal is weak, a fact that is expected because the signal is dispersed in a large volume (fig. 7B). Notwithstanding the low fluorescence signal of LF, its distribution of the LF fluorescence is not exactly homogeneous throughout the cytoplasm, as there appears to be some concentration on cellular organelles; this interpretation is in agreement with the fact that LF is active on MEK isoforms that are known to be localized on organelles such as MEK-1 and -2 (Golgi and endosomes), MEK-6 (mitochondria) (Wunderlich et al., 2001; Poderoso et al., 2008). At variance, EF-EGFP gives a spotty and perinuclear fluorescence distribution and shows an extensive colocalization with the LBPA specific

marker of late endosomes (fig. 7A). Together with the fact that, after 90 minutes, EF-EGFP has translocated across the late endosomal membrane and has already caused an large increase in cAMP level (fig. 1), this picture clearly indicates that in vivo EF translocates from the lumen of late endosomes to the cytosol in such a way as to remain associated to the cytosolic surface of these intracellular compartments. We are currently investigating the molecular basis of this specific association, and have already excluded that the N-terminal domain of EF is involved.

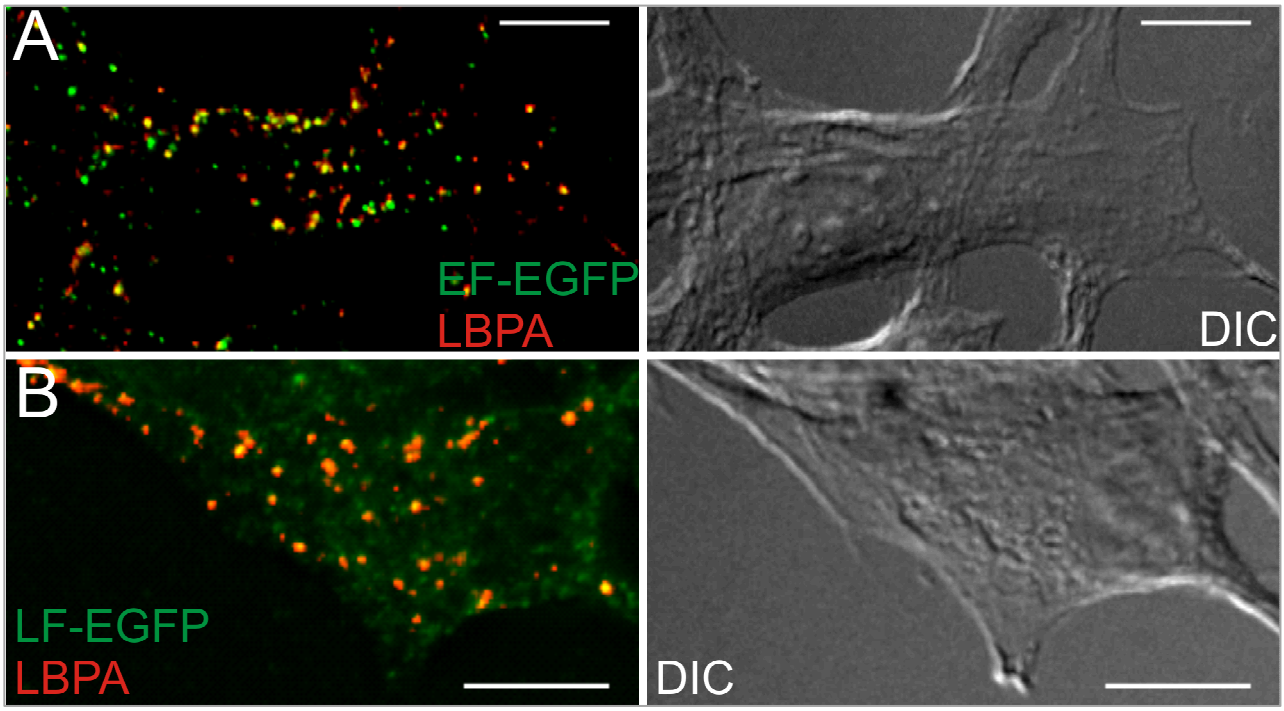

Figure 7. EF and LF have a different intracellular localization. Edema factor fluorescent derivative remains associated to the cytosolic surface of late endosomal organelles after a long incubation, whilst lethal factor chimeric subunit is cytosolic. BHK cells were incubated with PA and EF-EGFP (A) or LF-EGFP (B) at 37°C for 90 min to detect their intracellular distribution after translocation from $(PA_{63})_7$ pore (see Fig.1 and text). Cell samples were fixed and immunostained with appropriate antibodies. DIC images and merged 2D channels, after restoration of a 3D image stacks, are shown. Scale bar, 10 µm.

It has been recently shown that diphtheria toxin and Clostridium botulinum C2 toxin cross the endosomal membrane and refold into the cytosol with the contribution of chaperone proteins that are inhibited by radicicol and cyclosporin A (Ratts et al., 2003; Kalser et al., 2009). The presence of these two drugs together did not cause any reduction in the entry into the cytosol, monitored by enzymatic activity, western blotting and fluorescence, of the native LF and EF proteins or of their conjugates with EGFP (not shown).

Discussion

This is the first study of the trafficking of the two anthrax toxins, LF and EF, in the same cell at the same time, a situation that mimics the in vivo one in which both toxins are released by the infecting B. anthracis. We found that EF and LF clearly follow the same pathway of entry from cell surface beginning from the concentration into plasma membrane microdomains, which leads to a rapid endocytosis involving multiple routes to early endosomes. The two toxins end up in the same late endosomes, wherefrom LF and EF translocate from the lumen into the cytosol, but reach two different intracellular localizations. EF remains associated with late endosomes, whilst LF diffuses into the cytosol. This is in agreement with the recently acquired knowledge that LF cleaves different MEK proteins that are known to have different intracellular distributions (Fanger et al., 1997; Vitale et al., 2000; Wunderlich et al., 2001; Poderoso et al., 2008), whilst EF generates a intracellular gradient of cAMP from the perinuclear area to the cortical sub-plasma membrane region (Dal Molin et al., 2006; Puhar et al., 2008).

The binding of LF and EF to cell surface bound $(PA_{63})_7$ gives a patched distribution on the plasma membrane which is fully consistent with the two toxins entering cholesterol-enriched microdomains. This was established previously by Abrami et al. (2003) for LF and it is extended here to EF. Here, we also found that several of these microdomains are enriched in sphingomyelin, as there is colocalization with Lysenin, a sphingomyelin binding protein (Yamaji et al., 1998). Cell surface binding was found to be rapidly followed by endocytosis. From the present study, it appears that the $(PA_{63})_7$-LF and $(PA_{63})_7$-EF complexes may enter various types of endocytic vesicles to reach early endosomal compartments, most of them marked by the presence of Rab5 and PI3P. It should be noted that, here, we have deliberately chosen not to use any method that may alter the physiological process of cell entry of these toxins, such as cholesterol depletion, cross-linking, inhibitors, siRNA, over-expression of different proteins, etc. The only "cell manipulation" procedure used was that of expressing the light chain of clathrin coupled to mRFP, but this protein was not shown to colocalize substantially with the two toxins. This result is at variance with the previous report of a clathrin-mediated endocytosis of LF in CHO cells (Abrami et al., 2003), and we have no satisfactory explanation for such a difference. However, different cell lines were used and fibroblasts are known to have multiple pathways of endocytosis (Doherty and McMahon, 2009). On the other hand, the present result is not surprising in light of the fact that other toxins that bind via an oligomeric binding protomer enter cells via non-clathrin dependent

trafficking (Sandvig et al., 2008) and that the majority of ligands that bind to raft microdomains are preferentially taken up via by clathrin-independent endocytosis (Nichols 2003).

No matter which initial traffic route is taken by LF and EF to early endosomes, eventually they reach the late endosomal compartments, wherefrom they translocate into the cytosol. We found that this translocation is not assisted by chaperons inhibited by radicicol or cyclosporin A, as was found to be the case for diphtheria toxin and Clostridium botulinum (Kalser et al., 2009). A remarkable finding presented here is that both LF and EF are capable of pulling the conjugated EGFP through the PA channel with high efficiency, whilst this is not the case of the mCherry fluorescent protein. The mCherry fluorescent protein is more resistant to unfolding than the EGFP protein (supplementary fig. S2). Taken together, these data provide further evidence in favor of the prevailing model of translocation of LF that envisages a low pH driven unfolding of the polypeptide chain to enter the PA channel and translocation of the unfolded chain that refolds in the neutral pH of the cytosol (Krantz et al., 2005; Collier, 2009). At the same time, the present reports shows that mCherry may not be an appropriate choice as reporter of intracellularly acting toxins.

Experimental Procedures

Cells, antibodies and reagents

BHK cells were maintained in DMEM (Gibco) containing 10% heat-inactivated foetal calf serum (FCS, Euroclone), penicillin (100 U/ml) and streptomycin (100 mg/ml). Antibodies were obtained from the following sources: anti-His tag monoclonal antibody from Novagen, monoclonal and polyclonal anti-GFP, -RFP, -EF and -LF polyclonal antibodies from Abcam, anti-caveolin and anti-EEA1 antibodies from BD Transduction Laboratories; anti-PI3P from Echelon, anti-Rab5 from Synaptic System, anti-LBPA (6C4) was a kind gift of J. Gruenberg (University of Geneva, CH), Tfn-Alexa555 and fluorescently labelled secondary antibodies from Molecular Probes. Lysenin and Lysenin antiserum were from Peptide Institute Inc.; FuGENE HD from Roche Diagnostics Corporation. The plasmid encoding mRFP-Clathrin Light Chain was from Addgene. Reagents were Sigma-Aldrich and Calbiochem.

Cloning, expression and purification of chimeric proteins

The EGFP gene was PCR-amplified from pEGFP-N1 (Clontech) using the following primers: forward 5'-AAAGAGCTCATGGTGAGCAAGGGCG-3' and reverse 5'-AAAGAATTCCTTGTACAGCTCGTCCAT-3'.

The mCherry gene was PCR-amplified from pREST B, generously gift from RY Tsien, using the following primers: forward 5'-AAAGAGCTCATGGCCACTGGTGGACAG-3' and reverse 5'-AAAGAATTCTAGGCGCCGGYGGAGT-3'. Both fragments were digested with SacI and EcoRI and inserted in pRSET A (Invitrogen) containing LF or EF respectively, as previously described (Dal Molin et al., 2006), downstream from an N-terminal His-tag coding region. The sequences were confirmed by DNA sequencing. LF chimeric derivatives were expressed in E. coli BL21(DE3) and EF chimeric proteins in E. coli BL21 (DE3)-Codon Plus-RIL (Stratagene) grown at 37°C in LB broth containing 100 mg/ml ampicillin or 100 mg/ml ampicillin and 34 mg/ml chloramphenicol. After 4 h of induction with 1 mM isopropyl-1-thio-a-D-galactopyranoside at 30°C, the pellet was resuspended in buffer A (50 mM Na2HPO4, 500 mM NaCl, pH 8) and lysozyme (0.1 mg/ml). Bacterial cells were disrupted by ultrasonic dispersion and centrifuged, and the supernatant was loaded onto a Hi-trap column charged with Cu2SO4 and equilibrated with buffer A. The column was washed with buffer A, the protein was eluted with a 0–100 mM imidazole gradient, and the fractions containing chimeric proteins were pooled and dialysed against binding buffer (50 mM Tris, 20 mM NaCl and 1 mM EDTA, pH 7.5) to remove imidazole and NaCl. The identities of chimeric proteins were assessed by immunoblotting with anti-His tag, anti-LF, anti-EF and anti-GFP or anti-mRFP antibodies. We used this antibody, which recognizes a conserved epitope on mCherry, because no other was available for this red variant.

FRET imaging of cAMP intracellular dynamics

BHK cells (2.0×105) were co-transfected with 1 μg of two pcDNA3.1 plasmids, one carrying the catalytic (C) subunit of PKA fused to YFP (C-YFP) and one carrying the regulatory (R) subunit of PKA fused to CFP (RII-CFP) (Lissandron et al., 2005) using FuGENE HD, following manufacturer's instructions. Forty eight hours after transfection, cells were incubated in a balanced salt solution (NaCl 135 mM, KCl 5mM, KH2PO4 0.4mM, MgSO4 1 mM, HEPES 20mM, CaCl2 1.8 mM, glucose 5.4 mM, pH 7.4) in a microscope-adapted micro-incubator equipped with a temperature controller (HTC, Italy) at 37°C and constant 5% CO2 pressure. Toxins were added after about 15 minutes of imaging, and images were taken every 20 seconds for the indicated time periods. Integration time was 200 msec. At each time point, the intracellular cAMP level was estimated by measuring the ratio between the background-subtracted CFP emission image and the YFP emission image upon excitation of CFP (R CFP/YFP) (Mongillo et al., 2005). Images were acquired using an oil immersion 40X PlanApo 1.4 NA objective on a Leica DMI6000 microscope. FRET images were collected

through a BP 436/20-nm excitation filter and a custom-made optical beam splitter built with a 515-nm dichroic mirror and ET 480/40-nm and ET 535/30-nm emission filters. All optical filters were obtained from Chroma Technologies. A cooled camera from OES (Padova, Italy) with a 1,4 Megapixel CCD and a sensor resolution of 1360 × 1024 Pixel was used. The acquisition software was from OES (Padova, Italy). Recorded images were processed with WCIF ImageJ v1.40 (http://rsb.info.nih.gov/ij).

MEK3 cleavage by chimeric lethal factor

BHK cells (1.5×104) were incubated with PA 400 nM and 200 nM lethal factor or LF-EGFP in DMEM plus 1% BSA at 37°C for different time periods in a 96-well plate. After removal of the culture medium, the cells were lysed, subjected to SDS-PAGE, and immunoblotted for the isoform 3 of MEK with a specific polyclonal antibody from Santa Cruz Biotechnology (USA). Samples were developed with ECL plus detection system (Amersham Biosciences), and chemiluminescence emission was detected with ChemiDoc™ XRS (Biorad). Band intensities were quantified with the Quantity One software from Biorad.

Fluorescence microscopy

Sub-confluent BHK cells grown on glass coverslips were rinsed two times with DMEM plus 2% w/v BSA and intoxicated for different periods of time with EF-mCherry and/or LF-EGFP (200 nM) and PA (600 nM). Then cells were washed with PBS, fixed with ice-cold acetone for 5 min at room temperature to localize the toxins along the endocytic pathway or with PFA 4% (10 min at room temperature) to mark endocytic lipids and incubated sequentially with a mixture of primary antibodies and a mixture of fluorescent secondary antibodies. To monitor cell surface binding, cells were first treated with PA_{83} for 12 minutes, washed, incubated with LF or EF derivatives for 2 minutes at 37°C and immediately washed and fixed. All antibody incubations were performed for 1 hour at room temperature. Images were acquired sequentially with a FITC and Texas Red® filter set (Chroma Technology corp., USA) with 250 msec or longer integration times by using an oil immersion 63X PlanApo 1.40 NA objective on a Leica DMIRE3 widefield inverted microscope equipped with a DC 500 digital camera with 1300x1030 pixels resolution from Leica. The acquisition software was FW4000 (Leica). Images were processed with ImageJ v1.40 (http://rsb.info.nih.gov/ij) and colocalization analysis on raw images was performed using the JaCoP plug-in (Bolte and Cordelières, 2006) and OBCOL plug-in (Woodcroft et al., 2009) under

ImageJ. Colocalization is expressed as ratio of objects that contain the fluorescent pairs on red objects

Translocation of chimeric proteins across artificial membranes

Planar phospholipid bilayers were formed by standard methods (Janowiak et al., 2009). Once a membrane was formed, WT PA_{63} prepore (25 pM) was added to the cis compartment, held at a $\Delta\psi$ = + 20 mV with respect to the trans compartment. Free PA_{63} not inserted into the membrane was removed by perfusion. Binding cargo (LF, EF, or chimeric proteins) was added to the cis compartment (1 μg/ml), and the progress of binding to PA channels was monitored by the decrease in conductance. Free was removed by buffer exchange. Translocation was initiated by raising the pH of the trans compartment to pH 7.2 with 2 M KOH, while maintaining the cis compartment pH at 5.5. At the same time, we increased the membrane potential from $\Delta\psi$ = +20 mV to $\Delta\psi$ = +50mV. Experiments were normalized to controls lacking cargo protein ($n \geq 3$). All planar phospholipid experiments were performed in a Warner Instruments Planar Lipid Bilayer Workstation (BC 525D, Hamden, CT).

Supplementary Experimantal procedures

EGFP and mCherry guanidine hydrochloride-induced equilibrium unfolding

Protein samples (0.050 mg/ml in 50 mM TRIS, pH 8.0) were incubated for 20 hours at 25 °C in the presence of various concentrations of guanidine hydrochloride. Unfolding curves were determined by exciting the samples at 365 nm and detecting the emitted fluorescence at 510 nm for EGFP and at 610 nm for mCherry. Fluorescence was recorded in a quartz-microcuvette cell (105.250-QS, Hellma, Milan) kept at 25°C on a Perkin–Elmer LS-50 spectrofluorimeter. The data were analyzed with Origin v. 7.5 software.

References

- Abrami, L., Liu, S., Cosson, P., Leppla, S.H. and van der Goot, F.G. (2003) Anthrax toxin triggers endocytosis of its receptor via a lipid raft-mediated clathrin-dependent process. J Cell Biol 160: 321-328.

- Abrami, L., Lindsay, M., Parton, R.G., Leppla, S.H. and van der Goot, F.G. (2004) Membrane insertion of anthrax protective antigen and cytoplasmic delivery of lethal factor occur at different stages of the endocytic pathway. J Cell Biol 166: 645-651.
- Abrami, L., Reig, N. and van der Goot, F.G. (2005) Anthrax toxin: the long and winding road that leads to the kill. Trends Microbiol 13: 72-78.
- Abrami, L., Leppla, S.H. and van der Goot, F.G. (2006) Receptor palmitoylation and ubiquitination regulate anthrax toxin endocytosis. J Cell Biol 172: 309-320.
- Abrami, L., Kunz, B., Deuquet, J., Bafico, A., Davidson, G. and van der Goot, F.G. (2008) Functional interactions between anthrax toxin receptors and the WNT signalling protein LRP6. Cell Microbiol 10: 2509-2519.
- Abrami, L., Kunz, B., Iacovache, I. and van der Goot, F.G. (2008#1) Palmitoylation and ubiquitination regulate exit of the Wnt signaling protein LRP6 from the endoplasmic reticulum. PNAS 105: 5384-5389.
- Ascenzi, P., Visca, P., Ippolito, G., Spallarossa, A., Bolognesi, M. and Montecucco, C. (2002) Anthrax toxin: a tripartite lethal combination. FEBS Lett 531: 384-388.
- Baldari, C.T., Tonello, F., Paccani Rossi, S. and Montecucco, C. (2006) Anthrax toxins: A paradigm of bacterial immune suppression. Trends Immunol 27: 434-440.
- Beall, F.A., Taylor, M.J. and Thorne, C.B. (1962) Rapid lethal effect in rats of a third component found upon fractionating the toxin of *Bacillus anthracis*. J Bacteriol 83: 1274-1280.
- Beyer, W. and Turnbull, P.C.B. (2009) Anthrax in animals. Mol Aspects Med 30: 481–489
- Boll, W., Ehrlich, M., Collier, R.J. and Kirchhausen, T. (2004) Effects of dynamin inactivation on pathways of anthrax toxin uptake. Eur J Cell Biol 83: 281-288.
- Bolte, S. and Cordelières, F.P. (2006) A guided tour into subcellular colocalization analysis in light microscopy. J Microsc 224: 213-232.
- Collier, R.J. (2009) Membrane translocation by anthrax toxin. Mol Aspects Med 30:413-422.
- Cybulski, R.J.J., Sanz, P. and O'Brien, A.D. (2009) Anthrax vaccination strategies. Mol Aspects Med 30: 490–502.
- Dal Molin, F., Tonello, F., Ladant, D., Zornetta, I., Zamparo, I., Di Benedetto, G., et al. (2006) Cell entry and cAMP imaging of anthrax edema toxin. EMBO J 25: 5405-5413.

- Dixon, T.C., Meselson, M., Guillemin, J. and Hanna, P.C. (1999) Anthrax. N Engl J Med 341: 815-826.
- Doherty, G.J. and McMahon, H.T. (2009) Mechanisms of endocytosis. Annu Rev Biochem 78: 857-902.
- Drum, C.L., Yan, S., Bard, J., Shen, Y., Lu, D., Soelaiman, S., .et al. (2002) Structural basis for the activation of anthrax adenylyl cyclase exotoxin by calmodulin. Nature 415: 396-402.
- Duesbery, N.S., Webb, C.P., Leppla, S.H., Gordon, V.M., Klimpel, K.R., Copeland, T.D., et al. (1998) Proteolytic inactivation of MAP-kinase-kinase by anthrax lethal factor. Science 280: 734-737.
- Fanger, G.R., Johnson, N.L. and Johnson, G.L. (1997) MEK kinases are regulated by EGF and selectively interact with Rac/Cdc42. EMBO J 16: 4961-4972.
- Firoved, A.M., Miller, G.F., Moayeri, M., Kakkar, R., Shen, Y., Wiggins, J.F., et al. (2005) Bacillus anthracis edema toxin causes extensive tissue lesions and rapid lethality in mice. Am J Pathol 167: 1309-1320.
- Fouet, A. (2009) The surface of Bacillus anthracis. Mol Aspects Med 30: 374–385.
- Gaestel, M. (2006) MAPKAP kinases - MKs - two's company, three's a crowd. Nat Rev Mol Cell Biol 7: 120-130.
- Janowiak, B.E., Finkelstein, A. and Collier, R.J. (2009) An approach to characterizing single-subunit mutations in multimeric prepores and pores of anthrax protective antigen. Protein Sci 18: 348-358.
- Kaiser, E., Pust, S., Kroll, C. and Barth, H. (2009) Cyclophilin A facilitates translocation of the Clostridium botulinum C2 toxin across membranes of acidified endosomes into the cytosol of mammalian cells. Cell Microbiol 11: 780-795.
- Kobayashi, T., Stang, E., Fang, K.S., de Moerloose, P., Parton, R.G. and Gruenberg, J. (1998) A lipid associated with the antiphospholipid syndrome regulates endosome structure and function. Nature 392: 193-197.
- Koehler, T.M. (2009) Bacillus anthracis physiology and genetics. Mol Aspects Med 30: 386-396.
- Krantz, B.A., Melnyk, R.A., Zhang, S., Juris, S.J., Lacy, D.B., Wu, Z., et al. (2005) A phenylalanine clamp catalyzes protein translocation through the anthrax toxin pore. Science 309: 777-781.

- Lissandron, V., Terrin, A., Collini, M., D'Alfonso, L., Chirico, G., Pantano, S. et al. (2005) Improvement of a FRET-based indicator for cAMP by linker design and stabilization of donor-acceptor interaction. J Mol Biol 354: 546-555.
- Moayeri, M. and Leppla, S.H. (2009) Cellular and systemic effects of anthrax lethal toxin and edema toxin. Mol Aspects Med 30: 439-455.
- Mongillo, M., Terrin, A., Evellin, S., Lissandron, V. and Zaccolo, M. (2005) Study of cyclic adenosine monophosphate microdomains in cells. Methods Mol Biol 307: 1-13.
- Neumeyer, T., Tonello, F., Dal Molin, F., Schiffler, B. and Benz, R. (2006) Anthrax edema factor, voltage-dependent binding to the protective antigen ion channel and comparison to LF binding. J Biol Chem 281: 32335-32343.
- Nichols, B.J. (2002) A distinct class of endosome mediates clathrin-independent endocytosis to the Golgi complex. Nat Cell Biol 4: 374-378.
- Nichols, B. (2003) Caveosomes and endocytosis of lipid rafts. J Cell Sci 116: 4707-4714.
- Paccani Rossi, S., Tonello, F., Ghittoni, R., Natale, M., Muraro, L., D'Elios, M.M., et al. (2005) Anthrax toxins suppress T lymphocyte activation by disrupting antigen receptor signaling. J Exp Med 201: 325-331.
- Parton, R.G. and Simons, K. (2007) The multiple faces of caveolae. Nat Rev Mol Cell Biol 8: 185-194.
- Pelkmans, L., Kartenbeck, J. and Helenius, A. (2001) Caveolar endocytosis of simian virus 40 reveals a new two-step vesicular-transport pathway to the ER. Nat Cell Biol 3: 473-483.
- Pellizzari, R., Guidi-Rontani, C., Vitale, G., Mock, M. and Montecucco, C. (1999) Anthrax lethal factor cleaves MKK3 in macrophages and inhibits the LPS/IFNgamma-induced release of NO and TNFalpha. FEBS Lett 462: 199-204.
- Poderoso, C., Converso, D.P., Maloberti, P., Duarte, A., Neuman, I., Galli, S., Maciel, F.C., Paz, C.et al. (2008) A mitochondrial kinase complex is essential to mediate an ERK1/2-dependent phosphorylation of a key regulatory protein in steroid biosynthesis. PLoS One 3: e1443.
- Puhar, A. and Montecucco, C. (2007) Where and how do anthrax toxins exit endosomes to intoxicate host cells?. Trends Microbiol 15: 477-482.
- Puhar, A., Dal Molin, F., Horvath, S., Ladants, D. and Montecucco, C. (2008) Anthrax edema toxin modulates PKA- and CREB-dependent signaling in two phases. PLoS One 3: e3564.

- Ratts, R., Zeng, H., Berg, E.A., Blue, C., McComb, M.E., Costello, C.E., et al. (2003) The cytosolic entry of diphtheria toxin catalytic domain requires a host cell cytosolic translocation factor complex. J Cell Biol 160: 1139-1150.
- Sandvig, K., Torgersen, M.L., Raa, H.A. and van Deurs, B. (2008) Clathrin-independent endocytosis: from nonexisting to an extreme degree of complexity. Histochem Cell Biol 129: 267-276.
- Shaner, N.C., Campbell, R.E., Steinbach, P.A., Giepmans, B.N.G., Palmer, A.E. and Tsien, R.Y. (2004) Improved monomeric red, orange and yellow fluorescent proteins derived from Discosoma sp. red fluorescent protein. Nat Biotechnol 22: 1567-1572.
- Shaner, N.C., Steinbach, P.A. and Tsien, R.Y. (2005) A guide to choosing fluorescent proteins. Nat Methods 2: 905-909.
- Shen, Y., Zhukovskaya, N.L., Guo, Q., Florián, J. and Tang, W. (2005) Calcium-independent calmodulin binding and two-metal-ion catalytic mechanism of anthrax edema factor. EMBO J 24: 929-941.
- Smith, H. and Keppie, J. (1954) Observations on experimental anthrax; demonstration of a specific lethal factor produced in vivo by Bacillus anthracis. Nature 173: 869-870.
- Smith, H., Keppie, J., Stanley, J.L. and Harris-Smith, P.W. (1955) The chemical basis of the virulence of Bacillus anthracis. IV. Secondary shock as the major factor in death of guinea-pigs from anthrax. Br J Exp Pathol 36: 323-335.
- Smith, H., Tempest, D.W., Stanley, J.L., Harris-Smith, P.W. and Gallop, R.C. (1956) The chemical basis of the virulence of Bacillus anthracis. VII. Two components of the anthrax toxin: their relationship to known immunising aggressins. Br J Exp Pathol 37: 263-271.
- Tonello, F. and Montecucco, C. (2009) The anthrax lethal factor and its MAPK kinase-specific metalloprotease activity. Mol.Aspects Med 30: 431-438.
- Tournier, J., Quesnel-Hellmann, A., Mathieu, J., Montecucco, C., Tang, W., Mock, M., Vidal, D.R. and Goossens, P.L. (2005) Anthrax edema toxin cooperates with lethal toxin to impair cytokine secretion during infection of dendritic cells. J Immunol 174: 4934-4941.
- Tournier, J., Ulrich, R.G., Quesnel-Hellmann, A., Mohamadzadeh, M. and Stiles, B.G. (2009) Anthrax, toxins and vaccines: a 125-year journey targeting Bacillus anthracis. Expert Rev Anti Infect Ther 7: 219-236.

- Van Der Goot, G. and Young, J.A.T. (2009) Receptors of anthrax toxin and cell entry. Mol Aspects Med 30: 406-412.
- Vitale, G., Pellizzari, R., Recchi, C., Napolitani, G., Mock, M. and Montecucco, C. (1998) Anthrax lethal factor cleaves the N-terminus of MAPKKs and induces tyrosine/threonine phosphorylation of MAPKs in cultured macrophages. Biochem Biophys Res Commun 248: 706-711.
- Vitale, G., Bernardi, L., Napolitani, G., Mock, M. and Montecucco, C. (2000) Susceptibility of mitogen-activated protein kinase kinase family members to proteolysis by anthrax lethal factor. Biochem J 352: 739-745.
- Woodcroft, B.J., Hammond, L., Stow, J.L. and Hamilton, N.A. (2009) Automated organelle-based colocalization in whole-cell imaging. Cytometry 75: 941-950.
- Wunderlich, W., Fialka, I., Teis, D., Alpi, A., Pfeifer, A., Parton, R.G., et al.(2001) A novel 14-kilodalton protein interacts with the mitogen-activated protein kinase scaffold mp1 on a late endosomal/lysosomal compartment. J Cell Biol 152: 765-776.
- Yamaji, A., Sekizawa, Y., Emoto, K., Sakuraba, H., Inoue, K., Kobayashi, H. et al. (1998) Lysenin, a novel sphingomyelin-specific binding protein. J Biol Chem 273: 5300-5306.
- Young, J.A.T. and Collier, R.J. (2007) Anthrax toxin: receptor binding, internalization, pore formation, and translocation. Annu Rev Biochem 76: 243-265.

Acknowledgements

This work has been supported by the MIUR program FIRB Internazionalizzazione and the Istituto Superiore di Sanità and NIH grants 1F32 AI077280 to BEJ and 5R01 AI022021 to RJC, who holds equity in PharmAthene, Inc

Chapter VI: Conclusions

The first part of my Ph.D. thesis was focused on cAMP imaging of cells treated with edema toxin using fluorescent PKA-based probes [Dal Molin 2006] and the method was extended to other toxins which increase intracellular cAMP concentration [Dal Molin 2008].

The process of anthrax toxin cell entry and trafficking along endocytic pathway attracted then my attention. The available data on binding and internalization of these toxins are limited and suggested that the lethal anthrax toxin exploits clathrin-dependent endocytic route to enter into cells [Abrami 2003]. It found that PA, after antibody cross-linking, reached both clathrin-coated pits and vesicles as well as sometimes nonclathrin-coated invagination of the plasma membrane.

To clarify the question of anthrax toxins cell entry, imaging techniques based on fluorescent chimeric proteins consisting of a fluorescent domain linked to the toxin seemed to be promising. I prepared these tools and I found out that the strength of the fluorescence signal was not optimal and needed to be optimized by using anti-GFP antibodies, a technique which did not alter the pattern of fluorescence distribution. Using chimeric fluorescent catalytic subunits, I found that the two toxins follow exactly the same pathway of entry, segregate into plasma membrane rafts and have similar kinetics under experimental conditions that mimic the *in vivo* situation. The chimeric proteins enter caveolin-1 containing compartments in BHK cells. This result is at variance with clathrin-mediated entry, however these data are not surprising in light of the fact that other toxins enter cells via clathrin-independent route [Sandivig 2008] and that the majority of ligands that bind to raft microdomains are preferentially taken up via by clathrin-independent endocytosis [Nichols 2003].

Anthrax recombinant toxins enter caveolin-1 containing compartments and then endosomes marked by PI3P and Rab5, but not by EEA1 and transferrin. After 40 minutes, both EF and LF chimerae are in the late endosomal compartments marked by the lipid molecule LBPA.

It was also important to address the question of the cellular site from where EF and LF enter the cytosol because the available data are contradictory. It was proposed that LF reaches the cytosol solely from EEs in RAW264.7 macrophage cell line [Guidi-Rontani 2000] but was also suggested that it reaches its cytosolic substrates with a time course consistent with its exit at the late endosomal stages in baby hamster kidney (BHK) cell line [Abrami 2003]. Similar to LF, EF was found in late endosomes in HeLa cells [Dal Molin 2006]. Although these discrepancy can be explained by different experimental conditions, this point is crucial and needs to be addressed.

It was shown that the two toxins end up in the same late endosomes, wherefrom LF and EF translocate from the lumen into the cytosol. However, they reach two different intracellular localizations. EF remains associated with late endosomes, whilst LF diffuses into the cytosol. This point is under investigation, but we could exclude that the N-terminal domain of EF is involved.

Many outstanding questions remain open such as the molecular mechanism which dictate the toxins entry routes, the involvement of ESCRT complex in the endocytic sorting of ubiquitinated anthrax proteins into ILVs of late compartments, the efficiency of EF and LF translocation from the endosomes, the molecular partner that retains EF bound to late endosomes. Recent advances in imaging techniques seem to be promising; recent reports show the ability of these techniques to achieve super-resolution (up to 20 nm in the focal plane) in biological samples [Hell 2007] and the possibility to perform two-colour time-lapse imaging of mammalian cells [Donnert 2007]. Although simple FPs, such as GFP and YFP Citrine, have been used in super-resolution imaging [Hein 2008, Willig 2006], most of these techniques exploit the intrinsic ability of certain FPs to change their spectral properties on irradiation with light of a specific wavelength. It should be possible to study anthrax toxin chimerae trafficking at high resolution and address many open questions.

Chapter VII: References

1. Driks A. The *Bacillus anthracis* spore. Mol Aspects Med (2009) 30: pp. 368-373
2. Russell BH, Vasan R, Keene DR & Xu Y. *Bacillus anthracis* internalization by human fibroblasts and epithelial cells. Cell Microbiol (2007) 9: pp. 1262-1274.
3. Mesnage S, Tosi-Couture E, Gounon P, Mock M & Fouet A. The capsule and S-layer: two independent and yet compatible macromolecular structures in *Bacillus anthracis*. J Bacteriol (1998) 180: pp. 52-58.
4. Fouet A. The surface of *Bacillus anthracis*. Mol Aspects Med (2009) 30: pp. 374-385.
5. Smith H, Tempest DW, Stanley JL, Harris-Smith PW & Gallop RC. The chemical basis of the virulence of *Bacillus anthracis*. VII. Two components of the anthrax toxin: their relationship to known immunising aggressins. Br J Exp Pathol (1956) 37: pp. 263-271.
6. Smith H & Stanley JL. Purification of the third factor of anthrax toxin. J Gen Microbiol (1962) 29: pp. 517-521.
7. Koehler TM. *Bacillus anthracis* physiology and genetics. Mol Aspects Med (2009) 30: pp. 386-396.
8. Ascenzi P, Visca P, Ippolito G, Spallarossa A, Bolognesi M & Montecucco C. Anthrax toxin: a tripartite lethal combination. FEBS Lett (2002) 531: pp. 384-388.
9. Petosa C, Collier RJ, Klimpel KR, Leppla SH & Liddington RC. Crystal structure of the anthrax toxin protective antigen. Nature (1997) 385: pp. 833-838.
10. Lacy DB, Wigelsworth DJ, Melnyk RA, Harrison SC & Collier RJ. Structure of heptameric protective antigen bound to an anthrax toxin receptor: a role for receptor in pH-dependent pore formation. Proc Natl Acad Sci U S A (2004) 101: pp. 13147-13151.
11. Hammamieh R, Ribot WJ, Abshire TG, Jett M & Ezzell J. Activity of the *Bacillus anthracis* 20 kDa protective antigen component. BMC Infect Dis (2008) 8: p. 124.
12. Wesche J, Elliott JL, Falnes PO, Olsnes S & Collier RJ. Characterization of membrane translocation by anthrax protective antigen. Biochemistry (1998) 37: pp. 15737-15746.
13. Zhang S, Udho E, Wu Z, Collier RJ & Finkelstein A. Protein translocation through anthrax toxin channels formed in planar lipid bilayers. Biophys J (2004) 87: pp. 3842-3849.
14. Krantz BA, Melnyk RA, Zhang S, Juris SJ, Lacy DB, Wu Z, Finkelstein A & Collier RJ. A phenylalanine clamp catalyzes protein translocation through the anthrax toxin pore. Science (2005) 309: pp. 777-781.

15. Mogridge J, Mourez M & Collier RJ. Involvement of domain 3 in oligomerization by the protective antigen moiety of anthrax toxin. J Bacteriol (2001) 183: pp. 2111-2116.
16. Blaustein RO, Koehler TM, Collier RJ & Finkelstein A. Anthrax toxin: channel-forming activity of protective antigen in planar phospholipid bilayers. Proc Natl Acad Sci U S A (1989) 86: pp. 2209-2213.
17. Milne JC & Collier RJ. pH-dependent permeabilization of the plasma membrane of mammalian cells by anthrax protective antigen. Mol Microbiol (1993) 10: pp. 647-653.
18. Sellman BR, Mourez M & Collier RJ. Dominant-negative mutants of a toxin subunit: an approach to therapy of anthrax. Science (2001) 292: pp. 695-697.
19. Sellman BR, Nassi S & Collier RJ. Point mutations in anthrax protective antigen that block translocation. J Biol Chem (2001#1) 276: pp. 8371-8376.
20. Janowiak BE, Finkelstein A & Collier RJ. An approach to characterizing single-subunit mutations in multimeric prepores and pores of anthrax protective antigen. Protein Sci (2009) 18: pp. 348-358.
21. Pannifer AD, Wong TY, Schwarzenbacher R, Renatus M, Petosa C, Bienkowska J, Lacy DB, Collier RJ, Park S, Leppla SH, Hanna P & Liddington RC. Crystal structure of the anthrax lethal factor. Nature (2001) 414: pp. 229-233.
22. Tonello F & Montecucco C. The anthrax lethal factor and its MAPK kinase-specific metalloprotease activity. Mol Aspects Med (2009) : 30: pp. 431-436.
23. Arora N, Klimpel KR, Singh Y & Leppla SH. Fusions of anthrax toxin lethal factor to the ADP-ribosylation domain of *Pseudomonas* exotoxin A are potent cytotoxins which are translocated to the cytosol of mammalian cells. J Biol Chem (1992) 267: pp. 15542-15548.
24. Arora N & Leppla SH. Residues 1-254 of anthrax toxin lethal factor are sufficient to cause cellular uptake of fused polypeptides. J Biol Chem (1993) 268: pp. 3334-3341.
25. Arora N & Leppla SH. Fusions of anthrax toxin lethal factor with shiga toxin and diphtheria toxin enzymatic domains are toxic to mammalian cells. Infect Immun (1994) 62: pp. 4955-4961.
26. Milne JC, Blanke SR, Hanna PC & Collier RJ. Protective antigen-binding domain of anthrax lethal factor mediates translocation of a heterologous protein fused to its amino- or carboxy-terminus. Mol Microbiol (1995) 15: pp. 661-666.

27. Blanke SR, Milne JC, Benson EL & Collier RJ. Fused polycationic peptide mediates delivery of diphtheria toxin A chain to the cytosol in the presence of anthrax protective antigen. Proc Natl Acad Sci U S A (1996) 93: pp. 8437-8442.
28. Liang X, Young JJ, Boone SA, Waugh DS & Duesbery NS. Involvement of domain II in toxicity of anthrax lethal factor. J Biol Chem (2004) 279: pp. 52473-52478.
29. Ladant D & Ullmann A. *Bordetella pertussis* adenylate cyclase: a toxin with multiple talents. Trends Microbiol (1999) 7: pp. 172-176.
30. Tang W & Guo Q. The adenylyl cyclase activity of anthrax edema factor. Mol Aspects Med (2009) 30: pp. 423-430.
31. Drum CL, Yan S, Bard J, Shen Y, Lu D, Soelaiman S, Grabarek Z, Bohm A & Tang W. Structural basis for the activation of anthrax adenylyl cyclase exotoxin by calmodulin. Nature (2002) 415: pp. 396-402.
32. Shen Y, Lee Y, Soelaiman S, Bergson P, Lu D, Chen A, Beckingham K, Grabarek Z, Mrksich M & Tang W. Physiological calcium concentrations regulate calmodulin binding and catalysis of adenylyl cyclase exotoxins. EMBO J (2002) 21: pp. 6721-6732.
33. Van Der Goot G & Young JAT. Receptors of anthrax toxin and cell entry. Mol Aspects Med (2009) 30: pp. 406-412.
34. Bradley KA, Mogridge J, Mourez M, Collier RJ & Young JA. Identification of the cellular receptor for anthrax toxin. Nature (2001) 414: pp. 225-229.
35. Scobie HM, Rainey GJA, Bradley KA & Young JAT. Human capillary morphogenesis protein 2 functions as an anthrax toxin receptor. Proc Natl Acad Sci U S A (2003) 100: pp. 5170-5174.
36. Liu S & Leppla SH. Cell surface tumor endothelium marker 8 cytoplasmic tail-independent anthrax toxin binding, proteolytic processing, oligomer formation, and internalization. J Biol Chem (2003) 278: pp. 5227-5234.
37. Scobie HM & Young JAT. Interactions between anthrax toxin receptors and protective antigen. Curr Opin Microbiol (2005) 8: pp. 106-112.
38. Lacy DB, Wigelsworth DJ, Melnyk RA, Harrison SC & Collier RJ. Structure of heptameric protective antigen bound to an anthrax toxin receptor: a role for receptor in pH-dependent pore formation. Proc Natl Acad Sci U S A (2004) 101: pp. 13147-13151.
39. Santelli E, Bankston LA, Leppla SH & Liddington RC. Crystal structure of a complex between anthrax toxin and its host cell receptor. Nature (2004) 430: pp. 905-908.

40. Bradley KA, Mogridge J, Jonah G, Rainey A, Batty S & Young JAT. Binding of anthrax toxin to its receptor is similar to alpha integrin-ligand interactions. J Biol Chem (2003) 278: pp. 49342-49347.
41. Wigelsworth DJ, Krantz BA, Christensen KA, Lacy DB, Juris SJ & Collier RJ. Binding stoichiometry and kinetics of the interaction of a human anthrax toxin receptor, CMG2, with protective antigen. J Biol Chem (2004) 279: pp. 23349-23356.
42. Liu S, Leung HJ & Leppla SH. Characterization of the interaction between anthrax toxin and its cellular receptors. Cell Microbiol (2007) 9: pp. 977-987.
43. Liu S, Crown D, Miller-Randolph S, Moayeri M, Wang H, Hu H, Morley T & Leppla SH. Capillary morphogenesis protein-2 is the major receptor mediating lethality of anthrax toxin in vivo. Proc Natl Acad Sci U S A (2009) 106: pp. 12424-12429.
44. Rainey GJA, Wigelsworth DJ, Ryan PL, Scobie HM, Collier RJ & Young JAT. Receptor-specific requirements for anthrax toxin delivery into cells. Proc Natl Acad Sci U S A (2005) 102: pp. 13278-13283.
45. Liu S & Leppla SH. Cell surface tumor endothelium marker 8 cytoplasmic tail-independent anthrax toxin binding, proteolytic processing, oligomer formation, and internalization. J Biol Chem (2003) 278: pp. 5227-5234.
46. Go MY, Kim S, Partridge AW, Melnyk RA, Rath A, Deber CM & Mogridge J. Self-association of the transmembrane domain of an anthrax toxin receptor. J Mol Biol (2006) 360: pp. 145-156.
47. Bonuccelli G, Sotgia F, Frank PG, Williams TM, de Almeida CJ, Tanowitz HB, Scherer PE, Hotchkiss KA, Terman BI, Rollman B, Alileche A, Brojatsch J & Lisanti MP. ATR/TEM8 is highly expressed in epithelial cells lining *Bacillus anthracis'* three sites of entry: implications for the pathogenesis of anthrax infection. Am J Physiol Cell Physiol (2005) 288: p. C1402-10.
48. Maldonado-Arocho FJ, Fulcher JA, Lee B & Bradley KA. Anthrax oedema toxin induces anthrax toxin receptor expression in monocyte-derived cells. Mol Microbiol (2006) 61: pp. 324-337.
49. Rmali KA, Al-Rawi MAA, Parr C, Puntis MCA & Jiang WG. Upregulation of tumour endothelial marker-8 by interleukin-1beta and its impact in IL-1beta induced angiogenesis. Int J Mol Med (2004) 14: pp. 75-80

50. Banks DJ, Barnajian M, Maldonado-Arocho FJ, Sanchez AM & Bradley KA. Anthrax toxin receptor 2 mediates *Bacillus anthracis* killing of macrophages following spore challenge. Cell Microbiol (2005) 7: pp. 1173-1185.
51. Milne JC, Furlong D, Hanna PC, Wall JS & Collier RJ. Anthrax protective antigen forms oligomers during intoxication of mammalian cells. J Biol Chem (1994) 269: pp. 20607-20612.
52. Mogridge J, Cunningham K & Collier RJ. Stoichiometry of anthrax toxin complexes. Biochemistry (2002) 41: pp. 1079-1082.
53. Young JAT & Collier RJ. Anthrax toxin: receptor binding, internalization, pore formation, and translocation. Annu Rev Biochem (2007) 76: pp. 243-265.
54. Kintzer AF, Thoren KL, Sterling HJ, Dong KC, Feld GK, Tang II, Zhang TT, Williams ER, Berger JM & Krantz BA. The protective antigen component of anthrax toxin forms functional octameric complexes. J Mol Biol (2009) 392: pp. 614-629.
55. Mayor S & Pagano RE. Pathways of clathrin-independent endocytosis. Nat Rev Mol Cell Biol (2007) 8: pp. 603-612.
56. Doherty GJ & McMahon HT. Mechanisms of endocytosis. Annu Rev Biochem (2009) 78: pp. 857-902.
57. Mousavi SA, Malerød L, Berg T & Kjeken R. Clathrin-dependent endocytosis. Biochem J (2004) 377: pp. 1-16.
58. Moya M, Dautry-Varsat A, Goud B, Louvard D & Boquet P. Inhibition of coated pit formation in Hep2 cells blocks the cytotoxicity of diphtheria toxin but not that of ricin toxin. J Cell Biol (1985) 101: pp. 548-559.
59. Sandvig K, Olsnes S, Petersen OW & van Deurs B. Acidification of the cytosol inhibits endocytosis from coated pits. J Cell Biol (1987) 105: pp. 679-689.
60. Sandvig K & van Deurs B. Delivery into cells: lessons learned from plant and bacterial toxins. Gene Ther (2005) 12: pp. 865-872.
61. Conner SD & Schmid SL. Regulated portals of entry into the cell. Nature (2003) 422: pp. 37-44.
62. Kirkham M & Parton RG. Clathrin-independent endocytosis: new insights into caveolae and non-caveolar lipid raft carriers. Biochim Biophys Acta (2005) 1745: pp. 273-286.

63. Gruenberg J. The endocytic pathway: a mosaic of domains. Nat Rev Mol Cell Biol (2001) 2: pp. 721-730.
64. Cullen PJ. Endosomal sorting and signalling: an emerging role for sorting nexins. Nat Rev Mol Cell Biol (2008) 9: pp. 574-582.
65. Mari M, Bujny MV, Zeuschner D, Geerts WJC, Griffith J, Petersen CM, Cullen PJ, Klumperman J & Geuze HJ. SNX1 defines an early endosomal recycling exit for sortilin and mannose 6-phosphate receptors. Traffic (2008) 9: pp. 380-393.
66. Woodman PG & Futter CE. Multivesicular bodies: co-ordinated progression to maturity. Curr Opin Cell Biol (2008) 20: pp. 408-414.
67. Sönnichsen B, De Renzis S, Nielsen E, Rietdorf J & Zerial M. Distinct membrane domains on endosomes in the recycling pathway visualized by multicolor imaging of Rab4, Rab5, and Rab11. J Cell Biol (2000) 149: pp. 901-914.
68. Gruenberg J & Stenmark H. The biogenesis of multivesicular endosomes. Nat Rev Mol Cell Biol (2004) 5: pp. 317-323.
69. Raiborg C & Stenmark H. The ESCRT machinery in endosomal sorting of ubiquitylated membrane proteins. Nature (2009) 458: pp. 445-452.
70. Rink J, Ghigo E, Kalaidzidis Y & Zerial M. Rab conversion as a mechanism of progression from early to late endosomes. Cell (2005) 122: pp. 735-749.
71. Kobayashi T, Stang E, Fang KS, de Moerloose P, Parton RG & Gruenberg J. A lipid associated with the antiphospholipid syndrome regulates endosome structure and function. Nature (1998) 392: pp. 193-197.
72. White IJ, Bailey LM, Aghakhani MR, Moss SE & Futter CE. EGF stimulates annexin 1-dependent inward vesiculation in a multivesicular endosome subpopulation. EMBO J (2006) 25: pp. 1-12.
73. Kobayashi T, Beuchat M, Chevallier J, Makino A, Mayran N, Escola J, Lebrand C, Cosson P, Kobayashi T & Gruenberg J. Separation and characterization of late endosomal membrane domains. J Biol Chem (2002) 277: pp. 32157-32164.
74. Russell MRG, Nickerson DP & Odorizzi G. Molecular mechanisms of late endosome morphology, identity and sorting. Curr Opin Cell Biol (2006) 18: pp. 422-428.
75. Luzio JP, Pryor PR & Bright NA. Lysosomes: fusion and function. Nat Rev Mol Cell Biol (2007) 8: pp. 622-632.

76. Bright NA, Gratian MJ & Luzio JP. Endocytic delivery to lysosomes mediated by concurrent fusion and kissing events in living cells. Curr Biol (2005) 15: pp. 360-365.
77. Pryor PR & Luzio JP. Delivery of endocytosed membrane proteins to the lysosome. Biochim Biophys Acta (2009) 1793: pp. 615-624.
78. Puhar A & Montecucco C. Where and how do anthrax toxins exit endosomes to intoxicate host cells?. Trends Microbiol (2007) 15: pp. 477-482.
79. Wei W, Lu Q, Chaudry GJ, Leppla SH & Cohen SN. The LDL receptor-related protein LRP6 mediates internalization and lethality of anthrax toxin. Cell (2006) 124: pp. 1141-1154.
80. Abrami L, Kunz B, Deuquet J, Bafico A, Davidson G & van der Goot FG. Functional interactions between anthrax toxin receptors and the WNT signalling protein LRP6. Cell Microbiol (2008) 10: pp. 2509-2519.
81. Young JJ, Bromberg-White JL, Zylstra C, Church JT, Boguslawski E, Resau JH, Williams BO & Duesbery NS. LRP5 and LRP6 are not required for protective antigen-mediated internalization or lethality of anthrax lethal toxin. PLoS Pathog (2007) 3: p. e27.
82. Ryan PL & Young JAT. Evidence against a human cell-specific role for LRP6 in anthrax toxin entry. PLoS One (2008) 3: p. e1817.
83. Abrami L, Liu S, Cosson P, Leppla SH & van der Goot FG. Anthrax toxin triggers endocytosis of its receptor via a lipid raft-mediated clathrin-dependent process. J Cell Biol (2003) 160: pp. 321-328.
84. Abrami L, Leppla SH & van der Goot FG. Receptor palmitoylation and ubiquitination regulate anthrax toxin endocytosis. J Cell Biol (2006) 172: pp. 309-320.
85. Abrami L, Lindsay M, Parton RG, Leppla SH & van der Goot FG. Membrane insertion of anthrax protective antigen and cytoplasmic delivery of lethal factor occur at different stages of the endocytic pathway. J Cell Biol (2004) 166: pp. 645-651.
86. Dal Molin F, Tonello F, Ladant D, Zornetta I, Zamparo I, Di Benedetto G, Zaccolo M & Montecucco C. Cell entry and cAMP imaging of anthrax edema toxin. EMBO J (2006) 25: pp. 5405-5413.
87. Le Blanc I, Luyet P, Pons V, Ferguson C, Emans N, Petiot A, Mayran N, Demaurex N, Fauré J, Sadoul R, Parton RG & Gruenberg J. Endosome-to-cytosol transport of viral nucleocapsids. Nat Cell Biol (2005) 7: pp. 653-664.

88. Neumeyer T, Tonello F, Dal Molin F, Schiffler B & Benz R. Anthrax edema factor, voltage-dependent binding to the protective antigen ion channel and comparison to LF binding. J Biol Chem (2006) 281: pp. 32335-32343.
89. Krantz BA, Finkelstein A & Collier RJ. Protein translocation through the anthrax toxin transmembrane pore is driven by a proton gradient. J Mol Biol (2006) 355: pp. 968-979.
90. Melnyk RA & Collier RJ. A loop network within the anthrax toxin pore positions the phenylalanine clamp in an active conformation. Proc Natl Acad Sci U S A (2006) 103: pp. 9802-9807.
91. Collier RJ. Membrane translocation by anthrax toxin. Mol Aspects Med (2009) 30: pp. 413-422.
92. Ratts R, Zeng H, Berg EA, Blue C, McComb ME, Costello CE, vanderSpek JC & Murphy JR. The cytosolic entry of diphtheria toxin catalytic domain requires a host cell cytosolic translocation factor complex. J Cell Biol (2003) 160: pp. 1139-1150.
93. Tamayo AG, Bharti A, Trujillo C, Harrison R & Murphy JR. COPI coatomer complex proteins facilitate the translocation of anthrax lethal factor across vesicular membranes in vitro. Proc Natl Acad Sci U S A (2008) 105: pp. 5254-5259.
94. Duesbery NS, Webb CP, Leppla SH, Gordon VM, Klimpel KR, Copeland TD, Ahn NG, Oskarsson MK, Fukasawa K, Paull KD & Vande Woude GF. Proteolytic inactivation of MAP-kinase-kinase by anthrax lethal factor. Science (1998) 280: pp. 734-737.
95. Vitale G, Pellizzari R, Recchi C, Napolitani G, Mock M & Montecucco C. Anthrax lethal factor cleaves the N-terminus of MAPKKs and induces tyrosine/threonine phosphorylation of MAPKs in cultured macrophages. Biochem Biophys Res Commun (1998) 248: pp. 706-711.
96. Vitale G, Bernardi L, Napolitani G, Mock M & Montecucco C. Susceptibility of mitogen-activated protein kinase kinase family members to proteolysis by anthrax lethal factor. Biochem J (2000) 352 Pt 3: pp. 739-745.
97. Tonello F, Seveso M, Marin O, Mock M & Montecucco C. Screening inhibitors of anthrax lethal factor. Nature (2002) 418: p. 386.
98. Tonello F, Ascenzi P & Montecucco C. The metalloproteolytic activity of the anthrax lethal factor is substrate-inhibited. J Biol Chem (2003) 278: pp. 40075-40078.
99. Cummings RT, Salowe SP, Cunningham BR, Wiltsie J, Park YW, Sonatore LM, Wisniewski D, Douglas CM, Hermes JD & Scolnick EM. A peptide-based fluorescence resonance energy

transfer assay for *Bacillus anthracis* lethal factor protease. Proc Natl Acad Sci U S A (2002) 99: pp. 6603-6606.

100. Zakharova MY, Kuznetsov NA, Dubiley SA, Kozyr AV, Fedorova OS, Chudakov DM, Knorre DG, Shemyakin IG, Gabibov AG & Kolesnikov AV. Substrate recognition of anthrax lethal factor examined by combinatorial and pre-steady-state kinetic approaches. J Biol Chem (2009) 284: pp. 17902-17913.

101. Maynard JA, Maassen CBM, Leppla SH, Brasky K, Patterson JL, Iverson BL & Georgiou G. Protection against anthrax toxin by recombinant antibody fragments correlates with antigen affinity. Nat Biotechnol (2002) 20: pp. 597-601.

102. Zhao P, Liang X, Kalbfleisch J, Koo H & Cao B. Neutralizing monoclonal antibody against anthrax lethal factor inhibits intoxication in a mouse model. Hum Antibodies (2003) 12: pp. 129-135.

103. Turk BE, Wong TY, Schwarzenbacher R, Jarrell ET, Leppla SH, Collier RJ, Liddington RC & Cantley LC. The structural basis for substrate and inhibitor selectivity of the anthrax lethal factor. Nat Struct Mol Biol (2004) 11: pp. 60-66.

104. Friedlander AM. Macrophages are sensitive to anthrax lethal toxin through an acid-dependent process. J Biol Chem (1986) 261: pp. 7123-7126.

105. Friedlander AM, Bhatnagar R, Leppla SH, Johnson L & Singh Y. Characterization of macrophage sensitivity and resistance to anthrax lethal toxin. Infect Immun (1993) 61: pp. 245-252.

106. Tournier J, Rossi Paccani S, Quesnel-Hellmann A & Baldari CT. Anthrax toxins: a weapon to systematically dismantle the host immune defenses. Mol Aspects Med (2009) 30: pp. 456-466

107. Pellizzari R, Guidi-Rontani C, Vitale G, Mock M & Montecucco C. Anthrax lethal factor cleaves MKK3 in macrophages and inhibits the LPS/IFNgamma-induced release of NO and TNFalpha. FEBS Lett (1999) 462: pp. 199-204.

108. Boyden ED & Dietrich WF. Nalp1b controls mouse macrophage susceptibility to anthrax lethal toxin. Nat Genet (2006) 38: pp. 240-244.

109. Park JM, Greten FR, Wong A, Westrick RJ, Arthur JSC, Otsu K, Hoffmann A, Montminy M & Karin M. Signaling pathways and genes that inhibit pathogen-induced

macrophage apoptosis: CREB and NF-kappaB as key regulators. Immunity (2005) 23: pp. 319-329.

110. Rossi Paccani S, Tonello F, Patrussi L, Capitani N, Simonato M, Montecucco C & Baldari CT. Anthrax toxins inhibit immune cell chemotaxis by perturbing chemokine receptor signalling. Cell Microbiol (2007) 9: pp. 924-929.

111. Rossi Paccani S, Benagiano M, Capitani N, Zornetta I, Ladant D, Montecucco C, D'Elios MM & Baldari CT. The adenylate cyclase toxins of *Bacillus anthracis* and *Bordetella pertussis* promote Th2 cell development by shaping T cell antigen receptor signaling. PLoS Pathog (2009) 5: p. e1000325.

112. Moayeri M & Leppla SH. Cellular and systemic effects of anthrax lethal toxin and edema toxin. Mol Aspects Med (2009) 30: .

113. Moayeri M, Martinez NW, Wiggins J, Young HA & Leppla SH. Mouse susceptibility to anthrax lethal toxin is influenced by genetic factors in addition to those controlling macrophage sensitivity. Infect Immun (2004) 72: pp. 4439-4447.

114. Dal Molin F, Fasanella A, Simonato M, Garofolo G, Montecucco C & Tonello F. Ratio of lethal and edema factors in rabbit systemic anthrax. Toxicon (2008) 52: pp. 824-828.

115. Sirard JC, Mock M & Fouet A. The three *Bacillus anthracis* toxin genes are coordinately regulated by bicarbonate and temperature. J Bacteriol (1994) 176: pp. 5188-5192.

116. Firoved AM, Miller GF, Moayeri M, Kakkar R, Shen Y, Wiggins JF, McNally EM, Tang W & Leppla SH. *Bacillus anthracis* edema toxin causes extensive tissue lesions and rapid lethality in mice. Am J Pathol (2005) 167: pp. 1309-1320.

117. Dal Molin F, Zornetta I, Puhar A, Tonello F, Zaccolo M & Montecucco C. cAMP imaging of cells treated with pertussis toxin, cholera toxin, and anthrax edema toxin. Biochem Biophys Res Commun (2008) 376: pp. 429-433.

118. Boll W, Ehrlich M, Collier RJ & Kirchhausen T. Effects of dynamin inactivation on pathways of anthrax toxin uptake. Eur J Cell Biol (2004) 83: pp. 281-288.

119. Sandvig K, Torgersen ML, Raa HA & van Deurs B. Clathrin-independent endocytosis: from nonexisting to an extreme degree of complexity. Histochem Cell Biol (2008) 129: pp. 267-276.

120. Nichols B. Caveosomes and endocytosis of lipid rafts. J Cell Sci (2003) 116: pp. 4707-4714.

121. Guidi-Rontani C, Weber-Levy M, Mock M & Cabiaux V. Translocation of *Bacillus anthracis* lethal and oedema factors across endosome membranes. Cell Microbiol (2000) 2: pp. 259-264.

122. Hell SW. Far-field optical nanoscopy. Science (2007) 316: pp. 1153-1158.

123. Donnert G, Keller J, Wurm CA, Rizzoli SO, Westphal V, Schönle A, Jahn R, Jakobs S, Eggeling C & Hell SW. Two-color far-field fluorescence nanoscopy. Biophys J (2007) 92: p. L67-9.

124. Hein B, Willig KI & Hell SW. Stimulated emission depletion (STED) nanoscopy of a fluorescent protein-labeled organelle inside a living cell. Proc Natl Acad Sci U S A (2008) 105: pp. 14271-14276.

125. Willig KI, Kellner RR, Medda R, Hein B, Jakobs S & Hell SW. Nanoscale resolution in GFP-based microscopy. Nat Methods (2006) 3: pp. 721-723.